STUDIES OF BLOCK COPOLYMER

STABILIZERS FOR DISPERSION

POLYMERIZATION

by

GRAHAM TAYLOR

Supervisor :   DR. J.V. DAWKINS

A doctoral thesis submitted in partial fulfilment

of the requirements for the award of the Degree

of Doctor.of Philosophy of Loughborough University

of Technology.

October 1977   Department of Chemistry

ACKNOWLEDGEMENTS

ORIGINALITY

The work presented in this Thesis has been carried
out by the author, except where otherwise
acknowledged, and has not previously been submitted
to this University or any other Institution.

ABSTRACT

Anionic polymerization techniques have been used to prepare AB block copolymers of polystyrene and poly(dimethyl siloxane) having well-defined molecular weight and composition, and narrow molecular weight distribution. Block copolymers prepared over a range of molecular weights and compositions were characterized by gel permeation chromatography, osmometry and silicon analysis.

Such block copolymers have been used as stabilizers for non-aqueous dispersion polymerizations of styrene and methyl methacrylate in aliphatic hydrocarbon. The polymer particles thus produced were stabilized by well-defined surface layers of poly(dimethyl siloxane). The effects of varying the polymerization conditions, and the type and concentration of stabilizer present, were studied. Both radical and anionic polymerization mechanisms have been considered, and methods of preparing polymer particles of a narrow size distribution were developed.

Polymer particles were characterized by transmission electron microscopy to determine the shape and size. Small-angle X-ray scattering and light scattering studies confirmed the particle sizes and also detected the presence of the surface layer of poly(dimethyl siloxane). Gravimetric methods were used to determine the silicon content of the polymer particles, from which an estimate of the surface coverage was made. Surface coverage was studied as a function of the molecular weight of the poly(dimethyl siloxane).

Rheological studies confirmed the sphericity of the particles, and showed them to be non-flocculated under shear. An estimate of the hydrodynamic thickness of the surface layer was also obtained from rheology, and studied as a function of particle size and molecular weight of the poly (dimethyl siloxane). Hydrodynamic measurements were combined with surface coverage information to suggest that the configuration of the poly(dimethyl siloxane) chains was extended over a random coil configuration.

Theta-conditions were determined for poly(dimethyl siloxane) in mixtures of alkane and alcohol. The solvency of the dispersion medium of polymer dispersions was reduced until flocculation occurred. The flocculation conditions corresponded closely to theta-conditions for free poly(dimethyl siloxane), and thus the mechanism of dispersion stabilization was confirmed to be steric.

CONTENTS

CHAPTER 1

INTRODUCTION

Heterogeneous polymerization is an easily controllable method for preparing polymer particles within an inert medium. By far the most exploited system is that of aqueous emulsion polymerization, which has been widely studied over the past 35 years [1]. Emulsion polymerization can be used to prepare dispersions of high molecular weight polymer at high concentration whilst retaining a relatively low overall viscosity. These characteristics have promoted the extensive use of such products in the surface-coatings industry. Water represents a cheap, non-toxic and non-inflammable medium, but has disadvantages when used as a vehicle for surface coatings, such as a slow and uncontrollable rate of evaporation. Attention was, therefore, focused on a non-aqueous counterpart to emulsion polymerization, and non-aqueous dispersion polymerization techniques were developed.

The characteristics of the different heterogeneous poly- merization techniques available are discussed in Chapter 2. Polymer particles in a non-aqueous dispersion are prevented from flocculation by surrounding the particle with a surface layer of soluble polymeric stabilizer. Such particles are said to be sterically stabilized. The term "stabilizer" will be used in the present work to describe the agent which prevents flocculation of the dispersed particles. This should not be confused with the stabilizers often added to polymers to prevent thermal or photo-induced degradation.

Because of the obvious commercial potential of polymer dispersions, most of the work published has been confined to the patent literature. Early dispersion polymerizations employed rubbers which took part in grafting reactions during the polymerization to form grafted stabilizers [2,3]. Subsequent developments introduced the use of pre-formed block and graft copolymer stabilizers, which were often grafted onto the particles [4,5].

Quite recently, the preparation of non-aqueous polymer dispersions [6], and studies of the mechanism and kinetics of polymerization [7], have been described in the literature. Most studies to date have been based upon polymer particles stabilized by grafted copolymers. Very prominent among such systems are acrylic polymer particles stabilized by graft copolymers consisting of an acrylic backbone with short side chains such as poly[12-hydroxy stearic acid] [6].

Various types of polymerization mechanism are adaptable to dispersion polymerization, such as addition, condensation and ring-opening polymerization. Almost all the kinetic and mechanistic studies reported have concerned radical addition polymerization [7], again particularly of acrylic monomers. The anionic dispersion polymerization of styrene was described in the patent literature [8], and involved the use of grafted rubbers as the stabilizer. The only reference to such an anionic polymerization which could be found in the scientific journals is due to Stampa [9]. He reported the anionic dispersion polymerization of α-methyl styrene in the presence of a poly[vinyl ether] stabilizer. Barrett [10] has recently edited a book on the subject of dispersion poly-merization, which comprehensively reviews the work done to date.

In parallel with the work described above, much has been published in the literature concerning the concept of steric stabilization. These theoretical considerations were largely motivated by the work of Fischer [11] and Meier [12], and the major contributions have come from Dutch and British colloid schools and from Napper in Australia. There is currently much discussion in the literature as to the nature of steric interactions. The various theories have been reviewed [13] and will be discussed in Chapter 2.

Most of the theoretical work was developed in isolation from the practical systems studied largely in industrial laboratories. Some attempts to correlate theory and experiment have been made recently by Napper [e.g. see reference 14] and British workers [e.g. see reference 15]. Fundamental problems arose owing to the nature of the sterically stabilized dispersions commonly prepared. The stabilizing molecules were usually rather poorly-defined, and of such a short chain length that it is doubtful whether conventional polymer solution theories are applicable. A recent Science Research Council report [16] has highlighted the need for better-defined polymer layers at the surface of colloidal particles.

With this aim in mind, the present work sought to prepare well-defined, sterically stabilized dispersions of polymer particles in a non-aqueous medium. Studies based on such systems would lead to a better understanding of the stabilizing mechanism.

A simple AB-type of block copolymer stabilizer was chosen, consisting of a polystyrene [PS] block and a poly [dimethyl siloxane] [PDMS] block. Methods of synthesising

such copolymers of a predictable molecular weight and composition are known. The significantly different solubility parameters of PS and PDMS [9.1 [cal cc^{-1}]$^{1/2}$ and 7.4[cal cc^{-1}]$^{1/2}$ respectively [17]] suggested that PS-PDMS copolymers would be useful for stabilizing particles in a range of aliphatic hydrocarbon media. The soluble PDMS block would provide the stabilizing layer, and would be anchored to the particle by the insoluble PS anchor block.

A range of PS-PDMS block copolymers of differing composition and molecular weight has been synthesised, and their use as stabilizers in dispersion polymerization was studied. In order to prepare model systems, a knowledge of the characteristics of dispersion polymerizations involving adsorbed block copolymer stabilizers is desirable. A study of such dispersion polymerizations was, therefore, made.

Radical polymerization has been used to prepare dispersions of PS and polymethylmethacrylate [PMMA] particles in aliphatic hydrocarbon media. The preparation of a dispersion of PS, stabilized by a PS-PDMS block copolymer, has been described in the patent literature [18]. PMMA particles stabilized with an adsorbed PS-PDMS block copolymer represents a novel system, although Saam has reported the preparation of such particles stabilized with a grafted PDMS layer [19]. The use of anionic dispersion polymerization was also investigated for preparing dispersions of PS. The effects of varying polymerization conditions were extensively studied. The behaviour of the block copolymer stabilizers in a selective solvent was considered, and a series of micellar dispersions was prepared.

Three methods of measuring the particle size of the

dispersions were compared. The stability of the dispersed particles in a medium which is a θ-solvent for PDMS was studied. Rheological measurements gave an indication of the state of the dispersions, and were used to provide an estimate of the Hydrodynamic thickness of the PDMS layer. This study was combined with surface coverage information to suggest the configuration of the PDMS chains.

CHAPTER 2

THEORY

2.1 THE THEORY OF STERIC STABILIZATION

2.1.1 FORCES OF ATTRACTION

Non-aqueous polymer dispersions are prepared by poly-
merizing monomer dissolved in a suitable dispersion medium,
to give a polymer which·is insoluble in the medium and which,
therefore,precipitates out. This precipitated polymer is in
the form of a sub-micron dispersion, and the particle
collision frequency is such that the number of free particles
is quickly reduced to zero. This behaviour, which is known
as flocculation, is due to the mutual attraction of particles
arising from London dispersion forces. In order to appre-
ciate the mechanism of stabilizing such a system against
flocculation, it is useful to consider firstly the origin
and magnitude of the attractive forces between particles.

Interactions between the atoms and molecules of two
adjacent particles give rise to an attractive force between
the particles. The origin of such forces was described by
London [20], who showed that the interaction between the two
atoms of an inert gas was a quantum mechanical effect.
Applying the Heisenberg uncertainty principle, he showed that
the fluctuation in the electrical field of an atom or a mole-
cule gave rise to a transient dipole in another atom or
molecule. Since the total energy involved was less than
one quantum, no actual dissipation of energy occurred. The
random fluctuations of the electrical fields of the two

molecules become coupled and oscillate together, thus reducing the total free energy of the system. Hence, there is an attraction between molecules and they approach each other. Since random fluctuations of the electrical fields are involved, one molecule is able to participate in London oscillations with several other molecules at the same time. This effect is seen in a gas where one gas molecule attracts all its neighbouring molecules simultaneously. This quantum mechanical effect is essentially additive, based on "pair-wise" interactions, and·it can be shown that the attractive potential energy (V_A) decreases with the distance of separation (r) as described by

$$V_A = -L/r^6 \qquad\qquad (2.1)$$

where L is the London interaction constant.

The above concepts, based upon gaseous systems, were applied to condensed bodies in a vacuum by Hamaker [21]. Hamaker considered all the possible interactions between the attracting elements of two particles, and showed that the sum of all these "pair-wise" interactions could be replaced by a double integral. An integration of all these inter-actions results in an expression of the form:

$$V_A = A.H \qquad\qquad (2.2)$$

A is the Hamaker constant, which is a function of the strength of attraction between two elements, and is proportional to L and the square of their concentration. H is a geometrical function which for equal-sized spheres, where the distance between their surfaces (h) is much less than their radius (a), approximates to

$$H = a/12h \qquad (2.3)$$

The Hamaker integration predicts that attraction may occur over distances of several tens of nanometers between particles. These attractive forces are, however, significantly reduced owing to the retardation effect, as observed by Overbeek [22]. The distance between fluctuating dipoles is greater than the wavelength of the fluctuation frequency. Therefore, dipole oscillations can be out of phase, causing a subsequent reduction in the total attractive energy.

The Hamaker approach was derived from a model of condensed bodies within a vacuum and further modifications are required if the approach is to be applied to real colloidal dispersions. The dispersion medium modifies the attractive forces in two ways; a primary medium effect, which describes the influence of the liquid medium on the transmission of London forces, and a secondary medium effect which involves the finite attraction of the particles for the medium. The primary medium effect is a function of the dielectric constant of the medium and ultimately reduces the attractive forces, also causing retardation effects at much closer distances of separation. The secondary medium effect leads to the derivation of an "effective" Hamaker constant, A_{12} where

$$A_{12} = [A_1^{1/2} - A_2^{1/2}]^2 \qquad (2.4)$$

where subscript 1 refers to the particle and subscript 2 to the medium. As will be described in Section [2.1.2] the colloidal dispersions under consideration at present are composed of polymer particles surrounded by a surface layer

of adsorbed polymer of different Hamaker constant. It has been shown [23] that such particles behave as compound particles,with an overall Hamaker constant closer to that of the dispersion medium than that of the bare particle. The forces of attraction are,therefore,reduced although this reduction is negligible compared to the steric stabilization forces generated by adsorbed layers.

It should be noted that the Hamaker approach is based upon interactions of microscopic elements and is therefore subject to errors when applied to macroscopic particle systems. In such systems the attractive forces between elements just below the particle surface will be modified by the particle material.

An alternative approach suggested by Lifshitz [24] considers bodies as ideal continua with the same dielectric properties throughout. Modifications due to retardation and medium effects are,therefore,unnecessary since they are already incorporated. The approach requires very complex mathematical treatment however, and, therefore, the Hamaker approach still finds widespread use, despite its fundamental defects. The attractive forces calculated using the macroscopic continuum model are often in reasonable agreement with those calculated by the microscopic Hamaker approach, although the agreement may well be due to compensating errors.

Both quantitative predictions from theory and experimental results for polymer particles in organic media, suggest that the attractive forces in many cases are less than kT [where k is the Boltzmann constant and T is absolute temperature] even at separations of 5-10 nm. Refinements in both theoretical calculations and experimental conditions

are still required,however,for an exact interpretation of attractive forces.

2.1.2 STABILIZATION OF COLLOIDAL DISPERSIONS AGAINST FLOCCULATION

In the absence of some mechanism of stabilization, a dispersion of colloidal particles would flocculate almost immediately as particles are mutually attracted by the forces described above. Studies of the stabilization of colloidal dispersions against flocculation have been largely confined to aqueous systems, both in theoretical and experimental considerations, and the nature of stabilization is well understood. In an ionizing aqueous medium the predominant mechanism is that of electrostatic charge stabilization, and quantitative theories have been developed based on the Derjaguin-Landau-Verwey-Overbeek [D.L.V.O.] theory [22,25].

For colloidal dispersions in non-aqueous media, the dispersion medium is generally non-ionizing and a different mechanism of stabilization must be sought. Stabilization is achieved by surrounding the particles with a surface layer of soluble polymer and such a mechanism is known as steric stabilization. The concept of steric stabilization is less well understood than that of electrostatic stabilization, and the origin and magnitude of the repulsive forces is still under discussion. Vincent [13] has reviewed theories of electrostatic charge stabilization and compares them with some of those derived for steric stabilization.

Consider two spherical particles surrounded by surface layers of soluble polymer chains as in figure [2.1].

FIGURE 2.1

STERICALLY STABILIZED PARTICLES
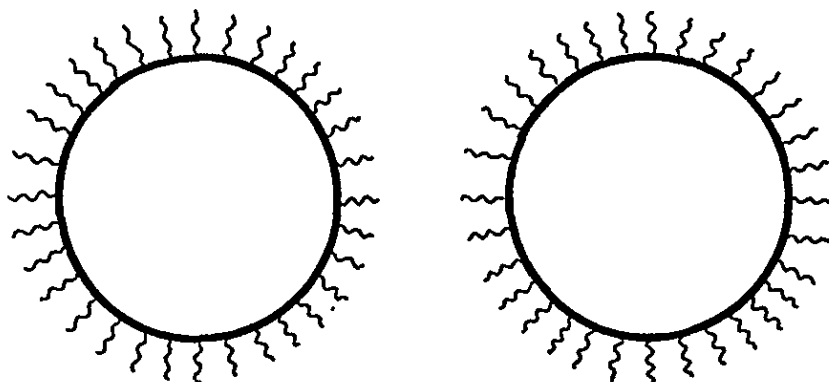
When particles approach one another a repulsive force is generated by the interaction of the soluble stabilizing chains. Repulsive forces between particles may be described by two models, the equilibrium adserption model and the constant adsorption model. The repulsive forces in the former arise from the work done in desorbing stabilizer chains as the particles approach. This model is only applicable to weakly adsorbed chains and,therefore,finds little consideration in the adsorption of polymeric stabilizers.

A polymeric stabilizer chain may be attached to the particle surface at one or more points and may adopt the so-called loop, train and tail configurations as seen in figure (2.2).

FIGURE 2.2

CONFIGURATIONS OF ADSORBED POLYMERS

tail   train   loop
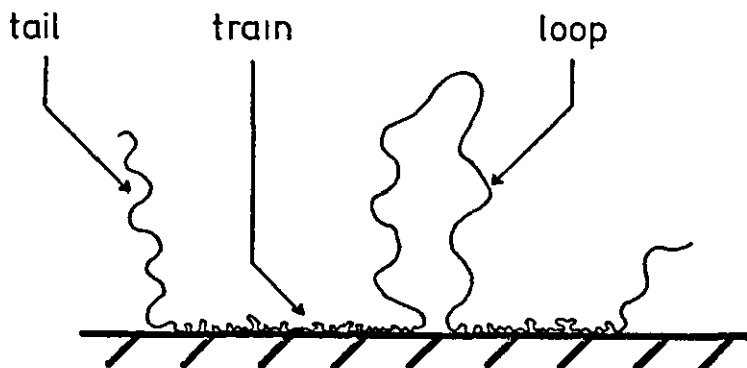
In the constant adsorption model the fraction of polymer

segments adsorbed at the interface [i.e. for homopolymers

the fraction in trains] remains constant. The loops and

tails extend into solution and may redistribute themselves

as two particles approach one another, although there is no

desorption of trains. It is this redistribution of polymer

segments in solution which gives rise to the repulsive forces

maintaining stability. Two limiting cases of particle inter-

action have been described and each will be considered

individually,

Interpenetration or "mixing" model

Figure [2.3] illustrates the situation where two

particles are brought together and the impinging soluble

layers overlap with no compression of chains. Such a model

might be approached for particles surrounded by high molecular

polymer since the segment density at the periphery is low and

interpenetration may occur without chain interaction at low

FIGURE 2.3

INTERACTION OF STERICALLY STABILIZED PARTICLES - THE MIXING MODEL
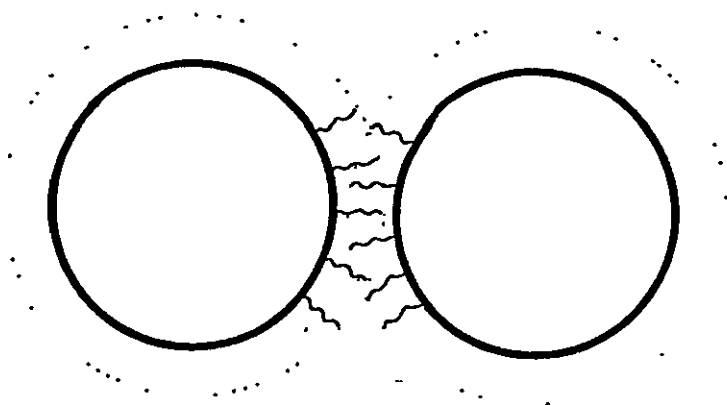
overlap. A similar situation would exist for conditions of low surface coverage but in the present models maximum coverage is assumed.

Fischer [11] initially considered this model and assumed that the segment density in the adsorbed layer was uniform. The concentration of polymer chains in the region of overlap was then equal to the sum of the concentrations in each layer. Using the Flory-Krigbaum [26] theory of dilute polymer solutions, Fischer derived the change in free energy (ΔG_M) obtained by doubling the concentration of polymer within the lens-shaped region of overlap. Applying the Flory-Krigbaum theory to a small volume (δV) of the region of overlap gives an expression for the free energy of mixing $\delta(\Delta G_M)$ of segments and solvent molecules:

$$\delta(\Delta G_M) = kT \ [\delta n_1 \ \ln \phi_1 + \chi \ \delta n_1 \phi_2] \qquad (2.5)$$

where δn_1 is the number of solvent molecules contained in δV,
ϕ_1 and ϕ_2 are the volume fractions of solvent and polymer respectively,

χ is the Flory-Huggins interaction parameter.
The change in the free energy of mixing for the total inter-
action volume (V) is,therefore,given by summing over the
changes in all the volume elements comprising V.

The total repulsive force is,therefore,a function of the
degree of overlap of the souble layers.   Fischer obtained
an expression for spherical particles for ΔG_M of the form:

$$\Delta G_M = A'.B \qquad\qquad (2.6)$$

B is the second virial coefficient and

$$A' = 4/3.\pi k T C^2 [\,\delta - \tfrac{h}{2}]^2 (3a + 2\delta + \tfrac{h}{2}) \qquad (2.7)$$

where C is the concentration of segments in the adsorbed layer

a is the radius of the particle

h is the surface to surface separation

δ is the adsorbed layer thickness

k and T are as defined above.

The term A' is a geometric term and term B is a thermodynamic
term (the second virial coefficient) which may be expressed
as

$$B \equiv \frac{\psi_1 - K_1}{v_1} \equiv \frac{(1 - \theta/T)\,\psi_1}{v_1} \equiv \frac{\frac{1}{2} - \chi}{v_1} \qquad (2.8)$$

where ψ_1 is the entropy parameter

K_1 is the enthalpy parameter

v_1 is the partial molar volume of the solvent

θ is the theta-temperature

χ is the polymer-solvent interaction parameter.

Similar expressions have been derived by Ottewill and
Walker [27] and Napper [14,28].   The major defect of this
model is the assumption that the polymer segment density is

constant throughout the layer. This leads to an overestimation of repulsive forces generated under conditions of low overlap. Hesselink [29] has calculated the theoretical segment density distribution for flat plates,as will be discussed later. He was then able to improve Fischer's expression for the total free energy of mixing, although,as will be discussed Hesselink's model was derived from unrealistic volumeless chains.

Fischer's approach also assumes no redistribution of polymer segments (loops and tails) within the region of over-lap, and therefore becomes meaningless beyond "half overlap" i.e. when h < δ . A model which allows for redistribution has been suggested by Doroszkowski and Lambourne [15] who consider redistribution over a torroidal volume of interaction.

Compression or "Volume Restriction" Model

FIGURE 2.4

INTERACTION OF STERICALLY STABILIZED PARTICLES
- COMPRESSION OR VOLUME RESTRICTION MODEL
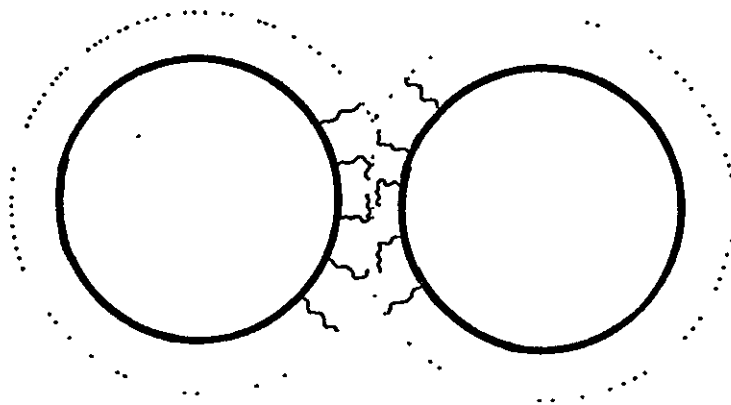
In this second model, repulsive forces are derived from a mixing term plus an entropic "volume restriction" term. Figure (2.4) illustrates the basis of the model in which

impinging layers of soluble polymer are compressed when particles are brought together, with no interpenetration. Such a model might perhaps be approximated to in the close approach of particles surrounded by low molecular weight or branched polymer layers, in which the layers are composed of a relatively high concentration of polymer chains.

This approach was first suggested by Mackor [30] who considered a model of a rigid rod terminally adsorbed and freely jointed at a flat surface, as shown in figure [2.5].

FIGURE 2.5

MODEL FOR VOLUME RESTRICTION TERM AFTER MACKOR
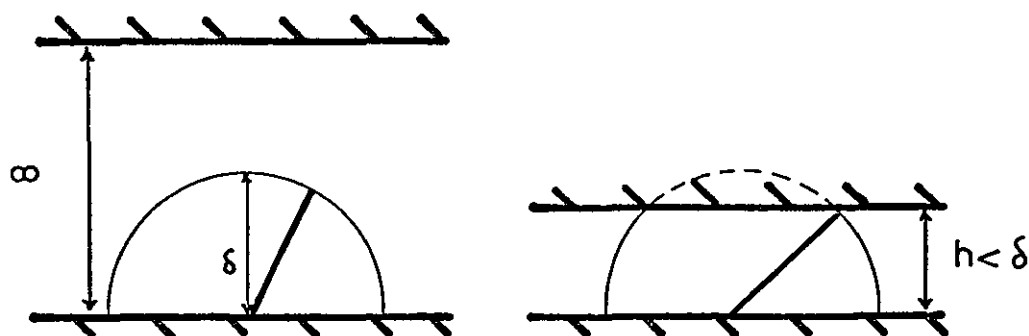
The repulsive force (ΔG_{VR}) generated upon the approach of a second flat plate was calculated from the loss of configurational entropy [S] calculated from the Boltzmann relationship:

$$S = k \ln \Omega \qquad [2.9]$$

where Ω is proportional to the area swept out by the free end of the rod. Assuming all possible orientations of the rod at the surface had an equal probability of occurrence, he

derived an expression

$$\Delta G_V = kTN[1 - h/b] \qquad (2.10)$$

where N is the number of chains per unit area and

b is the length of the rod; $b = \delta$ in this case.

Mackor considered the rods to be volumeless, hence there is no interaction between the rods covering a second approaching surface, and no interaction between neighbouring rods on the same surface. This model can,therefore,only be taken as a crude basis for consideration of real,flexible polymer chains.

Meier [12] modified Mackor's approach by considering the interaction of multisegment chains terminally adsorbed on a plane surface, as a function of the distance from a second plane surface. He derived firstly an expression for the free energy change due to the reduction of available configurations of a random flight chain. This "volume restriction" term has subsequently been calculated analytically by Dolan and Edwards [31]. Again using the Flory theory of dilute polymer solutions [32], Meier calculated the free energy of mixing of the polymer molecules and summed the two terms to give the total energy of interaction. Hesselink [29] has subsequently shown Meier's calculation of the segment density distribution to be incorrect. Hesselink, Vrij and Overbeek [33] further extended Meier's approach using a six-choice cubic lattice upon which was generated a chain. This chain was attached at one end to a flat impenetrable surface, and was generated with no restriction in bond angle or occupation of a parti- cular site. A second chain was generated, this time in the presence of a second flat impenetrable barrier at a set

distance from the primary surface. The reduction in the number of possible configurations between the second and first situations leads to an evaluation of the repulsive energy generated at the given distance of separation. Again the total interaction was described by the sum of a "volume restriction" and a "mixing" term.

Fundamental defects in the above analysis arise from the consideration of unrealistic volumeless chains which experience no interaction with adjacent chains on the same surface or with chains adsorbed onto an approaching surface. The evaluation of the total interaction as the sum of a "mixing" term and a "volume restriction" term has also been criticised by Osmond, Vincent and Waite [34] who suggest that the basic models used to calculate the two terms are so different that simply adding them would hardly give the correct result. They point out that the model must over-estimate the repulsive forces, due to significant double counting of repulsions. This arises since no consideration is given to the fact that the calculated "mixing" term, based on Flory-Krigbaum theories, already contains a configurational term of sorts, to which a second configurational term [the "volume restriction" term] is added.

A similar analysis to that of Hesselink has been performed by Clayfield and Lumb [35,36]. These workers used computer techniques to generate chains on a four-choice cubic lattice with the restriction that the bond angle was fixed at 90° and segments were not allowed to enter previously occupied sites [i.e. the chains possess real volume]. This model predicts a lower energy of repulsion than Hesselink's model since although the loss of configurations in the

restricted chain is a large proportion of the total number of configurations, the total number of configurations lost is less than that in Hesselink's model. Clayfield and Lumb's approach, however, neglects polymer-segment/solvent interactions, and so must only be considered as approaching a real situation under athermal mixing conditions. Other defects in the model stem from consideration of a 90° bond angle, and an absence of an adsorbed layer on the second approaching plane surface.

2.1.3 IMPLICATIONS OF STERIC STABILIZATION THEORIES

Total interaction

The total interaction ΔG_T between two polymer-covered particles is given by

$$\Delta G_T = V_A + V_R + \Delta G_S \tag{2.11}$$

where V_A is the attractive potential energy

V_R is the repulsive potential energy (small for uncharged polymer particles)

ΔG_S is the total steric interaction.

Summarizing the theories outlined above, Meier and Hesselink suggest that ΔG_S consists of the sum of ΔG_{VR} and ΔG_M, whereas Napper claims that ΔG_M describes completely the total interaction.

All the models described above contain assumptions which are not valid for real systems, although it is possible that certain models become more valid under some conditions.

The magnitude and range of total interaction

The authors of the above theories are in agreement that in a thermodynamically "good" solvent, the "mixing term" will

be the dominant repulsive term, at least for conditions of low overlap. This can be derived from a consideration of the geometry involved and the fact that most of the possible configurations are lost as a result of interactions between polymer chains before the stage of half-overlap is reached. The variation of net potential energy with interparticle distance, for sterically stabilized spheres in a "good" solvent for the stabilizing layer, is shown in figure [2.6.b]. The potential energy of repulsion exceeds that of attraction by an ever-increasing amount as particles approach one another. The net repulsive energy is, therefore, always positive and increases rapidly with decreasing particle separation. The attractive forces between uncharged polymer particles are relatively small and, as pointed out by Evans and Napper [37], may be conveniently neglected in a consideration of the total repulsive energy.

The net potential energy curve for an electrostatically stabilized system is shown in figure [2.6.a] for comparison. Unlike such electrostatically stabilized systems, a steric barrier is of a finite dimension, so that the very large repulsive energy generated by the soluble polymer falls to zero beyond the effective range of the interacting soluble chains. It is conceivable that for certain combinations of layer thickness and particle size, a significant attractive trough might exist in this region [figure [2.6.b]] giving rise to a secondary minimum similar to that seen in electrostatically stabilized systems. Such systems would then show the type of behaviour corresponding to the weak flocculation at the secondary minimum observed for aqueous charge -stabilized systems. Such an effect has not, however, been

FIGURE 2.6

FORM OF NET POTENTIAL ENERGY [V] CURVES AS A FUNCTION OF PARTICLE SURFACE SEPARATION [h]

(a) Charge stabilization

(b) Steric stabilization
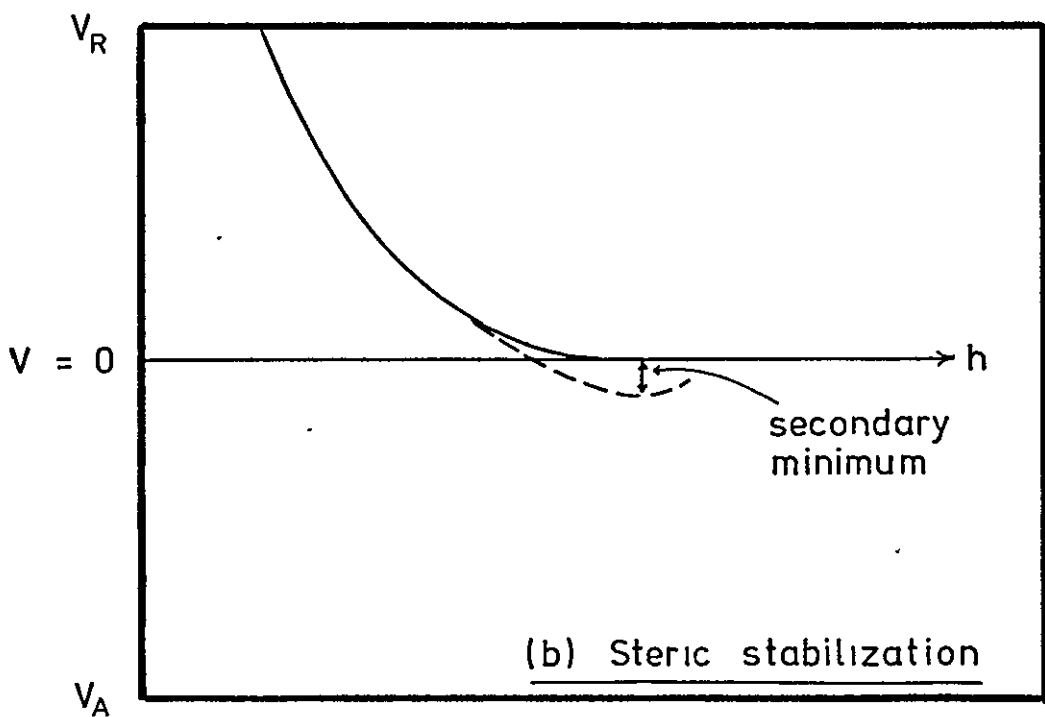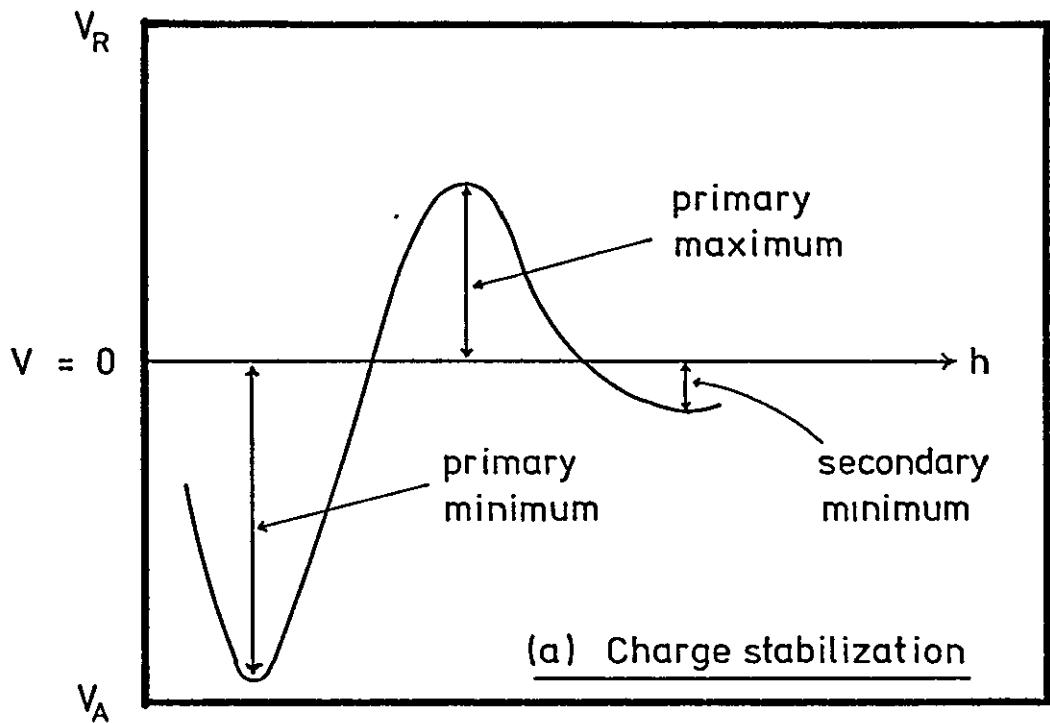
shown to occur in the non-aqueous systems reported to date.

The idea that repulsive forces are generated only when the soluble layers interact is fundamental to the concept of steric stabilization and both the predictions of theoretical models (33, 35,38) and experimental measurements (39, 40) are in agreement.

Stability of sterically stabilized systems under theta — conditions

From equation (2.8) describing the "mixing term" it is seen that ΔG_M is a function of (½ - χ). Therefore,if the solvency of the dispersion medium is reduced to θ-conditions for the stabilizing chains, χ becomes 0.5 and ΔG_M becomes zero. In the absence of a repulsive force, particles would be expected to flocculate, and,therefore,if there were any contribution from a volume restriction term, ΔG_{VR}, this would be apparent at θ-conditions.

Napper (14 .28) has studied the behaviour of several sterically stabilized systems under theta-conditions, and has indeed found that the systems become unstable at close to theta conditions. Napper in fact finds that flocculation is observable at slightly better than theta-conditions, which he accounts for in terms of V_A [14]. He therefore concludes that the total interaction can be completely described by the "mixing term". If this is so, for small degrees of over-lap it may be concluded that interprenetration rather than compression occurs.

As mentioned above, if the total interaction is descri-bed by the sum of the "mixing term" plus a volume restriction term, a repulsive force should still be observed under

θ-conditions, since ΔG_{VR} is still operative. Ooroszkowski and Lambourne [39] do indeed claim to have detected a small repulsive force under θ-conditions, during the compression of a monolayer of sterically stabilized particles on a surface balance. It should be noted that the particles used in these studies did appear flocculated during compression, and it has been suggested that the measured repulsive force is an experimental artefact due to the time period of the compression cycles [38].

Osmond, Vincent and Waite [34] suggest the apparent differences in behaviour are a result of Napper's determination of the θ-conditions. Napper used a modified Elias [41] method for determing the θ-temperature, which involves extrapolation of a plot of the reciprocal temperature of phase separation against polymer concentration to pure polymer [42]. It is more usual to derive θ-conditions at infinite dilution by extrapolation to zero concentration [43]. Other areas from which errors could arise include Napper's use of stabilizing chains of a relatively broad molecular weight distribution, and the experimental difficulties concerning the detection of incipient flocculation in dispersions. It should also be noted that θ-conditions determined for a free molecule in solution do not necessarily represent the θ-conditions for the same molecule when it is terminally adsorbed at an interface.

2.2 THE DESIGN AND SYNTHESIS OF STABILIZERS

2.2.1 THE ROLE OF THE STABILIZER

Steric stabilization is achieved by surrounding particles with a layer of soluble polymer as described above. One of

the main requirements for a suitable stabilizer for a disper-
sion of polymer particles is that the soluble polymer is
firmly anchored to the particle which it is stabilizing.
The stabilizing polymer should ideally be not easily desorbed
or laterally displaced when particles approach each other
closely. This requirement excludes the use of soluble homo-
polymers and random copolymers for use as stabilizers of
polymer particles. Such homopolymers are only weakly
adsorbed on the low energy polymer surfaces, although they
have been used to stabilize dispersions of inorganic materials
[44]. The soluble component of a random copolymer is normally
unable to form loops large enough to provide a stabilizing
barrier. The soluble polymer may be chemically attached to
the particle by the incorporation of suitable functional
groups, which are reacted with complementary functional groups
(e.g. acid-base interactions) on the particle surface.

The most widely reported stabilizers used for non-aqueous
polymer dispersions are those based upon block and graft
copolymers. Such copolymers are chosen to comprise one com-
ponent which is soluble, and one component which is insoluble,
in the dispersion medium. The stabilizing copolymer is
firmly attached to the polymer particle by its insoluble
component or anchor (designated "A"), which is physically
adsorbed onto the particle surface owing to its insolubility
in the dispersion medium. The anchor component may be
chemically reacted with the dispersed polymer after adsorp-
tion, if desired. The soluble stabilizing component of the
copolymer (designated "B") is chosen to have little or no
affinity for the particle surface and,therefore,extends into
the dispersion medium to provide a stabilizing barrier.

Figure (2.7.a) shows block and graft copolymers adsorbed in this way. It is possible to combine suitable A and B components into many forms of block and graft copolymers. Figure (2.7.b) shows a few of these combinations which might be suitable for use as steric stabilizers. The present study concerns systems stabilized by simple AB block copolymers of the type (ii) in figure (2.7.b).

2.2.2 THE BEHAVIOUR OF STABILIZERS IN SOLUTION

Block and graft copolymers consisting of essentially incompatible components as described above, are known to form aggregates in both solution and under bulk conditions [45, 46 ,47]. The formation of these aggregates is somewhat analogous to the micellar structures observed in aqueous soap solutions, and this micellar behaviour of block and graft copolymers in solution has recently been reviewed [48].

The aggregates, or micelles formed, can adopt a variety of configurations depending upon the concentration, size and composition of the polymer, the solvent environment and the temperature. At very low concentrations, copolymer molecules exist in an unassociated manner as in a conventional homopolymer solution. At concentrations of a few percent, copolymer molecules aggregate to give a micelle in which the core is composed of the least soluble component of the copolymer (figure (2.8)).

At higher concentrations [> 20%) these aggregates coalesce into regular and periodic structures of three main types: spheres, rods or cylinders, and lamellae [49].

Dispersion polymerization usually involves block or graft copolymer stabilizers at a few percent concentration

FIGURE 2.7
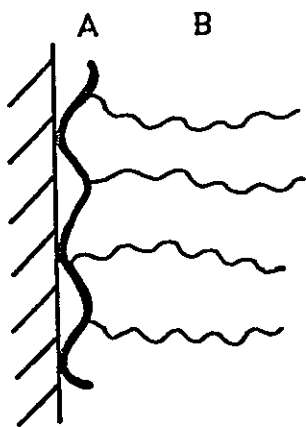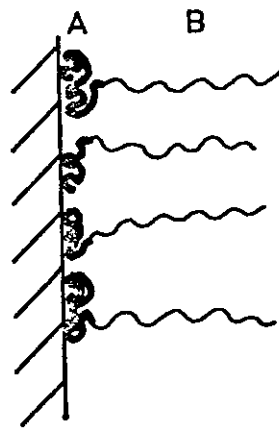
Graft copolymer   Block copolymer

(a)   Block and Graft copolymers used
       as stabilizers

(i)   (ii)   (iii)
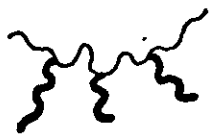
(iv)   (v)   (vi)

(b)   Suitable combinations of A and B
       for use as stabilizers

FIGURE 2.8

BLOCK COPOLYMER MICELLES

[a]

Unassociated
block copolymer
molecules

[b]

Block copolymer
micelles
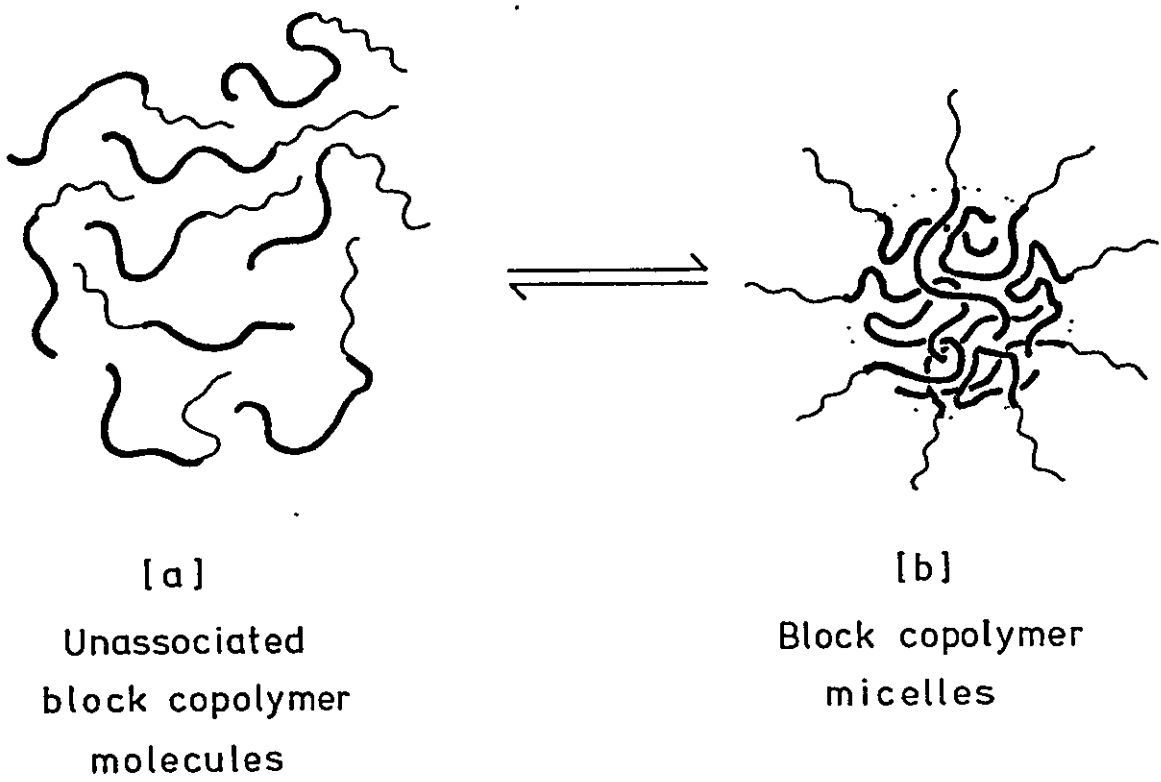
level, and the dispersion medium is a selective solvent for the stabilizing B component. The size of the micelle formed depends largely upon the ratio of the A and B components, and the concept of an anchor/soluble balance [ASB] analogous to the hydrophile/lipophile balance [HLB] system for emulsifiers, was introduced. At ASB values close to unity, block and graft copolymers at concentrations of a few percent aggregate to form micelles in equilibrium with free copolymer molecules, as shown in figure [2.8]. The existence of "monomolecular-micelles" in very dilute solution has been proposed [45]. Such monomolecular micelles comprise a collapsed core of the insoluble component, surrounded by a layer of the soluble component, and it is suggested that as the concentration is increased, these would aggregate to form multimolecular micelles.

At higher ASB values, the equilibrium in figure [2.8] is displaced towards the aggregated structure, and in the limit the copolymer may be irreversibly associated in micelles. At very high ASB values, it becomes impossible to surround the insoluble component with a layer of the soluble component, and the polymer forms a flocculated mass rather than spherical micelles.

The size of micelle formed is predicted to increase as the cube root of the degree of polymerization of the copolymer [50]. It also follows that the size will increase as the interfacial contact·energy per unit area between the core and the solvated outer layer becomes larger. This implies that larger micelles will be formed as the incompatibility of A and B increases. Once formed, such a micelle is prevented from combining with other micelles by steric stabilization

forces, as described above.

It is possible to calculate the number of copolymer molecules required to form a continuous layer of soluble polymer around an insoluble core [10]. Values must be taken for the area of a particle that could be stabilized by one copolymer molecule, and the molecular weight of the copolymer must be known. The so-called micellization number "n" is given by

$$n = \frac{36\,\pi}{(0.6023)^2} \left[\frac{M_A}{\varrho}\right]^2 \frac{1}{c^3\,x^3} \qquad (2.12)$$

where M_A is the molecular weight of the insoluble chains,

C is the surface area $(\overset{\circ}{A}{}^2)$ stabilized by one soluble chain,

x is the number of soluble chains attached to each insoluble chain,

ϱ is the density of the particle core (assumed),

n is the number of copolymer molecules per micelle

and the micelle core radius r is given by

$$r = \left[\frac{3nM_A}{4\pi\varrho \times 0.6023}\right]^{\frac{1}{3}} \qquad (2.13)$$

The ability of such block and graft copolymers to "solubilize" homopolymers has also relevance for studies of dispersion polymerization. Solubilization is of course the mechanism proposed to explain the behaviour of soaps [51]. Hydrocarbons show apparently increased "solubility" in soap solution, since they dissolve in the hydrocarbon-like interior of a soap micelle. In an analogous fashion, homopolymer can be "solubilized" by dissolving in the like-component of a block copolymer [52,53,54]. The quantity of homopolymer that can be solubilized is highly dependent

on the ratio M_H/M_A of the molecular weight of the homopolymer M_H to that of the similar block M_A in the block copolymer. If appreciable quantities (say, equal volumes) are to be solubilized M_H/M_A must be less than unity. The amount decreases rapidly with increasing values of the ratio above unity.

2.2.3 SYNTHESIS OF THE STABILIZER

The advent of anionic polymerization and subsequent improvements in experimental technique has provided a way of producing well-defined block copolymers consisting of blocks with predictable and narrowly distributed molecular weights. The first reported synthesis of such copolymers was due to Szwarc and co-workers [55]. These workers showed that it was possible to initiate the polymerization of styrene using a sodium-naphthalene complex formed in the presence of tetrahydrofuran (THF) under perfectly moisture-free conditions. The red solution of polystyrene still contained active polymer chains and even when all the monomer had been consumed, polymerization could be continued by simply adding further monomer. Thus, the term "living polymers" was coined. If the monomer used in the second addition differs from that polymerized first and if the anion of the first monomer is capable of initiating polymerization in the second monomer, a block copolymer is formed.

Such an anionic polymerization proceeds with very little chain transfer and is devoid of a spontaneous termination step. These systems are,however,extremely susceptible to termination by any impurities able to donate protons such as water and alcohols. If the rate of initiation is fast

compared to the rate of propagation, all polymer chains
will be initiated before any propagation can occur, and all
chains will then propagate simultaneously. This leads to a
polymer of very narrow molecular weight distribution which,
as predicted by Flory [56], is in fact a Poisson distribution.
Each molecule of a monofunctional initiator is capable of
initiating one polymer chain, and,therefore,any desired
molecular weight polymer may be generated by varying the
ratio of monomer to initiator. A monofunctional initiator
will,therefore,generate.polymer chains with number average
molecular weight $(\bar{M}_n)$ given by

$$\bar{M}_n = \frac{\text{grammes of monomer}}{\text{moles of initiator}} \qquad [2.14]$$

In practice the problem of eliminating impurities sets
the upper limit for $\bar{M}_n$. It should,however,be noted that
polystyrene of molecular weight 43.7×10^6 has been prepared
anionically [57], which represents the highest molecular
weight synthetic polymer synthesized to date.

Initiators commonly used for anionic polymerization
include alkali metals, their alkyls and hydrides. Anionic
systems and the applicability of various initiators have
been extensively reviewed [58, 59, 60].

The block.copolymers considered in this research are
A-B block copolymers of polystyrene [PS] and polydimethyl-
siloxane [PDMS]. The synthesis of such polymers has been
described in the literature [61-65]. The method of Davies
and Jones [62] was followed, with the requisite conditions
of high purity being met by high vacuum and inert gas
blanket techniques.

Styrene was polymerized in toluene solution using n-butyl

lithium as initiator:

$$n\text{-BuLi} + m\text{CH}_2\text{=CH} \longrightarrow \text{Bu}(\text{CH}_2\text{-CH})_{m-1}\text{CH}_2\overset{-}{\text{CH}} \text{Li}^+$$
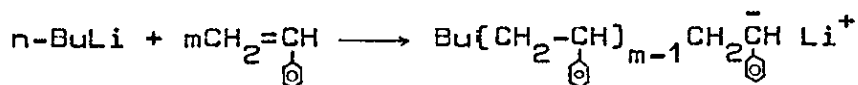
The propagation rate for this reaction in toluene is slower than the initiation rate, and therefore toluene provides a suitable solvent in which to prepare near monodisperse product. Polystyryllithium has been shown to be associated in pairs in hydrocarbon media, thus slowing down the rate of propagation [66]. The addition of trace amounts of THF breaks down these dimers by forming a monoetherate of the ion-pair which is highly reactive, and augments the propagation without changing the kinetic order with respect to the initiator. n-Butyl lithium is also known to be highly associated in hydrocarbon media and it has been shown that the predominant form is the hexamer [67]. Worsfold and Bywater [68,69] suggest that this associated species is unreactive towards the monomer and that only free (unassociated) n-butyl lithium is able to initiate polymerization, which leads to the equilibrium:
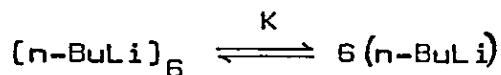
$$(n\text{-BuLi})_6 \overset{K}{\rightleftharpoons} 6\,(n\text{-BuLi})$$

$$K = \frac{[n\text{-BuLi}]^6}{[(n\text{-BuLi})_6]} \tag{2.15}$$

These workers indeed found the 1/6th rate order to hold for the initiation of styrene, but have shown in subsequent work [69] reaction orders ranging from 1/6 to nearly first order are possible. It has been suggested [70] that the amount of unassociated organolithium present would not be enough to account for the observed reaction rates, and so a reaction has been proposed between the monomer and the

associated species.

AB block copolymers of PS-PDMS were obtained by reacting polystyryllithium with hexamethylcyclotrisiloxane (D_3) to give a lithium dimethylsilanolate anion at the end of each polymer chain. In the presence of an ether promotor, polymerization of further D_3 occurs, as shown below:

$$Bu-\!\!-\!\!(CH_2\underset{\underset{\textcircled{0}}{|}}{CH})_{m-1} CH_2\overset{-}{\underset{\underset{\textcircled{0}}{|}}{CH}} Li^+$$

$$\Big\downarrow \quad P/3 \ \left((CH_3)_2SiO\right)_3$$

$$Bu-\!\!-\!\!(CH_2-\underset{\underset{\textcircled{0}}{|}}{CH})_{m} (SiMe_2O)_{p-1} SiMe_2O^- Li^+$$

$$\Big\downarrow \quad \text{termination with } Me_3SiCl$$

$$Bu-\!\!-\!\!(CH_2\underset{\underset{\textcircled{0}}{|}}{CH})_m (SiMe_2O)_p SiMe_3$$
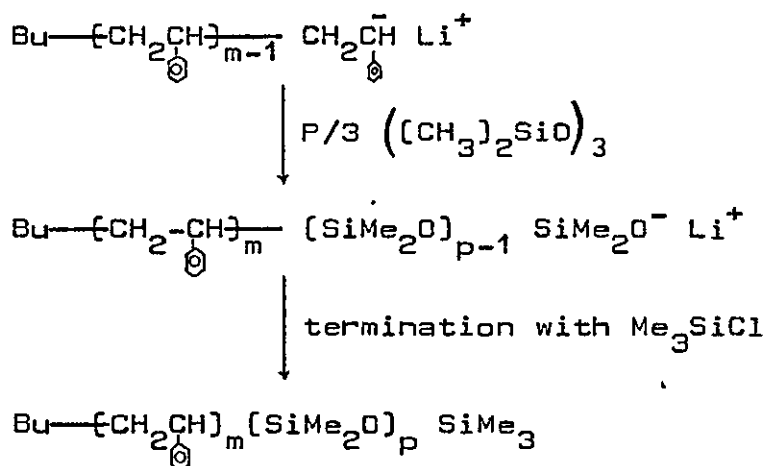
The "living" polystyryllithium solution turns from orange to colourless as the D_3 polymerizes and the reaction is terminated by adding trimethylchlorosilane or methanol.

The reaction order for the above has been shown to be of the order 0.25-0.35 with respect to initiator [64] suggesting as before association of silanolate anions. Tert.-butoxylithium, which has a similar chemical nature to lithium silanolates, is known to be highly associated in hydrocarbon solvents [~ six-fold association] and even in ether solvents [~ four-fold association] [71].

The cyclic trimer D_3 was chosen as monomer for the PDMS block in preference to the eight-membered octamethylcyclo-tetrasiloxane (D_4), since the higher strain energy leads to a faster rate of reaction with minimal formation of cyclics and homoPDMS [72,73]. The reactivity of the silanolate anion is much less than that of the polystyryl anion;

therefore, a block copolymer cannot be prepared by adding styrene to a "living" PDMS system [73].

2.3 DISPERSION POLYMERIZATION

2.3.1 A COMPARISON OF HETEROGENEOUS POLYMERIZATION TECHNIQUES

Several heterogeneous polymerization techniques have been developed, and a brief comparison will serve to emphasise the essential characteristics of dispersion polymerization. The various techniques can be divided into two types, those which are heterogeneous throughout the polymerization, and those which are initially homogeneous until polymer precipitates and the reaction continues in a heterogeneous manner.

Emulsion polymerization is perhaps the most commonly used heterogeneous polymerization technique, and the subject has been reported extensively in the literature [1]. This technique is of the first type described above and is characterized by a low monomer solubility in the reaction medium, which is water; an initiator which is soluble in the reaction medium; ionic or non-ionic surfactants; a high rate of polymerization and a product of high molecular weight owing to radical isolation within the particles; and particles typically 0.1-0.3 μm diameter. A somewhat similar technique is that of suspension polymerization, which differs from emulsion polymerization since the initiator is soluble in the monomer, which itself is only sparingly soluble in the dispersion medium (again water). Lower levels of surfactant are required and polymerization occurs within the suspended monomer droplets in a "micro-bulk" fashion [74]. The particles produced by a suspension polymerization are coarser than those from emulsion polymerization, typically

greater than 5 μm. With certain monomers, an enhanced polymerization rate and high molecular weight polymer are obtained as a result of the "gel-effect" which will be discussed more fully below.

Precipitation polymerization [75] is of the second type described above and may be carried out in both aqueous and organic media. The initially soluble monomer is converted into an insoluble polymer which precipitates in the form of a coarse agglomerate or slurry. An increased rate of poly-merization [auto-acceleration] is observed as a result of radical-trapping within the highly viscous precipitated polymer.

An aqueous-type of dispersion polymerization has been reported [76] in which aqueous suspensions of polymer, particularly poly[vinyl acetate], are prepared and stabilized from flocculation by a relatively high concentration of water-soluble polymer such as poly[vinyl alcohol]. The particles produced are somewhat larger than those prepared by conventional emulsion polymerization and tend to settle out on further dilution of the aqueous phase. Having noted this exceptional case, the term dispersion polymerization will now be taken as describing dispersion polymerization in non-aqueous media, which will now be discussed.

2.3.2   CHARACTERISTICS OF NON-AQUEOUS DISPERSION POLYMERIZATION

Dispersion polymerization may be regarded as a special case of precipitation polymerization in which the precipitat-ing polymer particles are prevented from flocculation. A typical dispersion polymerization begins with a homogeneous solution of monomer, initiator and copolymer stabilizer of the type described in Section [2.2.1] in an organic diluent.

As monomer is polymerized the insoluble polymer precipitates within the stirred system as microscopic,discrete particles which are prevented from flocculation by the adsorption of the copolymer stabilizer. After the initial precipitation there is no new nucleation unless there is a drastic change in solvency or excess stabilizer is added to the system. Polymerization proceeds within the monomer-swollen particles and in many cases polymerization is much faster than a corresponding solution polymerization owing to the "gel-effect". Such an effect also occurs in bulk polymerization at high conversion [77], and is due to the restriction of normal chain termination processes by the reduced mobility of growing polymer radicals within the viscous environment.

Most types of polymerization mechanisms can be performed as dispersion polymerizations, such as radical and ionic addition, condensation and ring-opening polymerization. The mechanism and kinetics of dispersion polymerization have been largely derived from studies of radically polymerizing systems, and the following consideration will therefore be confined to such systems.

2.3.3 MECHANISM OF PARTICLE FORMATION

Polymerization begins as in a conventional solution polymerization with the thermal or radiation-initiated breakdown of initiator into a pair of free radicals:

e.g. $(C_6H_5COO)_2 \xrightarrow{\text{heat}} 2C_6H_5COO^* \longrightarrow 2C_6H_5^* + 2CO_2$

Benzoyl peroxide $\qquad\qquad\qquad\qquad (R^*)$
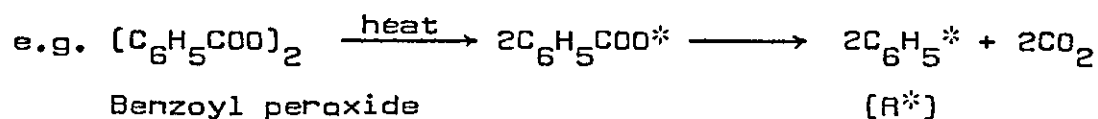
These radicals then react with monomer to form growing chains with a reactive radical at the end:

e.g. $R^* + CH_2=CHX \longrightarrow R-CH_2-\overset{*}{\underset{X}{CH}} \xrightarrow{[CH_2=CHX]_m} R-(CH_2-\underset{X}{CH})_m CH_2-\overset{*}{\underset{X}{CH}}$
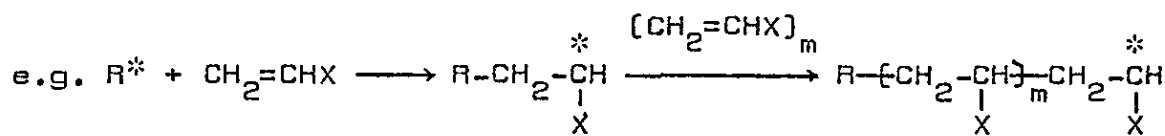
The polymer chain grows in solution until it reaches a threshold molecular weight at which it precipitates and is involved in the formation of a particle nucleus. Eventually termination occurs by either combination and/or disproportionation depending on the monomer:

$$R(CH_2-\underset{X}{CH})_m-CH_2-\overset{*}{\underset{X}{CH}} + \overset{*}{\underset{X}{HC}}-CH_2(\underset{X}{CH}-CH_2)_n-R$$

By combination $\quad R-(CH_2-\underset{X}{CH})_m-CH_2-\underset{X}{CH}-\underset{X}{CH}-CH_2(\underset{X}{CH}-CH_2)_n R$

By disproportionation $\quad R-(CH_2-\underset{X}{CH})_m-CH_2-\underset{X}{CH}_2 + \underset{X}{CH}=CH(\underset{X}{CH}-CH_2)_n R$
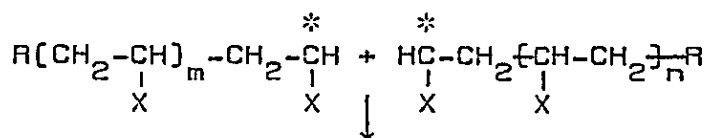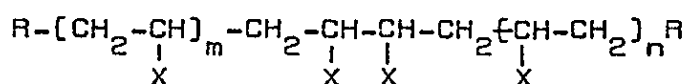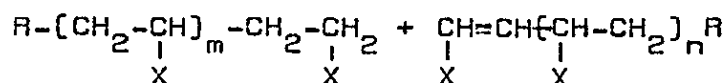
Three different models are proposed for the nucleation of growing chains described above. The models are illustrated in figure (2.9).

(a) <u>Self nucleation</u> [78] (figure (2.9.a))

A polymer chain grows in solution until it reaches a threshold molecular weight at which it collapses into a condensed state and forms a particle nucleus. The threshold molecular weight is dependent upon the solvency of the dispersion medium and every growing chain will form a new nucleus unless it is captured by diffusion into a particle before it reaches the threshold molecular weight.

(b) <u>Aggregative nucleation</u> [79] (Figure (2.9.b))

The theory of homogeneous nucleation suggests that as polymer chains grow they tend to associate until a certain threshold molecular weight and concentration is reached when

FIGURE 2.9

PARTICLE NUCLEATION

primary radicals   initiation and growth of polymer chains   nucleation
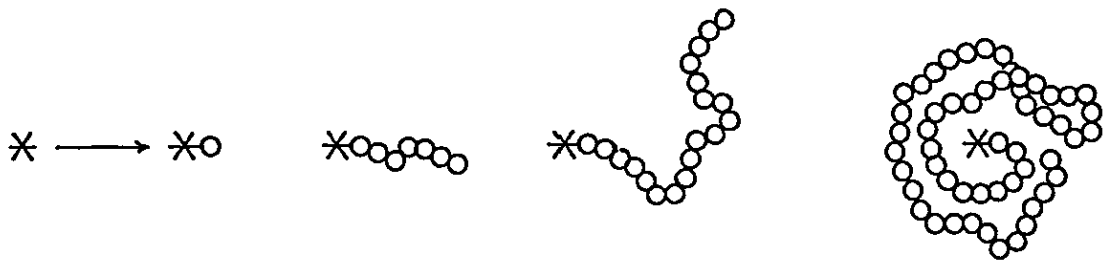
(a) self-nucleation
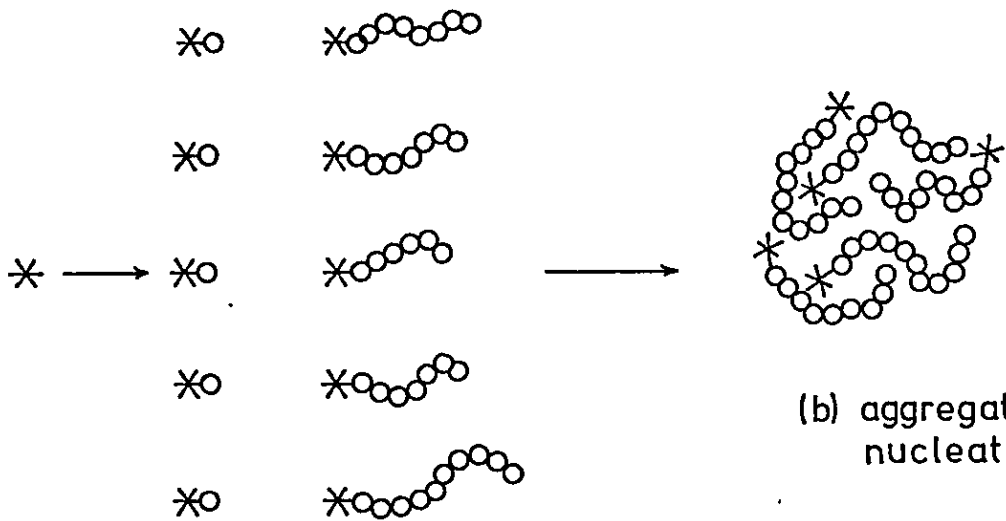
(b) aggregative nucleation
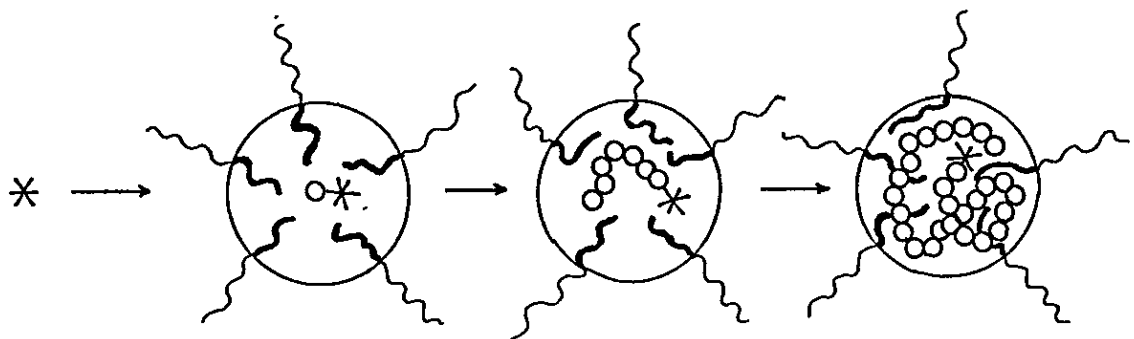
(c) nucleation from monomer-swollen micelles

they are irreversibly associated and become a particle nucleus. Again growing chains only form a nucleus if they are not firstly adsorbed onto existing particles.

(c) Nucleation from micelles (figure (2.9.c))

As discussed in Section (2.2.2) the block and graft copolymers employed as stabilizers are capable of forming micelles in the dispersion medium. It is suggested that chains are initiated and grow within monomer-swollen micelles until the critical threshold molecular weight is reached when a nucleus is formed. This idea is akin to the model proposed by Harkins [80] for emulsion polymerization.

Of these three models for nucleation, the micelle model may be disregarded since the monomer is completely soluble in the organic, dispersion medium, unlike emulsion polymerization, and stabilizer micelles might be regarded merely as a reservoir of stabilizer. Both self-nucleation and aggregative-nucleation are thought to occur within a real system, with a bias towards one mechanism depending upon monomer solubility, polymerization rate, etc.

In the absence of a competing process, the formation of particle nuclei would be expected to continue throughout the course of a polymerization, until monomer is depleted. In practice, however, the rate of nucleation falls to a negligible level very early in the course of polymerization. It is,therefore,suggested that growing oligomers are captured by existing particles before they reach their threshold molecular weight for precipitation. Fitch and Tsai [78] suggest the adsorption of oligomers is a diffusion-controlled process, and that after adsorption the chain is irreversibly

captured. Barrett [10] proposes an equilibrium adsorption model in which at least the low molecular weight growing species are in equilibrium between the dispersion medium and the surface of existing particles. Irreversible capture in this model occurs when the growing chain passes into the interior of the particle, where it grows to its threshold molecular weight before it could escape.

The above models for nucleation represent systems in the absence of stabilizing copolymers. It is found that in the presence of such copolymers the nucleation process is enhanced and more nuclei are formed. This effect occurs since the stabilizing copolymer associates with the growing oligomers, which raises the probability of forming a nucleus and lowers the probability of capture by existing particles. In the self-nucleation model, the stabilizing copolymer associates with a single growing chain, as shown in figure (2.10.a) protecting it from capture at existing particles at lower molecular weight. Therefore the probability of the chain forming a nucleus is increased and more nuclei are produced. In the aggregative nucleation model (figure (2.10.b], the stabilizing copolymer participates in forming incipient nuclei and reduces the interfacial tension. Thus smaller nuclei are produced and the total number of nuclei is increased. It follows then that an increase in concentration of a copolymer stabilizer in the dispersion medium will enhance the number of nuclei formed, with a consequent reduction in the particle size of the final dispersion.

2.3.4 A KINETIC MODEL FOR DISPERSION POLYMERIZATION

From a study of the dispersion polymerization of methyl-methacrylate in petroleum ethers [7] the following kinetic

FIGURE 2.10

MODIFICATION OF PARTICLE NUCLEATION
IN THE PRESENCE OF STABILIZER
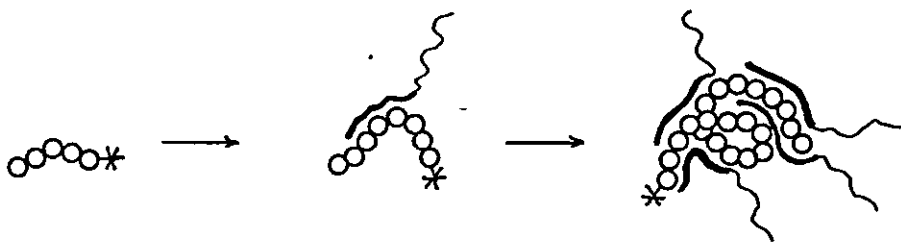
(a) self-nucleation
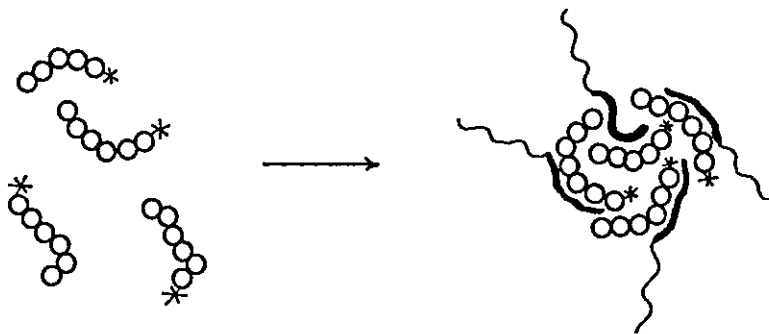
(b) aggregative-nucleation

features were apparent:

(i) The increased rate of dispersion polymerization over that of an equivalent solution polymerization indicated that the polymer particle was the main site of polymerization.

(ii) The rate of dispersion polymerization was independent of particle size over a wide range, making a surface polymerization mechanism improbable.

(iii) The rate of dispersion polymerization was independent of the number of particles present and proportional to the square root of the initiator concentration. The isolation of radicals as in emulsion polymerization is, therefore, not occurring.

(iv) The polymer particles were significantly swollen by monomer during polymerization.

These observations were combined with the mechanistic models for particle formation described above to derive a kinetic model for dispersion polymerization. The following assumptions were made:

(i) Particle nucleation occurs early in the course of a polymerization and can thereafter be omitted from a consideration of particle growth.

(ii) Bulk polymerization takes place within the monomer-swollen particles.

(iii) Growing oligomers are rapidly captured by existing particles, after only a few monomer units have been polymerized. Therefore, initiation can be considered as taking place completely within the particles, although the initiators used are, in reality, distributed between the

dispersion medium and the particles.

If dispersion polymerization is then a type of micro-bulk polymerization, any kinetic model must be similar to ordinary bulk or solution kinetics. The kinetics of radical addition polymerization will be considered.

Free radical addition polymerization occurs in three stages; initiation, propagation and termination. Initiation may be considered in two steps. Firstly the initiator [I] decomposes to give free radicals [R*]

$$I \xrightarrow{k_d} 2R*$$
(2.16)

The radical then reacts with a monomer unit [M] to form a chain radical [M_1^*]

$$R* + M \xrightarrow{k_p} M_1^*$$
(2.17)

where the k's are rate constants with subscripts designating the reactions to which they refer. Subsequent propagation steps, of the general form

$$M_x^* + M \xrightarrow{k_p} M_{x+1}^*$$
(2.18)

are assumed to have the same rate constant k_p, since radical reactivity is taken as being independent of chain length.

The termination step involves either combination of radicals:

$$M_x^* + M_y^* \xrightarrow{k_{tc}} M_{x+y}$$
(2.19)

or disproportionation:

$$M_x^* + M_y^* \xrightarrow{k_{td}} M_x + M_y$$
(2.20)

The rates of the three stages may be expressed in terms of

concentrations of the species involved and rate constants.
Thus the rate of initiation (R_i) is given by

$$R_i = (\frac{d[M*]}{dt})_i = 2Fk_d[I]$$ (2.21)

where F is the efficiency of the initiator in initiating
chains. The rate of termination by disproportionation (e.g.
as with methylmethacrylate [74]) is given by

$$R_t = -(\frac{d[M*]}{dt})_t = k_t[M*]^2$$ (2.22)

In many cases the concentration of growing radicals $[M*]$
becomes essentially constant in the early stages of the
reaction, as radicals are formed and destroyed at the same
rate. In this steady state $R_i = R_p$ and the concentration of
growing radicals $[M*]$ is given by .

$$[M*] = (\frac{R_i}{k_t})^{\frac{1}{2}}$$ (2.23)

The rate of propagation is taken as the overall rate of
disappearance of monomer, hence

$$R_p = -\frac{d[M]}{dt} = k_p[M][M*]$$ (2.24)

and substituting from equation (2.22)

$$R_p = k_p[M](\frac{R_i}{k_t})^{\frac{1}{2}}$$ (2.25)

The average number of monomer units converted to polymer
by a single initiating radical is known as the kinetic chain
length ($\bar{\nu}$) and is given by

$$\bar{\nu} = k_p[M] / (R_i k_t)^{\frac{1}{2}}$$ (2.26)

The rate of radical polymerization sometimes increases
during the course of a polymerization owing to the gel effect.

This phenomenon is particularly marked in the bulk polymerization of methyl methacrylate [81,82]. The viscosity of the polymerization medium increases with increasing conversion, and whilst the diffusion of monomer molecules is still possible, diffusion of the much larger growing radicals is hindered. Thus the rate of termination is greatly reduced. The values of $k_p/k_t^{1/2}$ as in equation [2.25], therefore, increases and there is an increase in the overall rate of polymerization and molecular weight of polymer produced. At even higher conversion monomer diffusion is hindered by the high viscosity of the medium, and therefore k_p and the overall rate of polymerization fall. Since viscosity is temperature-dependent this so-called gel effect is less pronounced at higher temperatures of polymerization.

The kinetic model for bulk or solution polymerization can now be applied to dispersion polymerization. If the rate of initiation within the whole system is R_i and the volume fraction of particles is V, then the effective initiation rate within the particles will be given by:

$$R_{ip} = R_i / V \qquad (2.27)$$

If M_p is the monomer concentration within the particles, the rate of polymerization within the particles (R_{pp}) is given by an expression of the form of equation [2.25] for bulk polymerization:

$$R_{pp} = \left[M_p \right] k_p \left(R_{ip}/k_t \right)^{1/2} \qquad (2.28)$$

$$= \left[M_p \right] k_p \left(R_i/k_t V \right)^{1/2} \qquad (2.29)$$

Since essentially all polymerization takes place within the particles in the volume fraction V, the overall rate of

polymerization in the whole dispersion is given by.

$$R_p = VR_{pp} = \left[M_p\right] k_p \left(VR_i/k_t\right)^{1/2} \qquad (2.30)$$

The concentration of monomer within the particles depends upon the partition coefficient (α) between polymer and the dispersion medium. The overall rate of polymerization is, therefore, given by:

$$R_p = \alpha \left[M_d\right] k_p \left(VR_i/k_t\right)^{1/2} \qquad (2.31)$$

where $\left[M_d\right]$ is the concentration of monomer within the dispersion medium. Two limiting cases to describe the kinetic model have been derived [7].

If α and V are small, then $\left[M_d\right]$ may be taken as the overall monomer concentration $\left[M\right]$.. Here V is roughly equal to $\left[M_o\right].x.V_p$, where $\left[M_o\right]$ is the initial monomer concentration, x is the fractional conversion and V_p is the volume of polymer per mole of monomer. Then

$$R_p = \alpha \left[M_o\right] x^{1/2} (1-x)\left(\left[M_o\right] R_i V_p\right)^{1/2} k_p/k_t^{1/2} \qquad (2.32)$$

If α is large and most of the monomer is found within the particles, V is approximately equal to $\left[M_o\right] V_m$ where V_m is the molar volume of the monomer. $\left[M_p\right]$ is then roughly equal to $(1-x)/V_m$, and

$$R_p = (1-x)\left(\left[M_o\right] R_i/V_m\right)^{1/2} k_p/k_t^{1/2} \qquad (2.33)$$

The overall kinetic model, therefore, depends upon the system. It has been shown [7] that the model derived for low values of α describes well the kinetics of the dispersion polymerization of methyl methacrylate, whilst equation (2.33) describes the dispersion polymerization of more polar monomers such as acrylonitrile.

2.4 PROPERTIES OF NON-AQUEOUS DISPERSIONS

2.4.1 RHEOLOGY OF DISPERSIONS

A study of the rheological properties of a colloidal dispersion can provide much information about the nature of the dispersion, such as the state of coagulation, the thickness of adsorbed layers and particle anisotropy. The viscosity of a colloidal dispersion is greater than that of the medium in which the colloid is dispersed. This is a consequence of an enhanced rate of energy dissipation during laminar shear flow and is due to the perturbation of the streamlines by the colloidal particles.

Einstein [83] has considered a dilute system of small, spherical, rigid, non-interacting particles, in which the transfer of momentum between colliding particles is negligible. The viscosity (η) of the dispersion is proportional to the viscosity of the dispersion medium (η_o) and the volume fraction of the particles (ϕ) as in equation [2.34]

$$\frac{\eta}{\eta_o} = (1 + \frac{5}{2}\phi + 4\phi^2 + \frac{11}{2}\phi^3 + 7\phi^4 + \quad) \qquad [2.34]$$

Assuming that at such low concentrations the hydrodynamic interaction between particles can be ignored, the increase in viscosity produced by one particle can be summed over the total number of particles, hence equation [2.34] gives

$$\eta = \eta_o (1 + \frac{5}{2}\phi) \qquad [2.35]$$

by neglecting all terms in ϕ of higher order than unity.

This equation is the well known Einstein equation containing the Einstein coefficient (α_o) of 2.5, and is only strictly applicable at volume fractions approaching infinite dilution. At higher volume fractions up to about 0.25,

dispersions still show Newtonian behaviour, and much work
has been devoted to extending Einstein's approach to higher
concentrations. At volume fractions greater than 0.01 the
viscosity of a dispersion is increased due to the formation
of temporary doublets, triplets and higher orders of associa-
tion which enhance the rate of energy dissipation. The power
series in volume fraction in equation [2.34] becomes,for more
concentrated systems,of the form

$$\frac{\eta}{\eta_o} = 1 + k_1 \phi + k_2 \phi^2 + k_3 \phi^3 + k_4 \phi^4 \qquad (2.36)$$

This equation reduces to Einstein's equation for a dilute
system of rigid non-interacting spheres, hence k_1 is taken
as Einstein's coefficient 2.5. The coefficient k_2 describes
the perturbation of streamlines by collision doublets, and
k_3, k_4, etc., describe higher order collisions.

The values of k have been estimated by many workers,
and their results have been extensively reviewed [84 ,85 ,86].
Values of k_2, which under Einstein conditions has a limit of
4.0, have been placed within the range 5.1 to 10.5 [87 , 88].

The infinite power series of equation [2.36] is a
general form of an exponential function, and it has been
shown [84] that for disperse systems

$$\frac{\eta}{\eta_o} = e^{k_1/\phi} \qquad \{2.37\}$$

where k_1 is a constant, which is equal to 2.5 at infinite
dilution. A more general case for dispersed systems was
described by

$$\frac{\eta}{\eta_o} = \exp\left(\frac{k_1\, h\, \phi}{1 - h\phi}\right) \qquad (2.38)$$

where h is a solvation factor.

From geometric packing considerations, Mooney [89] has developed an equation identical in form to [2.38]:

$$\eta_{rel} = \frac{\eta}{\eta_o} = exp \left[\frac{2.5\, \phi}{1 - k\phi}\right] \qquad (2.39)$$

where the constant k is a crowding factor.

At even higher volume fractions ($\phi > 0.25$) dispersions become non-Newtonian and dilatancy is often apparent [90.91]. Clearly such shear rate dependent systems cannot be described completely by equations of the form [2.36].

The above equations, derived for rigid, non-interacting spheres, may be modified to study colloidal particles surrounded by an adsorbed layer. In such systems, the perturbation of the streamlines during flow is increased in proportion to the volume of the adsorbed layer, unless the layer is free draining. The effect due to the presence of the adsorbed layer can be expressed in two ways: as an increase in the disperse phase volume or the Einstein coefficient by a factor "f", or by an increase in the particle diameter D by a distance 2δ, where δ = the thickness of the adsorbed layer. Equation [2.36] now becomes

$$\frac{\eta}{\eta_o} = 1 + k_1\, f\phi + k_2\, f^2\, \phi^2 + \qquad \cdot \qquad (2.40)$$

in which k_1 is the Einstein coefficient (α_o) and is equal to 2.5 for rigid, non-interacting spheres.

Since $f = \phi/\phi_o$, where ϕ_o is the particle volume fraction and ϕ is the total volume fraction, for small values of $2\delta/D$ [159]

$$f = 1 + \frac{6\delta}{D} \qquad (2.41)$$

Saunders [90] included this factor into the Mooney equation (2.39) to give

$$\frac{\phi_0}{\ln \eta_{rel}} = \frac{1}{k_1 f} - \frac{k}{k_1} \phi_0 \qquad (2.42)$$

in which k_1 is again the Einstein coefficient, and $k_1 f$ can be thought of as the effective Einstein coefficient. For systems of very small particles, where the adsorbed layer thickness is significant compared with the particle diameter, the full form of equation (2.41) should be used [86], i.e.

$$f = (1 + \frac{2\delta}{D})^3 \qquad (2.43)$$

Hence the effective Einstein coefficient becomes

$$k_1 f = k_1 (1 + \frac{2\delta}{D})^3 \qquad (2.44)$$

2.4.2 LIGHT SCATTERING BEHAVIOUR OF NON-AQUEOUS DISPERSIONS

The scattering of light from a dilute dispersed system provides a useful method of determining the size of the dispersed particles in an essentially undisturbed state, provided the particle shape is known. Many methods of analysing the light scattering behaviour of such systems have been developed (92), and the choice of method is largely governed by the ratio of the particle size to the wavelength of light used, and the ratio of the refractive index of the particle to that of the dispersion medium. Light scattering methods are most effective for particles of the same order of size as the incident wavelength.

For very small particles, where the diameter D is less than about one twentieth the wavelength (λ) of the incident light, Rayleigh scattering is observed (93). The scattered

light intensity is proportional to the square of the particle volume and the scattering pattern is symmetrical about 90°.

For a system of particles where D is equal to or greater than the wavelength of light, the Mie theory describes the scattering behaviour [94]. Since the Mie theory is in a difficult form to interpret, partial solutions have been developed using certain boundary conditions. Provided the refractive index ratio of the particles to the dispersion medium is near unity, the Rayleigh-Gans approximation can be used for larger particles. Larger particles show asymmetric scattering about 90°, with more scattering in the forward direction than the backward direction. This is a result of a loss of intensity due to destructive interference in the backward direction.

Several methods of determining particle size have been developed from an observation of the scattering behaviour of such systems. An estimate of particle size has been made by finding the position of maxima and minima in the polar scattering pattern of visible light [95,96,97], for particles in the range 0.18-4.0 μm. For monosize isotropic spheres, the state of polarization of the scattered light has been used to determine the particle size of polystyrene latexes of size 0.135-1.117 μm [98,99]. Dissymmetry methods [100,101] and analysis of the intensity of scattering at forward angles [102] are methods which have also been used successfully. The many methods available for analysing the light scattering behaviour of dispersed systems have been reviewed extensively [103,104,105]. A dissymmetry method has been used in the present research.

Measurement of the intensity of scattered light at two

angles symmetrically about 90° can be used to define the scattering pattern from which the size of the scattering particles can be deduced [106]. The ratio of the intensity (I_{θ}) of light scattered at an angle θ $(\theta < 90^{\circ})$ to that scattered at its supplementary angle $(180^{\circ} - \theta)$ is called the dissymmetry of the scattering system. For spheres, the dissymmetry is given by

$$\frac{I_{\theta}}{I_{180-\theta}} = (\cot \tfrac{\theta}{2})^6 \left(\frac{\sin x_1 - x_1 \cos x_1}{\sin x_2 - x_2 \cos x_2}\right)2 \qquad (2.45)$$

where $x_1 = (\frac{2\pi D}{\lambda'}) \sin \frac{\theta}{2}$ and $x_2 = (\frac{2\pi D}{\lambda'}) \cos \frac{\theta}{2}$

and λ' is the wavelength of light within the medium of refractive index n_o $(= \frac{\lambda}{n_o})$.

This equation is valid when $2\pi\left((n_p/n_o)-1\right)(D/\lambda')$ is small compared to unity $(n_p$ is the refractive index of the particle). Dissymmetries calculated from this equation have been derived as a function of D/λ' for various pairs of angles of observation [107], as shown in figure [2.11]. The dissymmetry increases very rapidly with increasing particle diameter. The parameter D is strictly the largest dimension of the particle (i.e. the diameter for a sphere), and similar expressions have been developed for coiled and rod-like particles and aggregates of various numbers of spheres in contact [108].

2.4.3 Small-Angle X-ray Scattering from non-aqueous dispersions

In common with light scattering, small-angle X-ray scattering provides a method of measuring the particle size of a dispersion in an essentially undisturbed state. Several methods of determining the particle size of a two-phase

FIGURE 2.11   Dissymmetry as a function of D/χ'

for various pairs of angles $(\theta$ and $180°-\theta)$ of observation
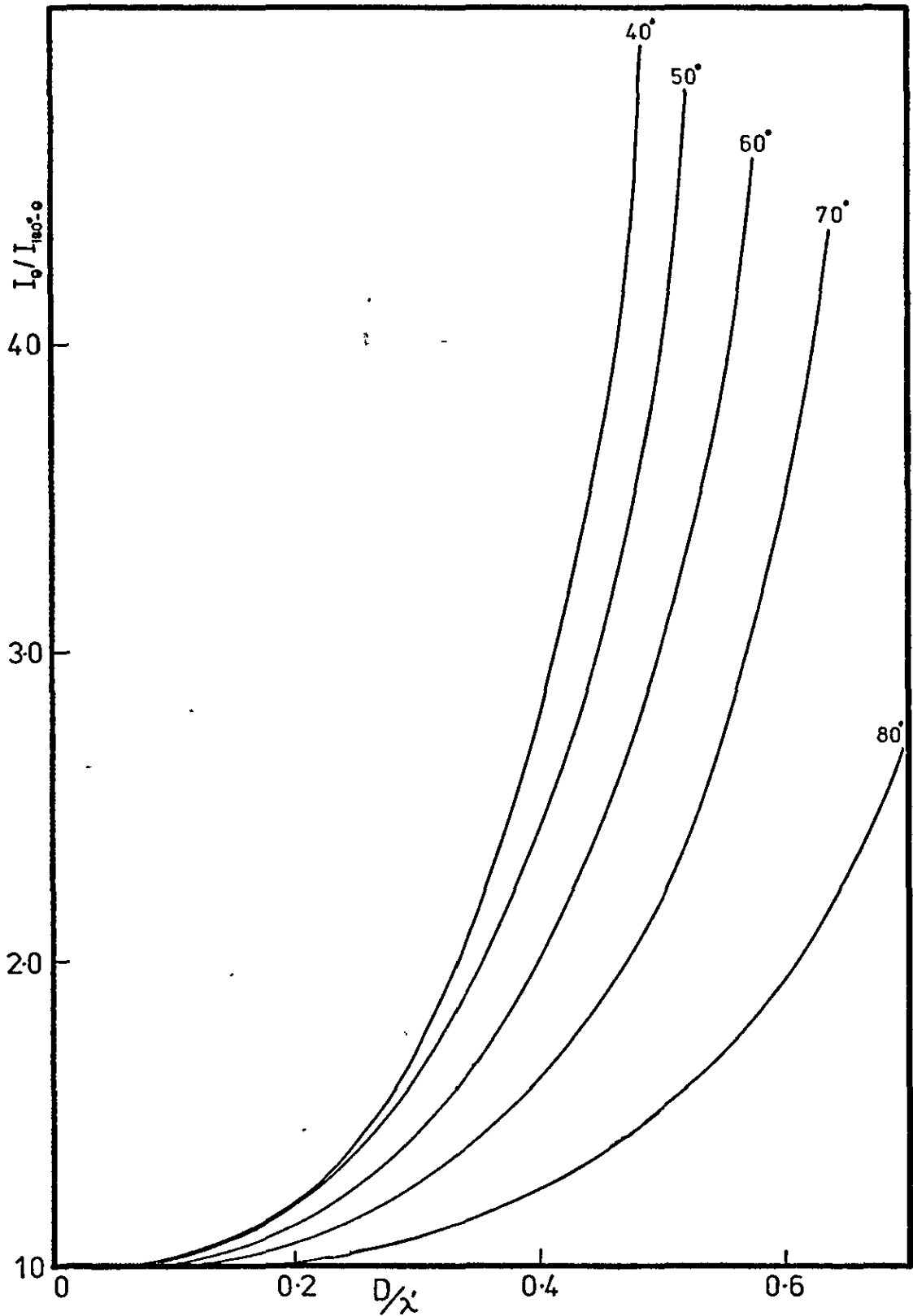
system of dispersed particles have been developed. The
particle size of such a monodisperse system can be determined
from a measurement of the total surface area of the particles
[109,110,111]. The surface area can also be determined for a
completely random two-phase system [112]. In the present
research the method due to Guinier has been used, which
determines the radius of gyration of the particle in a
dilute system [113].

Guinier's treatment was developed for pin-hole collima-
tion of the primary beam. In the present work slit collima-
tion was used to increase the beam intensity, and, therefore,
the experimental results must be mathematically modified or
"desmeared". The desmeared intensities approximate to those
which would have been detected with a pin-hole collimated
primary beam.

For a dilute, monodisperse system in which particles
assume all orientations with equal probability, Guinier
showed that the scattered intensity can be described by

$$I(\theta) = I(0) \exp\left(- \frac{1}{3} (\frac{4\pi\theta}{\lambda})^2 R^2\right) \tag{2.46}$$

where $I(\theta)$ and $I(0)$ are the desmeared intensities at θ and
zero angle respectively; R is the electronic radius of
gyration and λ is the wavelength of the X-rays. Equation
(2.46) is often expressed in logarithmic form:

$$\ln I(\theta) = \ln I(0) - \frac{1}{3} (\frac{4\pi\theta}{\lambda})^2 R^2 \tag{2.47}$$

Guinier's Law is obeyed when a plot of $I(0)$ against θ^2 is
Gaussian. The radius of gyration R is obtained from the
slope of the plot of $\ln I(\theta)$ against θ^2, which should be
linear over a relatively large angular range. Deviations

from linearity can occur owing to particle asphericity or polydisperse particle sizes. For spheres, the radius (a) of a particle is given by

$$a = (\frac{5}{3})^{1/2} R \qquad\qquad (2.48)$$

CHAPTER 3

EXPERIMENTAL

3.1 SYNTHESIS OF BLOCK COPOLYMER STABILIZERS

Block copolymer stabilizers of the type AB were prepared by anionic polymerization, where the A block was polystyrene (PS) and the B block was polydimethylsiloxane (PDMS). Such a "living" polymerization is highly susceptible to termination by impurities such as moisture and carbon dioxide, and , therefore,polymerizations must be performed under conditions of high purity. Two methods of providing such conditions have been used, namely polymerization under an inert gas blanket and polymerization under high vacuum.

3.1.1 INERT GAS BLANKET TECHNIQUE

Purification of reactants

Styrene (Fisons S.L.R. grade stabilized with tert. butyl catechol) was both destabilized and dried by passing a solution (20% w/v) in toluene down a 0.3 m column of active alumina, and stored over molecular sieve (Linde 3A type) for 20 h before use. Toluene (BDH A.R. grade) was dried for several days over freshly-baked molecular sieve. The cyclic trimer hexamethylcyclotrisiloxane (D_3) was supplied as a double-distilled white solid (boiling point 407K) by Dow Corning (114) and was initially purified (products B1-B3) by passing a solution (32% w/v) in toluene down a 0.3 m active alumina column. Owing to problems arising from the retention of D_3 on alumina columns, products B4-B7 were prepared using

D_3 which had simply been dissolved in toluene and purged with dry nitrogen under reflux. Oxygen-free nitrogen (B.O.C. "white spot") was dried by passing through successive columns of molecular sieve, silica gel and calcium hydride. Diglyme (diethylene glycol dimethyl ether, Fisons), which was used as a promotor, was purified by distillation from sodium wire onto sodium and naphthalene, and redistilled from the resulting dark-green complex before use. n-Butyl lithium (Pfizer) supplied as a solution in n-hexane (1.66 M) was standardized using a modified Gilman double titration method [115] and used without further purification.

Polymerization procedure

Polymerization was performed using techniques similar to those of Saam et al. [61]. The equipment comprised a 700 cm^3 split-necked R.B. flask equipped with stirrer, condenser and gas/reactant inlet necks, as illustrated in Figure (3.1). Using such apparatus up to 0.1 kg of block copolymer could be prepared at about a 20% w/v polymer concentration.

The empty reactor was baked by heating to over 473K with a heating mantle, left under a stream of nitrogen for several hours and then allowed to cool under a nitrogen blanket before use. The purified styrene solution and toluene were intro- duced directly into the reactor through glass wool filters. A calculated volume of n-butyl lithium solution was then added by syringe through a silicone-rubber septum to the stirred monomer solution. The solution turned a deep orange colour almost immediately, characteristic of polystyryl anions and the exothermic reaction was held below 313K by surrounding the reactor with a cold water bath. Polymerization was

FIGURE 3.1 REACTOR FOR ANIONIC
POLYMERIZATION UNDER N_2 BLANKET

stirrer motor

dry N_2in

monomer
solution

thermometer

rubber
septum

condenser

split
neck
flask

heating
mantle
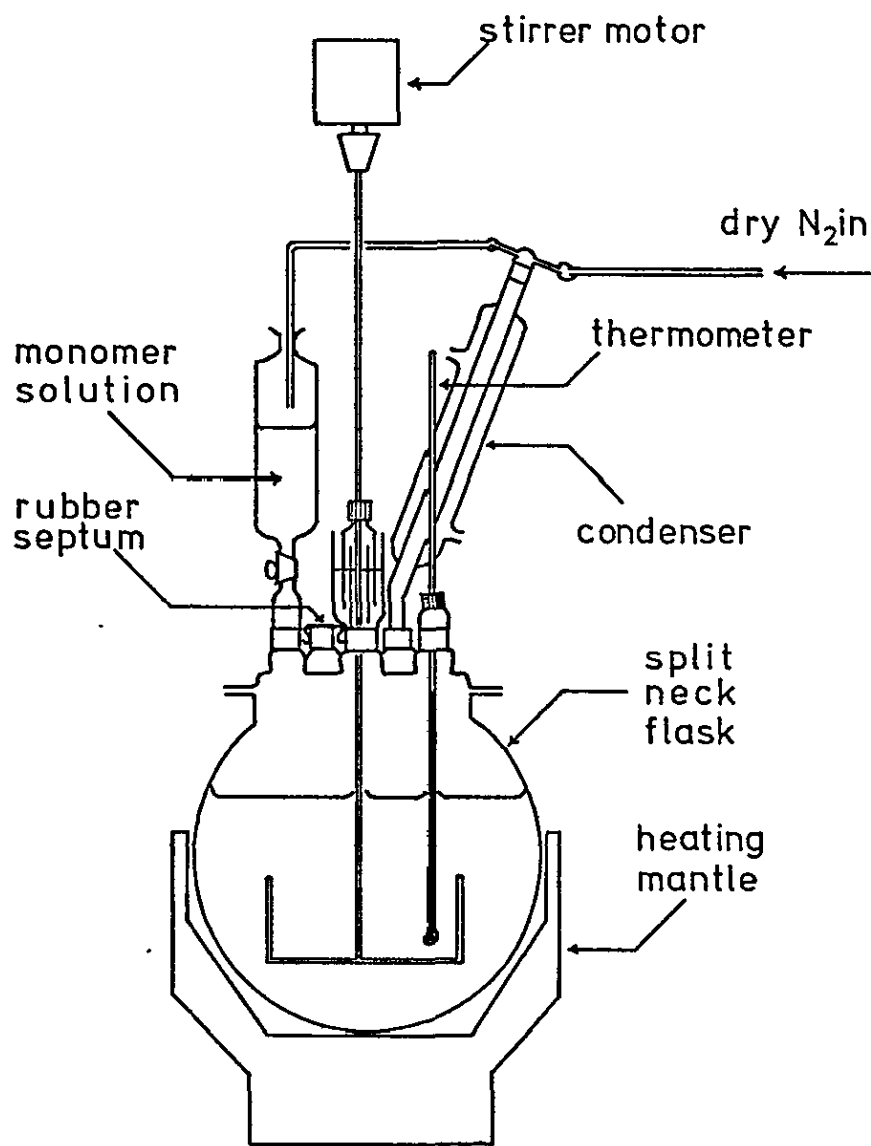
followed by the disappearance of the monomer peak in a g.l.c. analysis, and over 95% conversion was usually achieved within one hour. A sample of this homopolymer solution [5 cm^3] was removed by syringe for subsequent characterization of the A block, and the temperature was then raised to 333K. At this temperature the purified D_3 solution was added by syringe to the reactor, along with enough diglyme promotor to give a 4% v/v solution, and polymerization continued at 333-343K. At about 90% conversion of the D_3, again estimated by g.l.c. analysis, the "living" system was cooled and terminated with chlorotrimethylsilane [1 cm^3]. Block copolymer stabilizers B1-B7 were prepared according to the above technique.

3.1.2 HIGH VACUUM TECHNIQUE

The general principles of high vacuum work as described by Morton [116] and Fetters [59,60] were followed. Purifications and reactor preparation were performed on a purpose-built vacuum frame, illustrated in figure [3.2]. The pumping system consisted of a rotary oil pump and a mercury diffusion pump which was capable of producing a vacuum better than 0.1 Nm^{-2}. Greaseless PTFE O-ring taps and joints [J. Young 117] were used throughout the main section of the frame, and reactors and reactant ampoules were of an all-glass construction with extensive use being made of breakseals. Typical reactant ampoules are illustrated in figure [3.3]. All glassware was rigorously cleaned using freshly prepared chromic acid or Decon 90 [BDH], washed several times with tri-distilled water, and dried. Ampoules and reactors were then evacuated and strongly flamed to above 573K to remove adsorbed water molecules.

pirani
gauge
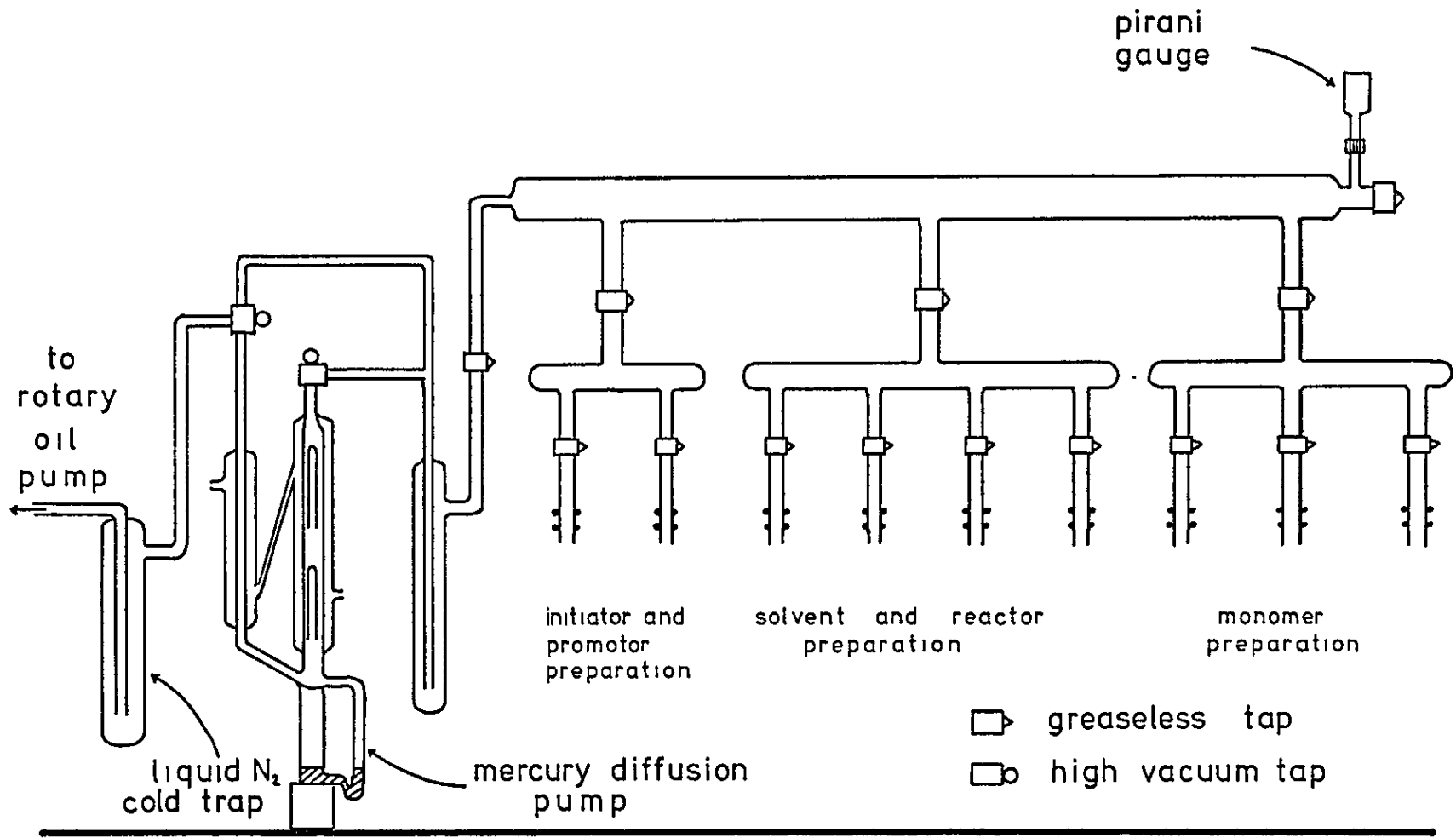
HIGH VACUUM FRAME

FIGURE 3.2

to
rotary
oil
pump

liquid N₂
cold trap

mercury diffusion
pump

initiator and
promotor
preparation

solvent and reactor
preparation

monomer
preparation

greaseless tap

high vacuum tap

FIGURE 3.3

TYPICAL HIGH-VACUUM REACTANT AMPOULES

initiator ampoule

rubber septum

breakseal

terminator ampoule

monomer ampoule
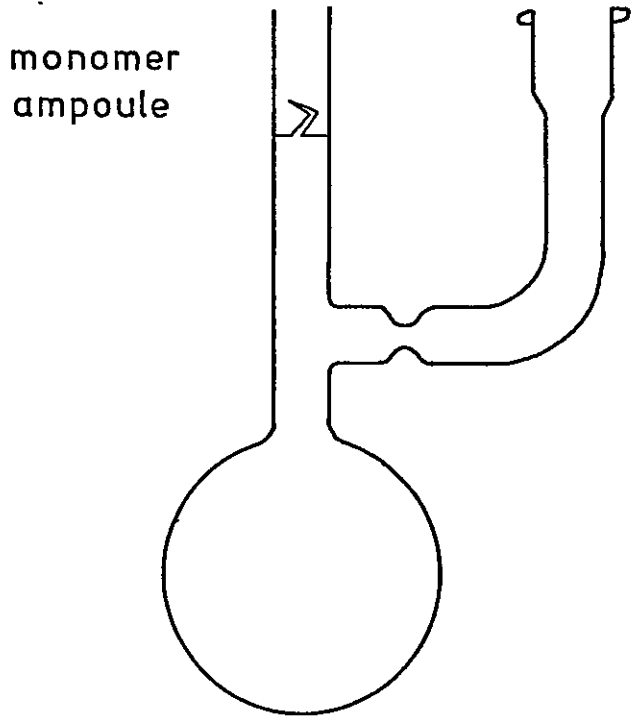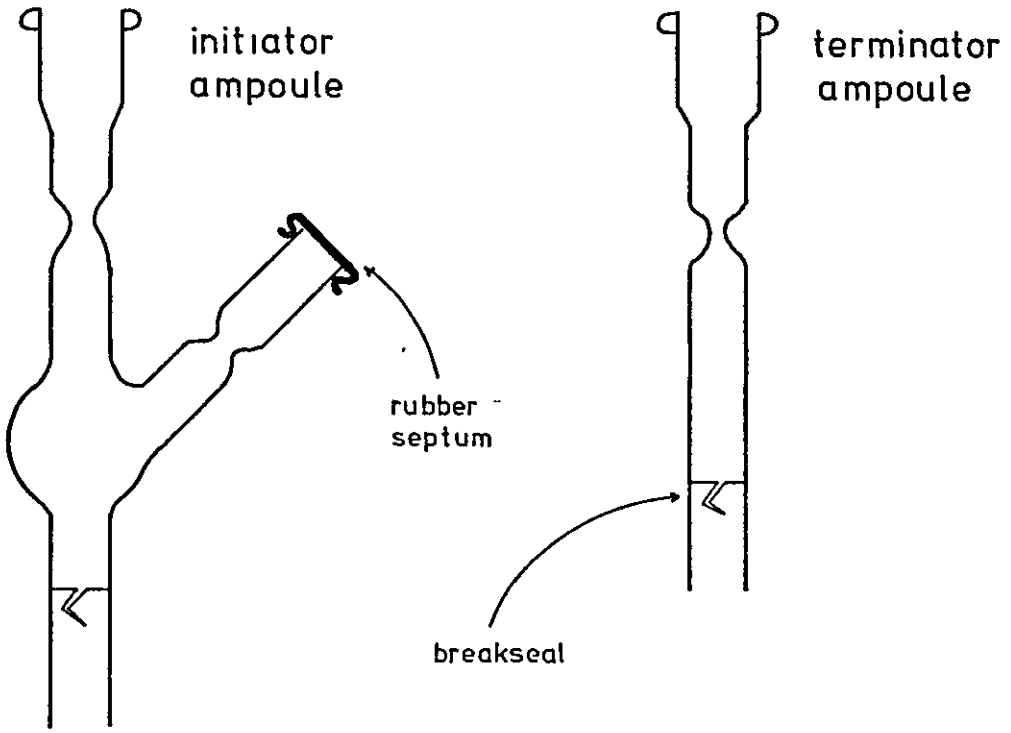
Purification of reactants

Styrene was destabilized by washing twice with aqueous KOH (10% w/v), washed twice with distilled water and dried by stirring under vacuum for several days over a slurry of ground calcium hydride. The monomer was degassed by the familiar freeze/degas/thaw cycles and final traces of moisture removed by distillation onto sodium mirrors until no further degradation of the mirror was evident. Exposure to two such sodium mirrors was usually considered adequate. Measured volumes of purified monomer were then distilled into a pre-flamed and cooled ampoule via a graduated measuring ampoule, and the monomer was further exhaustively degassed. The ampoule, which was equipped with a breakseal, was then sealed off from the vacuum frame and stored at 253K until required.

The required weight of D_3, obtained double-distilled as before, was dissolved in dry toluene and then stirred over a slurry of calcium hydride under vacuum for 24 h with intermittent degassing. The toluene was then distilled into a pre-flamed collection ampoule followed by the cyclic trimer, to give a purified solution which was then exhaustively degassed before the ampoule was sealed off and stored at 253K until required. The transfer of the D_3 solution in this manner was found to be quantitative. Products B8 and B9 were prepared using solutions of D_3 in toluene which had been dried over molecular sieve and syringed directly into nitrogen-filled pre-flamed ampoules before the usual degassing and sealing off operations. This purification technique proved less efficient than the first described method.

Diglyme was again distilled from sodium wire onto sodium and naphthalene, and distilled under vacuum from the resulting

dark-green complex directly into calibrated ampoules.
Products B8 and B9 utilized tetrahydrofuran (THF; Fisons
S.L.R. grade) as promotor, which was purified as for diglyme.
Toluene, stored over molecular sieve, was distilled onto
ground calcium hydride and stirred for several days under
vacuum with intermittent degassing. The solvent was then
distilled onto a 1:1 liquid alloy of sodium and potassium.
Such an alloy breaks up with stirring to give very many small
spheres with a large continually renewing surface area. This
provides a very efficient drying agent for solvents, although
care is required since the alloy is spontaneously combustible
in air. When required the dried toluene was distilled
directly into the polymerization reactor up to a pre-calibrated
mark.

n-Butyl lithium was supplied and standardized as before,
and the required volume was injected into a pre-flamed
initiator ampoule figure (3.3) through the rubber septum.
The septum arm was then immediately sealed off, so that the
initiator solution could be degassed and sealed off from the
line in the usual way. A lack of turbidity in the initiator
solution indicated successful transfer. A few drops of well-
degassed methanol (Fisons A.R. grade) sealed into a terminator
ampoule (figure (3.3)) served as terminator. Products B24
and B25 were terminated with a few drops of chlorotrimethyl-
silane (Fisons S.L.R. grade).

Polymerization procedure

The reactant ampoules were sealed onto an all-glass
reactor (figure (3.4)) containing two PTFE-covered magnetic
stirrer bars. The reactor was designed such that two
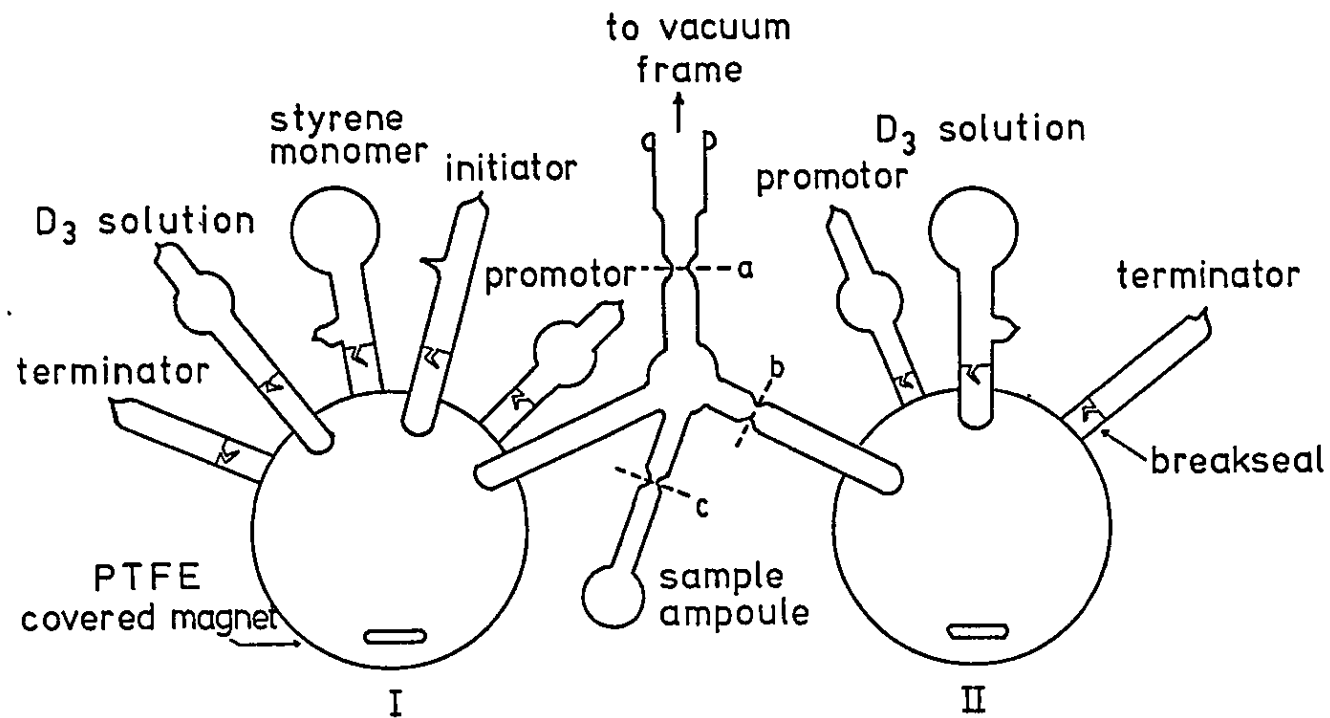
REACTOR FOR ANIONIC POLYMERIZATION

UNDER HIGH-VACUUM

products of equal A block length but differing B block lengths could be prepared simultaneously,by splitting a solution of "living" polystyryllithium and adding differing amounts of D_3 to each portion. The reactor was constructed from two 500 cm^3 bulbs and was used to synthesize up to 0.6 Kg of copolymer at about 20% polymer concentration.

The reactor was attached to the vacuum line, evacuated for several hours and strongly flamed. Purified toluene was distilled directly into bulb I of the reactor [see figure (3.4)] and exhaustively.degassed. The reactor was then sealed off from the line at "a". Bulb I was surrounded by a cold water bath and initiator added by breaking the appropriate breakseal with the magnetic stirrer bar. The initiator ampoule was rinsed with condensing solvent, and styrene monomer was then added dropwise to the stirred solution. The characteristic deep-orange colour of polystyryl anions developed virtually immediately and upon completion of the styrene addition, polymerization proceeded at room temperature. The exothermic reaction was again checked with a cold water bath. After one hour the bath could be removed and the polymerizing solution was left for a period of 3-5 hours to ensure almost complete monomer conversion.

The "living" polystyryllithium solution was then equally divided between bulbs I and II by tilting the reactor, and a sample (10 cm^3) introduced into the sample ampoule for subsequent characterization of the A block. The solutions in each section of the reactor were then frozen and the reactor separated at "b" and "c". The PS-homopolymer sample was immediately terminated by opening the ampoule under methanol.

Each half of the reactor was then treated separately. D_3 solution was added to the stirred solution of polystyryl-lithium at room temperature and the solution left for three hours. During this time, the colour of the solution faded to almost colourless, as each polystyryl anion was capped with one ring-opened trimer unit. Diglyme was then added to the solution to promote the further polymerization of D_3, and the stirred solutions were left to polymerize at room temperature (B12-B25) or at 333K (B8-B11). The time of polymerization was chosen according to the polymerization temperature and the length of the B block. Generally, up to 30 h was allowed for a PDMS block of $\bar{M}_n \sim$ 50 000 at the higher temperature, and up to 50 h for the same block at room temperature.

An increase in viscosity of the polymerizing solution was noted. This was particularly marked for higher molecular weight products (e.g. B17 and B25), which also showed opales-cence or slight turbidity owing to the phase separation of micelles at these concentrations. The "living" systems were terminated by adding the terminator via the appropriate break-seal, and particularly in the high molecular weight products, a significant drop in viscosity was noted, as a result of disassociation of the anions.

Block copolymer stabilizers B8-B25 were prepared according to the above method. Products B8, B9, B24 and B25 were prepared by adding promotor along with the D_3 solution to the polystyryllithium solution, as suggested by Zilliox et al. [64].

3.1.3 RECOVERY AND PURIFICATION

Block copolymers prepared using both the techniques described above were precipitated in excess methanol, washed twice with methanol and once with distilled water, and dried under vacuum at 333K for 30 h. The PS-homopolymer samples were similarly treated.

3.2 SOLUTION POLYMERIZATION OF HOMPOLYMERS

3.2.1 SYNTHESIS OF PDMS-HOMOPOLYMER

PDMS-homopolymer samples S2, S4 and S7 were prepared by polymerizing D_3 anionically using methods similar to those described by Saam et al. [61]. A high molecular PDMS sample (S5) prepared similarly was supplied by Dr. D.P. Jones [114]. The cyclic trimer, diglyme promotor and solvent were purified as described in Section (3.1.2). PDMS was prepared by adding a calculated volume of n-butyl lithium solution, standardized as before, to a solution of D_3. Each butyl lithium molecule reacted with one D_3 monomer unit only, and further polymerization occurred only upon addition of the diglyme promotor. Thus, products of narrow molecular weight distribution could be prepared.

Product S2 was prepared under nitrogen blanket in a similar reactor to that of figure (3.1). The polymerization solvent was cyclohexane, and polymerization was continued under reflux at 357K for 8 h, after which the living anions were terminated with a few drops of methanol. Products S4 and S7 were prepared under high vacuum using techniques similar to those described in Section [3.1.2]. Both products were prepared in toluene and polymerization was continued at room temperature for 23 h [S4] and 50 h [S7], terminating

each reaction as before with methanol.

The products were precipitated in excess methanol, washed twice with methanol and once with distilled water and dried at 333K under vacuum for 30 h.

3.2.2 ANIONIC SOLUTION POLYMERIZATION OF PS-HOMOPOLYMER

Polystyrene was prepared by homogeneous anionic polymerization techniques similar to those described in section [3.1]. Solution polymerzation S6 was performed under nitrogen blanket by polymerizing styrene dissolved in benzene [BDH A.R. grade; dried as for toluene] plus a trace [< 0.5% v/v] amount of THF, using n-butyl lithium as initiator. The reactor used was as described above and conversion of monomer was followed gravimetrically by periodically with-drawing samples [1.0 cm^3] of the polymerizing solution. The samples of known volume were then dried to constant weight at 373K in aluminium trays to determine the concentration of polymer in solution. The reaction conditions are recorded in table [3.1].

Solution polymerizations S3, S8 and S9 were performed in a similar manner using high vacuum techniques as described before. These polymerizations were carried out in the presence of pre-formed block copolymer, and the reaction conditions are again recorded in table [3.1].

3.3 CHARACTERIZATION OF HOMOPOLYMERS AND BLOCK COPOLYMERS

3.3.1 GEL PERMEATION CHROMATOGRAPHY

Gel Permeation Chromatography [GPC] was used to obtain a rapid characterization of the molecular weight and molecular weight distribution of the polymers prepared above.

Reaction Conditions for Solution Polymerizations

No.	Monomer and wt % w.r.t. solvent	Initiator (nBuLi) Conc. M $\times 10^4$	Solvent	Temp. (K)	Technique (a) N_2 blanket (b) High vacuum	Remarks
S2	D_3/25%	5.82	Cyclohexane	357	a	+ 4% diglyme
S4	D_3/50%	49.5	Toluene	298	b	+ 4% diglyme
S7	D_3/20%	14.5	Toluene	298	b	+ 4% diglyme
S3	Styrene/9%	11.0	Toluene	298	b	in presence of 2% B15 (+ 0.1% THF)
S8	Styrene/9%	11.0	Toluene	299	b	in presence of 2% B24 (+ 0.1% THF)
S9	Styrene/9%	11.0	Toluene	298	b	in presence of 2% B20 (+ 0.1% THF)
S6	Styrene/17%	14.5	Benzene	298	a	+ 0.1% THF

Table 3.1

A Waters ALC/GPC 501 instrument was used with four commercially available Styragel columns of nominal pore size 10^3 Å, 10^4 Å, 10^5 Å and 10^6 Å. The instrument was operated at room temperature using THF as eluent at a pumping rate of 2.5 cm^3 min^{-1}. GPC traces were obtained for polymer samples (0.2% w/v in THF) as described in the instruction manual [118]. The instrument was calibrated using a series of polystyrene standards [119] of narrow molecular weight distribution.

3.3.2 HIGH SPEED OSMOMETRY

The number average molecular weight ($\bar{M}_n$) of both homopolymers and block copolymers was determined by high speed membrane osmometry. A Hewlett-Packard 502 instrument was used as described in the instruction manual [120] at room temperature operating with degassed toluene as solvent. The osmotic pressure (π) of a series of polymer solutions at concentrations 4-10 gl^{-1} was measured for each sample.

3.3.3 SILICON ANALYSIS

Block copolymer samples were analysed for silicon by conversion of the silicon to silicate by fusion with sodium peroxide in a Parr bomb [121]. The silicate was then converted to silicomolybdate under controlled conditions, which on reduction yielded a blue colour owing to the formation of molybdenum blue. The conversion of the silicate to the molybdenum blue complex, and subsequent measurement of the optical density was carried out automatically on a Technicon Auto Analyser [122]. This analysis was performed by the Q.A.D. section of Dow Corning Ltd., Barry, U.K.

3.4   PREPARATION OF NON-AQUEOUS DISPERSIONS OF POLYSTYRENE

3.4.1   MICELLAR DISPERSIONS

Micellar dispersions have been prepared with block copolymers B1, B3, B4, B5 and B6 in n-dodecane (Fisons S.L.R. grade) and B1 in n-heptane (Fisons S.L.R. grade). The block copolymer (5.0 g) was dissolved in the solvent (50 cm^3) by heating (up to 473K in dodecane) in a R.B. flask equipped with a condenser and magnetic stirrer. The solution was cooled with stirring and phase separation was noted, giving a micellar dispersion. Such a dispersion was also prepared (D82) using a solution of B1 (5.0 g) dissolved in chloroform (30 g), which was poured with stirring into excess n-heptane (75 g). The chloroform was then distilled from the resulting dispersion.

3.4.2   RADICAL NON-AQUEOUS DISPERSION POLYMERIZATION OF STYRENE

Dispersions of polystyrene in aliphatic hydrocarbon media were prepared radically using block copolymers of PS-PDMS as stabilizers.

Styrene monomer was destabilized with aqueous KOH and dried over calcium hydride as before, degassed and distilled under vacuum immediately before use. Further degassing by repeated freeze/degas/thaw cycles ensured the removal of dissolved oxygen. Block copolymer stabilizer was dissolved in the degassed monomer and the resulting solution stirred into the selected dispersion medium (e.g. n-heptane previously dried over molecular sieve). Alternatively the stabilizer was dissolved in the dispersion medium and monomer stirred into the resulting solution. In both cases, the

entire solution was purged for 30 minutes with dry nitrogen
to remove air, after which the purge was converted to a
nitrogen blanket. Three radical-producing initiators were
used:

[i] Benzoyl peroxide [BDH] was used after drying for
several days under vacuum.

[ii] Azobisisobutyronitrile [AZBN] [BDH] was used after
recrystallization from ice-cold ethanol to give white
needle-like crystals.

[iii] bis[4.tert.butylcyclohexyl]peroxydicarbonate
["Perkadox 16" supplied by Akzo Chemie] was used as
obtained [98% peroxide content].

The apparatus [figure [3.5]] consisted of a 250 cm^3 three-
necked R.B. flask equipped with stirrer, condenser, rubber
septum and thermometer. The temperature of polymerization
was controlled [to ± 1K] by immersing the reactor in a
thermostatted water bath. Two polymerization techniques were
used:

"One-Stage" Polymerization Technique

Initiator was added to the monomer and stabilizer
dissolved in the dispersion medium and the temperature
raised to the desired polymerization temperature [usually
333-343K]. The initially clear solution soon became cloudy,
then opaque white, as the dispersion was produced. After the
desired polymerization time [typically 9-22 h] the dispersion
was cooled and transferred to a storage bottle flushed with
oxygen. Polymerizations were carried out at different
temperatures for differing lengths of time and the effects
of varying stabilizer concentration and composition were

FIGURE 3.5

REACTOR FOR NON-AQUEOUS DISPERSION
POLYMERIZATION

dry N$_2$

stirrer motor

condenser

rubber septum

thermometer

thermostatted water bath
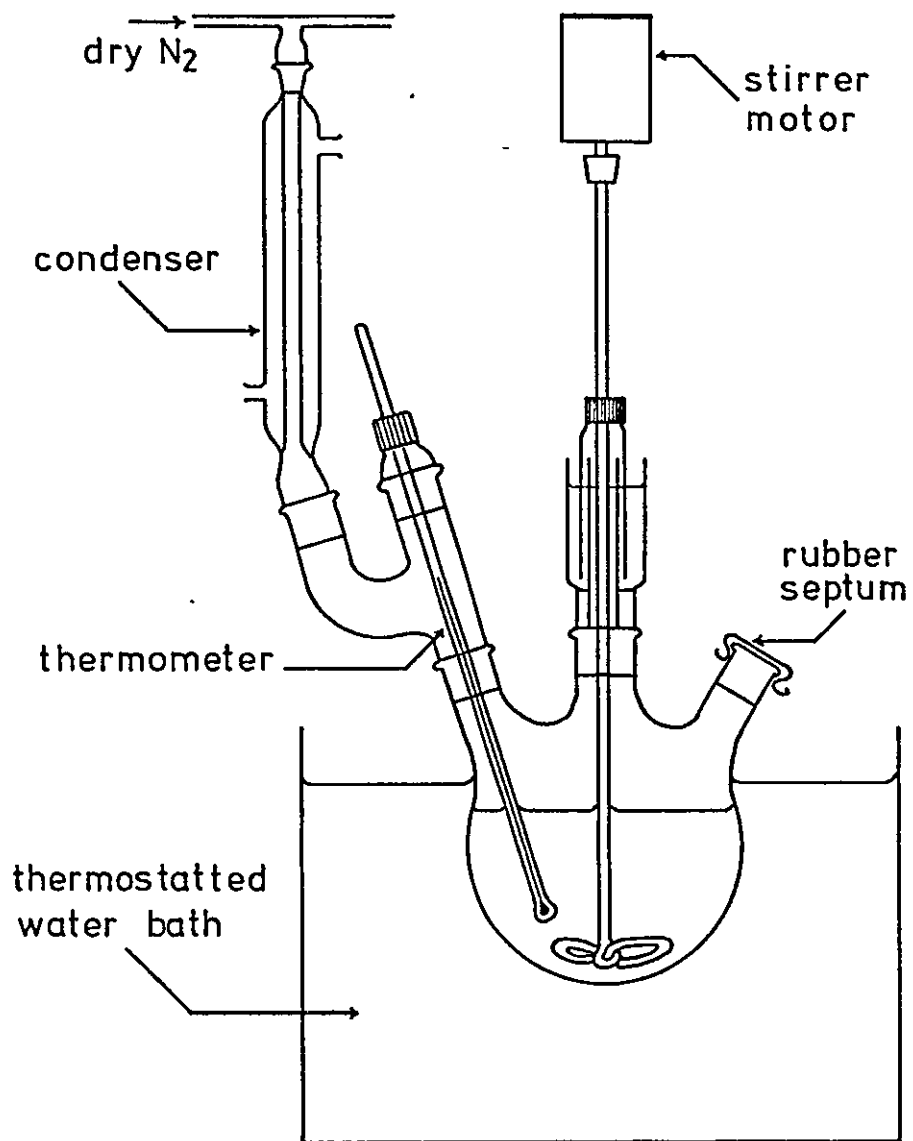
investigated. The extent of monomer conversion was estimated by determining the polymer content of a sample (1.0 cm^3) of the dispersion, as described in section (3.2.2). The reaction conditions used for individual dispersion polymerizations are recorded in table [3.2].

"Seeded" Polymerization Technique

This method involved polymerizing a "seed" portion (usually ~ 10%) of the total monomer with an equivalent amount of initiator and stabilizer, after which further monomer, initiator and stabilizer were added as a "feed" over a period of time. Typically the "seed" stage lasted 1-2 h and the "feed" was added dropwise or incrementally over a period of 9-12 h. The total reaction time was varied from 9 to 46 h,after which successful dispersions were cooled and stored as before. Again, the effects of varying initiator and stabilizer concentration and types were studied. The individual reaction conditions are given in table [3.2].

3.4.3 ANIONIC DISPERSION POLYMERIZATION OF STYRENE

Inert Gas Blanket Technique

The apparatus was similar to that used for radical dispersion polymerization (figure [3.5]). In order to prevent premature termination of the "living" anions, conditions of high purity were employed. The reactor was strongly flamed to over 573K to remove adsorbed moisture and allowed to cool under a blanket of dry nitrogen before use. Styrene monomer, destabilized and dried as before, was kept under nitrogen blanket during transfer and the dispersion medium (usually n-heptane or n-dodecane) was dried over

Reaction Conditions for the Radical Dispersion Polymerization of Styrene

No.	Dispersion medium	Initiator and conc. (weight %)	Monomer and conc. (weight %)	Stabilizer and conc. (weight %)	[a] one stage [b] seed/feed	Temp. [K]	Total polymerization time
D1	hexane	benzoyl peroxide/0.50	20.0	B9/20	a	333	18 h
D18	heptane	benzoyl peroxide/0.50	20.0	B3/1.9	a	333	9 h
D19	heptane	benzoyl peroxide/0.50	20.0	B3/2.0	b	333	21 h
D20	heptane	AZBN/0.30	20.0	B3/2.0	b	333	24 h
D23	heptane	AZBN/0.60	20.0	B3/2.0	b	333	46 h
D26	heptane	AZBN/0.56	20.0	B9/1.5	b	333	45 h
D29	heptane	AZBN/0.50	20.0	B11/2.0	b	335	50 h
D37	heptane	AZBN/1.00	20.0	B14/2.0	b	338	55 h
D48	pet. ether 40/60	"Perkadox 16"/0.50	20.0	B14/2.0	b	323	27 h
D67	heptane	AZBN/0.50	16.5	B14/5.3	a	342	21 h
D94	heptane	AZBN/0.25	20.0	B3/2.0	b	333	48 h

N.B. All concentrations are expressed as weight or mole percent with respect to the dispersion medium.

Table 3.2

molecular sieve or calcium hydride and distilled before use.
Initiators used were n-butyl lithium (~ 1.0 M in n-hexane)
and sec-butyl lithium (~ 1.3 M in cyclohexane) and both were
standardized as described previously. A trace amount (< 0.5%
v/v) of THF was added to systems initiated with n-butyl
lithium. The initiator solution was added dropwise from a
syringe to a stirred solution of monomer, stabilizer and
dispersion medium, until a faint pink colouration was seen,
indicative of the presence of polystyryl anions, and hence
the purity of the system. A further amount of initiator was
then added, calculated to give a product of the desired
molecular weight (typically ~ 25 000). The solution turned
immediately orange and very quickly the clear solution
became opaque as polymer particles formed. In many cases
this orange colour soon faded to give a white latex.
Dispersions prepared in n-dodecane were terminated in the
usual manner after 4 minutes, during which time the orange
colour had not faded. Dispersions D64, D73 and D81,
stabilized by B1 and B3 and polymerized in this way, retained
their orange colour for over two hours.

Polymerizations were carried out at temperatures
ranging from 293-348K and the application of a "seeding"
technique, as described above, was attempted. The addition
of initiator as an incremental feed was investigated, and as
before the effects of varying stabilizer and initiator types
and concentrations were studied. Individual reaction
conditions are presented in tables (3.3 ,3.4).

High Vacuum Technique

Anionic dispersion polymerization was carried out in a
reactor attached to the vacuum frame as seen in Figure (3.6).

Reaction Conditions for the Anionic Dispersion Polymerization of Styrene

No.	Dispersion medium	Initiator and conc. (mole % $\times 10^4$)	Monomer conc. (weight %)	Stabilizer and conc. (weight %)	Type [a] N_2 blanket [b] High vacuum	Temp. [K]	Total polymerization time
034	heptane	sec BuLi/5.0	20.0	B11/2.0	a	333	12 min
052	heptane	nBuLi/4.0	10.0	B11/2.0	b	298	22 min
056	heptane	nBuLi/6.6	16.5	B15/5.3	b	298	45 min
057	heptane	nBuLi/16.5	16.5	B15/5.3	b	298	75 min
062	heptane	nBuLi/13.0	10.0	B15/2.0	b	298	15 min
064	heptane	nBuLi/17.0	16.5	B1/5.3	a	298	4.0 h
072	heptane	bBuLi/9.9	16.5	B2/5.3	a	306	105 min
073	heptane	nBuLi/9.9	16.5	B1/5.3	a	298	125 min
077	heptane	nBuLi/9.9	16.5	B3/5.3	a	301	25 min
095	heptane	nBuLi/6.6	16.5	B24/5.3	a	298	105 min
097	heptane	nBuLi/60.0 as incremental feed	20.0	B24/2.0	a	298	-
098	decane	nBuLi/7.6	16.5	B24/5.3	b	298	2.5 h
099	decane	nBuLi/8.7	20.0	B24/2.0	b	298	45 min
0100	dodecane	nBuLi/8.7	20.0	B24/2.0	a	298	4 min
0103	dodecane	nBuLi/17.4	20.0	B14/1.48	a	298	4 min

Table 3.3

Reaction Conditions for the Anionic Dispersion Polymerization of Styrene (cont.)

No.	Dispersion medium	Initiator and conc. (mole % $\times 10^4$)	Monomer conc. (weight %)	Stabilizer and conc. (weight %)	(a) N2 blanket (b) High vacuum	Temp. (K)	Total polymerization time
D104	dodecane	nBuLi/17.4	20.0	B14/1.48	a	298	2 min
D106	dodecane	nBuLi/11.6	20.0	B14/2.0	a	298	5 min
D107	dodecane	nBuLi/8.7	20.0	B16/2.78	a	298	4 min
D108	dodecane·	nBuLi/4.3	20.0	B17/1.68	a	298	4 min
D110	dodecane	nBuLi/11.6	20.0	B21/1.06	a	298	4 min
D112	dodecane	nBuLi/17.3	16.5	B1/5.3	a	298	4 min

Table 3.4

FIGURE 3.6

VACUUM REACTOR FOR DISPERSION POLYMERIZATION
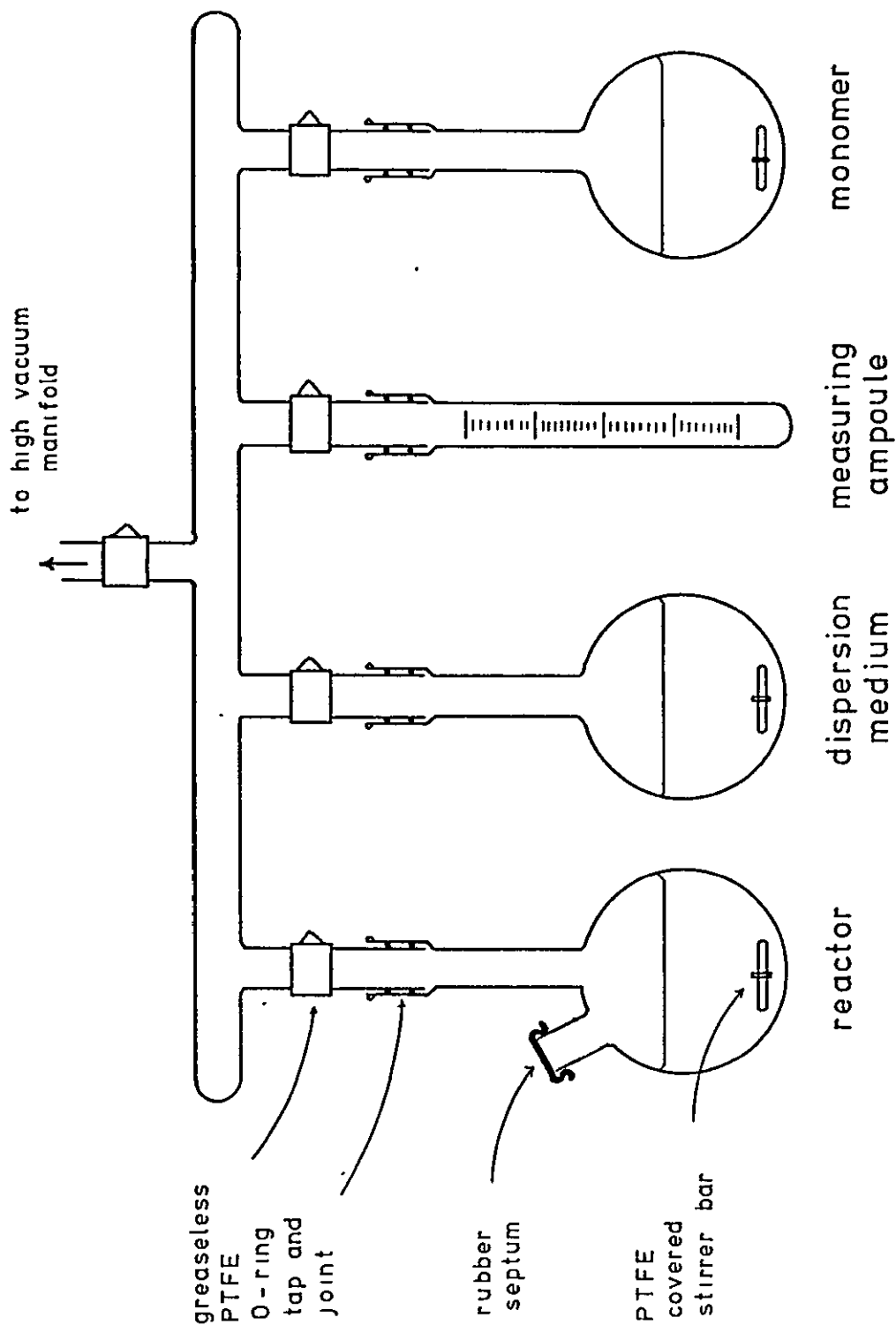
The initiator solution was sealed into an ampoule as described in section [3.1.2] and the ampoule sealed onto the reactor. Block copolymer stabilizer was weighed directly into the reactor and left overnight under vacuum. The conditions under which the stabilizer had been synthesized ensured its purity. The dispersion medium, which again contained a trace of THF promotor, was dried over ground calcium hydride under vacuum, and thoroughly degassed before being distilled into the reactor, The stabilizer was stirred to dissolve in the dispersion medium, using a magnetic stirrer bar, and a measured volume of styrene monomer, destabilized and dried as in section [3.1.2], was distilled in via a measuring ampoule. Initiator was added to the reactor through the breakseal, and polymerization proceeded as described above.

Occasionally a reactor containing reactants purified under vacuum was flushed with dry nitrogen, and polymerization initiated and proceeded with as under an inert gas blanket. Reaction conditions are again to be found in table [3.3].

3.5 PREPARATION OF NON-AQUEOUS DISPERSIONS OF
      POLY[METHYL METHACRYLATE]

Methyl methacrylate (MMA) [Fisons S.L.R. grade, stabilized with quinol] was destabilized with aqueous KOH as for styrene and dried over a slurry of ground calcium hydride under vacuum for several days. The monomer was degassed and distilled when required for use.

Polymerization techniques were similar to those described for the radical dispersion polymerization of styrene,

and both "one-stage " and "seeding" techniques were utilized.
AZBN was used as a radical-producing initiator and polymeriza-
tions were generally carried out in refluxing hexane at 342K.
A dispersion of low molecular weight poly[methyl meth-
acrylate] [PMMA] was prepared [D66] in the presence of
carbon tetrabromide [0.5% w/v] which acted as a chain transfer
agent.

The effects of varying stabilizer type and concentration,
and the amount of monomer in the "seed" stage were investi-
gated. The conditions of polymerization for each individual
dispersion are recorded in tables[3.5 , 3.6]

3.6 PURIFICATION OF NON-AQUEOUS DISPERSIONS BY REDISPERSION

In order to remove unconverted monomer, unadsorbed
stabilizer and initiator residues from the dispersions
prepared above, the dispersions were subjected to several
redispersion cycles. The dispersion was centrifuged at
10 000 r.p.m. for 15 minutes and the supernatant above the
precipitated polymer particles was replaced by fresh
dispersion medium. The particles were redispersed by
vigorous shaking or ultrasonic vibration, and the redisper-
sion cycle repeated. Analysis of the supernatant by infra-
red spectroscopy has shown that three such redispersion
cycles are usually sufficient to reduce to negligible pro-
portions the excess stabilizer content. Redispersion also
provided a way of exchanging the dispersion medium for a
different one, and products prepared in n-hexane have been
redispersed in n-heptane, n-decane, n-dodecane, cyclohexane
and Freon 113 [1,1,2-trichloro-1,2,2-trifluoroethane] in this
way.

Reaction Conditions for the Radical Dispersion Polymerization of Methyl Methacrylate

No.	Dispersion medium	Initiator and conc. [weight %]	Monomer conc. [weight %]	Stabilizer and conc. [weight %]	Mode [a] One stage [b] Seed/Feed	Temp. [K]	Total polymerization time
D43	heptane	AZBN/0.15	20.0	B11/2.0	a	353	7 h
D44	hexane	AZBN/0.023	16.5 ·	B15/5.3	b	342	8 h
D49	pet. ether 60/80	AZBN/0.023	16.5	B14/5.3	b	343	8.75 h
D51	pet. ether mixture	AZBN/0.023	16.5	B11/5.3	b	343	10 h
D55	hexane	AZBN/0.023	16.5	B15/5.3	a	342	3.2 h
D66	hexane	AZBN/0.023	16.5	B15/5.3	a'	343	5 h
D74	hexane	AZBN/0.023	16.5	B17/5.3	b	342	6.7 h
D75	hexane	AZBN/0.023	7.4	B17/4.7	a	342	8 h
D76	hexane	AZBN/0.023	16.5	B15/5.3	b	342	7.75 h
D78	hexane	AZBN/0.023	16.5	B10/5.3	b	342	4 h
D79	heptane	AZBN/0.023	16.5	B20/5.3	b	342	9 h
D80	hexane	AZBN/0.023	16.5	B21/5.3	b	342	8 h
D84	hexane	AZBN/0.023	16.5	B15/5.3	b	342	7 h
D88	hexane	AZBN/0.023	7.4	B23/5.3	a	342	5 h
D89	hexane	AZBN/0.023	12.1	B16/8.0	a	342	5.5 h

Table 3.5

Reaction Conditions for the Radical Dispersion Polymerization of Methyl Methacrylate [cont.]

No.	Dispersion medium	Initiator and conc. [weight %]	Monomer conc. [weight %]	Stabilizer and conc. [weight %]	Mode [a] One stage [b] Seed/feed	Temp. [K]	Total polymerization time
D90	hexane	AZBN/0.023	16.5	B15/3.95	b	342	6.75 h
D91	hexane	AZBN/0.023	16.5	B15/6.58	b	342	8.3 h
D101	hexane	AZBN/0.023	16.5	B25/5.3	b	342	7 h

Table 3.6

3.7 CHARACTERIZATION OF NON-AQUEOUS DISPERSIONS

3.7.1 PARTICLE SHAPE, SIZE AND SIZE DISTRIBUTION

Sedimentation

A rough estimate of the order of the particle size of a dispersion was made by observing the settling of particles under gravity. Very approximately, polymer particles in n-heptane of particle size > 1 μm settled out in less than an hour; particles of size $0.1-1$ μm settled within a few days; and particles smaller than 0.1 μm showed little settling over long periods of time.

Consideration of this behaviour was important when selecting systems for subsequent study of properties such as rheology and light scattering behaviour. For studies in which the experimental time scale is long and the particles are large, sedimentation problems could be minimised by redispersion in a denser dispersion medium.

Optical Microscopy

Optical microscopy was used to determine particle size and shape, but its application was limited to particles of size greater than ~ 1 μm.

Transmission Electron Microscopy

Transmission electron microscopy (TEM) was used extensively to determine particle size, shape and size distribution. Samples were prepared by placing one drop of diluted dispersion ($\sim 0.1\%$ w/v polymer content) directly onto a carbon-coated copper grid and evaporating to dryness. Samples were examined at magnifications of $2-100 \times 10^3$ times using an AEI EM6 instrument calibrated with a replica of a 2160 lines mm^{-1} grating. Particle size and size distribution

were calculated from direct measurement of individual particles on the micrographs.

Light Scattering

Dissymmetry measurements were obtained using a Sofica P.G.D. 42000M photogoniometer operating at ambient temperature. The green line of the mercury spectrum (λ = 546 nm) was used in a vertically polarized mode. Very dilute dispersions of PMMA ($< 2.10^{-4}$ gm^{-3}) in either Freon 113 (Fisons) (n_o = 1.356) or a mixture of n-dodecane and n-heptane (55:45 v/v) (n_o = 1.404) were contained in a cylindrical glass cell. The intensity of scattered light (I) was measured between 40° and 140° at 10° intervals. The samples were diluted further until no change in dissymmetry with concentration was observed. All diluents were filtered before use to remove dust. The dispersion sample was replaced by the pure dispersion medium and the intensity of scattering (I_B) at each angle was subtracted from the sample intensities.

Small Angle X-Ray Scattering

Samples of dispersions D87 and D84 redispersed in n-dodecane (at 2-8% w/v polymer content) were contained in sealed Lindemann tubes of diameter 1.0 mm. A sample of the dispersed phase of D84 was dried under vacuum and similarly treated. A Rigaku-Denki goniometer (Model 2202) was used for small angle X-ray scattering studies with slit-collimated nickel filtered CuK· radiation. The detector was a sodium iodide scintillation counter linked to a pulse height analyser, and the detected pulses were stored in a 100-channel multichannel analyser. A step scanner advanced the goniometer at angular increments of 0.01^o and samples were

scanned from 0.055^o to 1.045^o with 100 s counting time. Background intensities were determined by placing a sample in an absorbing position just in front of the detector and rescanning over the sample angular range.

3.7.2 SURFACE COVERAGE

The surface coverage of the particles could be conveniently estimated from a silicon analysis. Samples of the dispersions were washed by redispersion cycles, as described in section (3.6), to remove unadsorbed stabilizer. The dispersion medium was then evaporated under vacuum and the dried disperse phase subject to silicon analysis as described in section (3.3.3).

3.7.3 ISOLATION AND ANALYSIS OF THE STABILIZER ADSORBED ON A PMMA DISPERSION

The stabilizer (B15) adsorbed on a low molecular weight PMMA dispersion (D66, $\bar{M}_n$ = 15 800) was isolated from a washed and dried sample of the disperse phase. Acetonitrile (Fisons S.L.A. grade) was used as solvent in a Soxlet extraction, and the extraction continued for 70 h. The acetonitrile extracted the PMMA from the disperse phase to leave the stabilizing block copolymer, which was then washed with methanol and dried. The isolated block copolymer was then analysed by GPC.

3.8 PROPERTIES OF NON-AQUEOUS DISPERSIONS

3.8.1 RHEOLOGY

The relative viscosities of dispersions at dispersed phase volume fractions of 0.02-0.25 were measured using an

Ostwald-Fenske-type capillary viscometer of capillary diameter 0.65 mm. This diameter was very large compared to the diameter of the dispersion particles, thus corrections for wall-effects [123] could be neglected. Relative viscosities were determined for dispersions in n-heptane [PMMA particles],and n-dodecane [PS particles] at 298 ± 0.02K. Cumulative errors arising from dilution procedures were avoided by gravimetrically determining the polymer content of samples of the dispersion, as described before, at each dilution. The viscometer was washed with filtered heptane and filtered chloroform and dried between each determination.

Particles of the non-flocculated dispersions tend to accumulate with time on the walls of glass vessels. A method of preventing this [124] involved the prior adsorption of block copolymer stabilizer on the glass, but only slight improvement was noted. The problem was overcome completely by silating all galssware with a solution of chlorotrimethyl-silane [10% w/v] in chloroform. Glassware was baked for several hours at 373K before cooling and filling with the silating agent. After 24 h exposure to this silating agent, glassware was washed thoroughly with filtered chloroform and dried. The silation of a viscometer in such a manner remained effective for all the rheology studies performed.

3.8.2 FLOCCULATION STUDIES

Dispersions were flocculated by reducing the solvency of the dispersion medium in two ways; by adding ethanol, a non-solvent for PDMS; or by cooling a dispersion dispersed in a mixture of n-heptane and ethanol [51:49 v/v]. The conditions at which incipient flocculation was observed was termed the

critical flocculation volume (c.f.v.) of added non-solvent, and the critical flocculation temperature (c.f.t.).

Determination of c.f.v.

The dispersion sample (10 cm^3 at 0.001 g cm^{-3} polymer content) was contained in a cylindrical glass cell, as seen in figure (3.7). The cell was equipped with a magnetic stirrer and surrounded by a water bath thermostatted at 298 ± 0.02K. A light beam was arranged so that light scattered by the dispersion at about 45^0 from the transmitted beam could conveniently be observed by the human eye. Ethanol (99.9% pure) was added dropwise to the stirred dilute dispersion through a fine hypodermic needle and a suitable time for equilibration was allowed between additions. The drop size was such that ethanol could be added in increments of 6 x 10^{-3} cm^3, and the addition was continued until a change in turbidity was observed. The weight of ethanol added was found by weighing the cell before and after addition and hence the c.f.v. was calculated.

Determination of c.f.t.

The c.f.t. was determined using the same apparatus as above, and the temperature of the water bath was lowered from 341K at a rate of 10^0 h^{-1}. Ethanol was added to a sample of dilute dispersion (10 cm^3 at 0.001 g cm^{-3} polymer content) at 341K to give a dispersion medium of n-heptane (51%) and ethanol (49%). The stirred contents of the cell were cooled and the temperature at which a change in turbidity was visually observed was recorded as the c.f.t.

Flocculation was observed to be reversible, and addition of further n-heptane or an increase in temperature produced deflocculation.

FIGURE 3.7

APPARATUS FOR FLOCCULATION AND PHASE SEPARATION STUDIES

non solvent

thermostatted water bath

screen

angle of observation

lamp

stirred sample
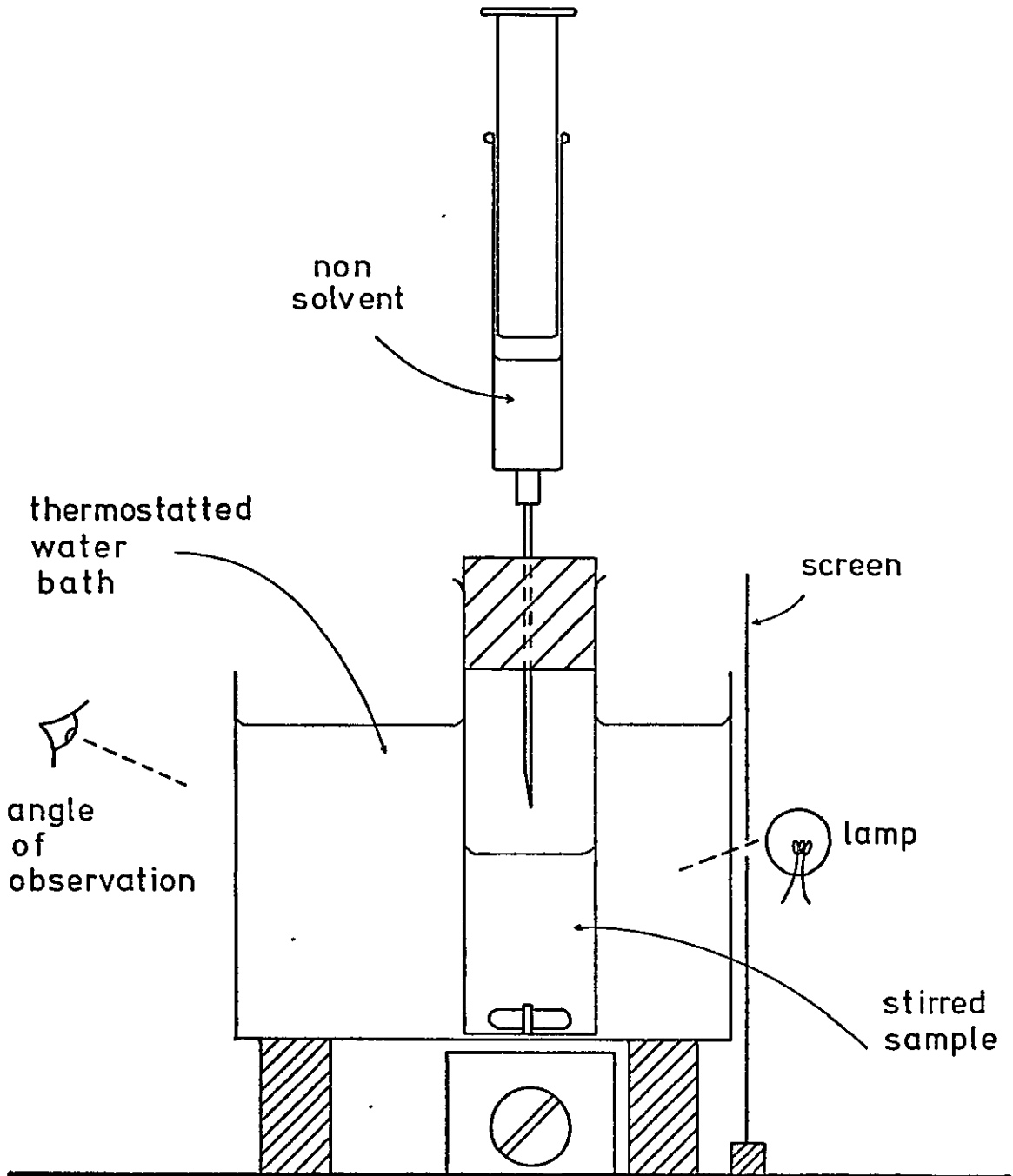
3.9 PHASE SEPARATION STUDIES

3.9.1 DETERMINATION OF THE THETA-COMPOSITION FOR POMS IN A HEPTANE/ETHANOL MIXTURE

The θ-composition for POMS in a mixture of ethanol and n-heptane at 298 ± 0.02K was determined using POMS samples S2, S4 and S7. A cloud-point titration method, as proposed by Elias [41] and later modified by Cornet and Ballegooijen [42] and Suh and Clarke [125] was used.

The apparatus and experimental techniques used were very similar to those used for the determination of the c.f.v. of dispersions as described in section [3.8.2]. Ethanol was added dropwise to a stirred solution of POMS in n-heptane [10 cm^3] until the originally clear solution showed a faint turbidity. The volume fraction of ethanol added was estimated by difference as before. The experiment was repeated for each POMS sample over a range of concentrations [1-9% w/v polymer content].

3.9.2 DETERMINATION OF THE THETA-TEMPERATURE FOR POMS IN A HEPTANE/ETHANOL MIXTURE

The θ-temperature for POMS in a n-heptane/ethanol mixture [51:49% v/v] was determined using two methods:

Suh and Clarke Method [125]

This method for determining θ-temperatures is analogous to the cloud-point method of determining θ-compositions described above. Again the apparatus and techniques used were as described above [section 3.8.2] , and POMS sample S7 was studied. The temperature at which turbidity developed in the stirred solution of POMS was noted and the experiment

repeated over a range of concentrations (1-9% w/v polymer content).

Talamini and Vidotto Method [126]

This method involved determining the temperature at which phase separation was observable for polymers of differing molecular weight at the same concentration. The apparatus and experimental techniques were again as described above. PDMS samples S7, S2 and S5 ($\bar{M}_n$ values 23 300, 33 500 and 267 300 respectively) were used at 4.62% w/v concentration in the n-heptane/ethanol mixture.

3.9.3 DETERMINATION OF THE THRESHOLD MOLECULAR WEIGHT FOR PRECIPITATION OF PS UNDER VARIOUS CONDITIONS

The solubility of PS in alkanes and freon 113

The solubility characteristics of a series of poly-styrene standards of narrow molecular weight distribution [119] in n-heptane, n-dodecane and Freon 113 were investigated. PS (0.05 g) was dissolved in the chosen solvent (5.0 cm^3) by warming if necessary, and the solution contained in the glass cell described in section (3.8.2.). The solution was cooled at 5° h^{-1} from a temperature about 5° above that of phase separation, and the temperature at which turbidity was seen was noted. The experiment was repeated for PS standards of molecular weight 600 to 15 000.

The solubility of PS in heptane/styrene monomer mixtures

This experiment represents an attempt to simulate the conditions during the very early stages of a non-aqueous dispersion polymerization of styrene. A series of PS standards and the apparatus and experimental techniques

described above were again used. PS [0.10 g] was dissolved in styrene monomer [5.0 g] and n-heptane added dropwise to the stirred solution until phase separation was observable. The volume of heptane added was determined in the usual manner. The experiment was repeated with a range of PS standards of molecular weights 600 to 20 000 at 298K and 333K. The lower temperature represents conditions of typical anionic dispersion polymerization, and the higher temperature the conditions of a typical radical dispersion polymerization.

The effect of the presence of block copolymer stabilizer on the solubility of PS was investigated by repeating the above series of experiments in the presence of B15 [1.6 g].

3.10 SOLUTION VISCOSITY STUDIES OF PDMS

In order to determine the expansion coefficient [α] of PDMS in various solvents, the relative viscosity of PDMS sample S2 was measured over a range of concentrations. The solvents considered were n-heptane, n-dodecane and Freon 113. The apparatus and techniques used were as previously described [section [3.8.1]], and measurements were made at 298 ± 0.02K.

3.11 MONOMER PARTITION STUDIES

The partition of methyl methacrylate monomer between PMMA particles and an alkane dispersion medium has been reported in the literature [7.127]. An estimate of the partition of styrene monomer between PS particles and

n-heptane has been made.

Styrene monomer (0.15 g) was added to a sample of D86 (5.8% w/v polymer content) in n-heptane. After equilibration (1 h) with constant shaking at room temperature, the dispersion was centrifuged and the supernatant removed. The refractive index of the supernatant was measured using an Abbe refractometer at 298 ± 0.02K. The refractive index of a series of concentrations of styrene in n-heptane was measured and a calibration curve constructed. Hence the weight of unadsorbed monomer in the supernatant was estimated, and the partition coefficient calculated.

CHAPTER 4

RESULTS

4.1 CHARACTERIZATION OF BLOCK COPOLYMER STABILIZERS

Block copolymer stabilizers were characterized by the following techniques, and the results are summarized in tables 4.1(a) and 4.1(b).

4.1.1 Gel Permeation Chromatography (G.P.C.)

A calibration curve for the G.P.C. instrument was obtained with a series of PS standards of narrow molecular weight distribution. The calibration curve is a plot of log(peak molecular weight) against elution volume, and is presented in figure 4.1. The elution volume of an internal standard (tetraphenylethylene of molecular weight 332) was taken as the total "path length" of a G.P.C. trace, which was divided into "counts" at 2% intervals. A computer program based on the method of Pickett et al. [128] and modified by Dr. Croucher [129] was used to calculate the molecular weight averages from the chromatograms. A comparison of the values of $\bar{M}_n$ determined by G.P.C. and by osmometry showed that the G.P.C. underestimated $\bar{M}_n$ by 15%. The values of $\bar{M}_n$ obtained were,therefore,corrected to compensate for peak broadening. The $\bar{M}_w$ values were uncorrected, and,therefore,the polydispersity ratio $\bar{M}_w/\bar{M}_n$ represents a maximum value.

Samples of the PS homopolymer A blocks were analysed by G.P.C., and a typical chromatogram is seen in figure 4.2(a). The G.P.C. trace of a PS standard is also given for comparison. Block copolymer stabilizers were analysed by G.P.C. to provide

Characterization of Block Copolymer Stabilizers

[i] Stabilizer Number	[ii] $\bar{M}_n$ PS block (from GPC)	[iii] $\bar{M}_n$ PDMS block (from [i] and [viii])	[iv] $\bar{M}_w/\bar{M}_n$ block copolymer (from GPC)	[v] $\bar{M}_n$ PS block (from osmometry)	[vi] $\bar{M}_n$ block copolymer (from osmometry)	[vii] $\bar{M}_n$ PDMS block ([vi]-[v])	[viii] % PDMS (from % Si)
B1	20 000	3 300	1.18				14.06
B2	74 800	9 800	1.57				11.63
B3	57 200	5 000	1.25				8.09
B4	72 000	4 000	1.10				5.26
B5	99 100	4 600	1.19				4.39
B6	150 200	4 200	1.52				2.72
B7	95 300	2 600	1.16				2.62
B8	44 400	1 200	1.10	48 900	49 900	1 000	2.38
B9	44 400	58 000	1.10	48 900	114 000	65 100	45.51
B10	10 600	2 400	1.24				18.61
B11	10 600	8 900	1.24				45.51
B12	45 700	28 500	1.31				38.37
B13	45 700	60 800	1.43				57.11

Table 4.1(a)

Characterization of Block Copolymer Stabilizers

[i] Stabilizer Number	[ii] $\bar{M}_n$ PS block (from GPC)	[iii] $\bar{M}_n$ PDMS block (from [i] and [viii])	[iv] $\bar{M}_w/\bar{M}_n$ block copolymer (from GPC)	[v] $\bar{M}_n$ FS block (from osmometry)	[vi] $\bar{M}_n$ block copolymer (from osmometry)	[vii] $\bar{M}_n$ PDMS block [[vi]-[v]] *[[vi]-[ii]]	[viii] % PDMS (from % Si)
B14	8 800	7 000	1.18				44.32
B15	8 800	11 200	1.14				56.00
B16	43 600	13 700	1.17	44 000			23.89
B17	43 600	29 800	1.20	44 000	74 000	30 000	40.54
B18	17 800	3 000	1.10				14.51
B19	17 800	32 800	1.13				64.86
B20	12 700	3 200	1.19				20.30
B21	12 700	23 800	1.24				65.23
B22	33 400	13 800	1.14				29.12
B23	33 400	48 000	1.22				59.07
B24	16 400	9 100	1.23			7 600*	35.59
B25	16 400	16 100	1.30			16 000*	74.42

Table 4.1(b)

GPC CALIBRATION CURVE
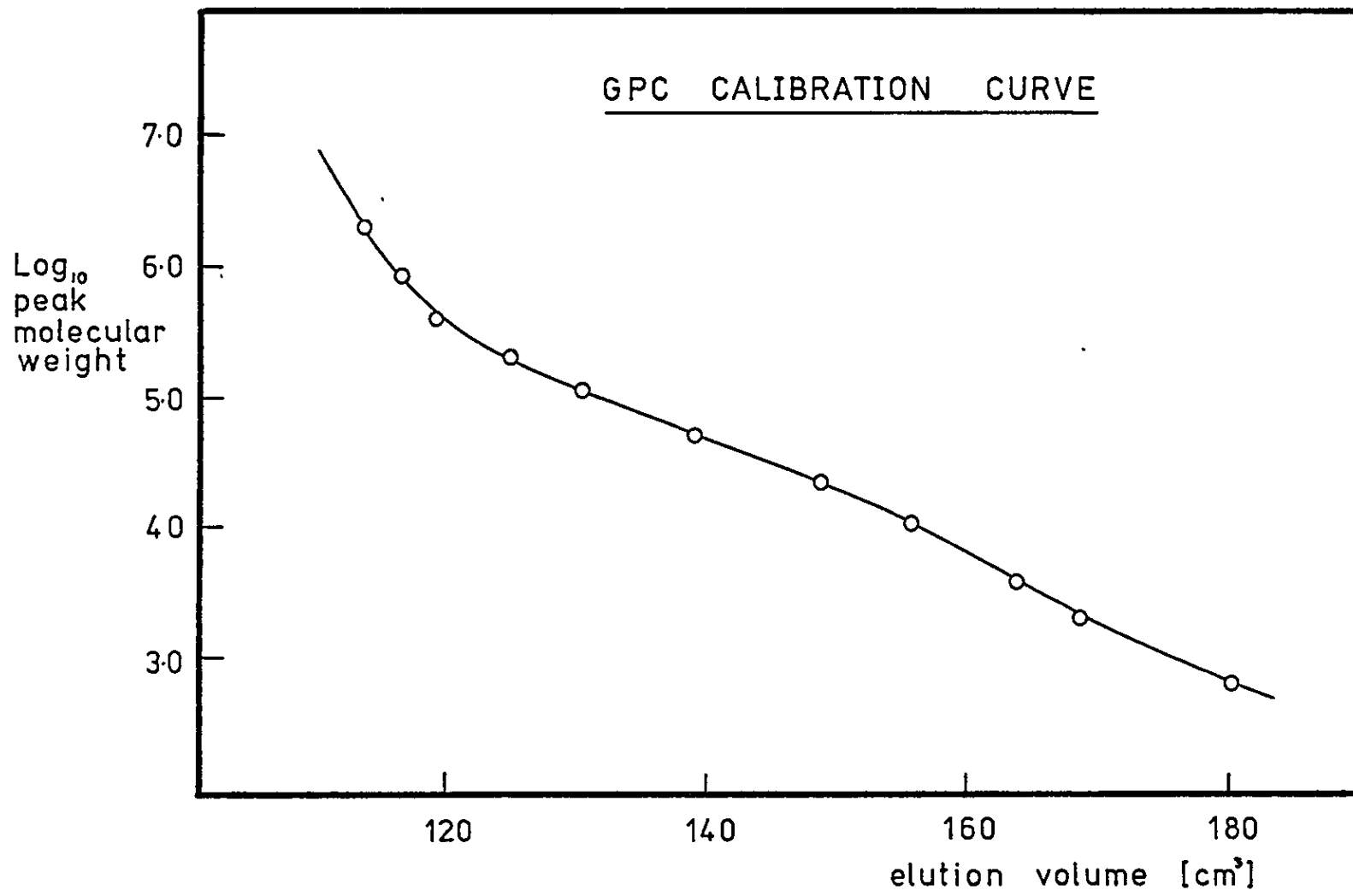
FIGURE 4.1

FIGURE 4 2

GEL PERMEATION CHROMATOGRAMS
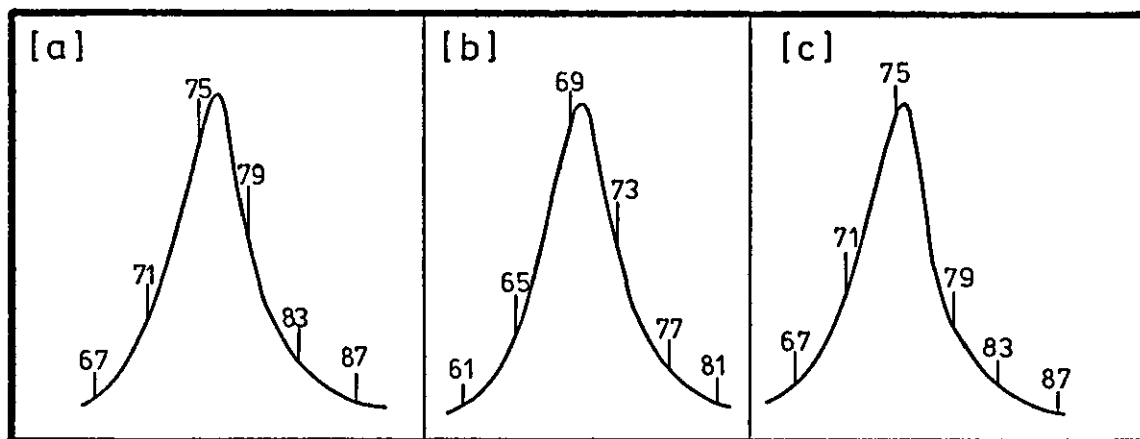
[a]   PS homopolymer   A – block of   B15   ($\overline{M}_n = 8800$)

[b]   Block copolymer   B15   ($\overline{M}_n$ = 20 000)

[c]   PS   standard   ($\overline{M}_n$ = 9 800)
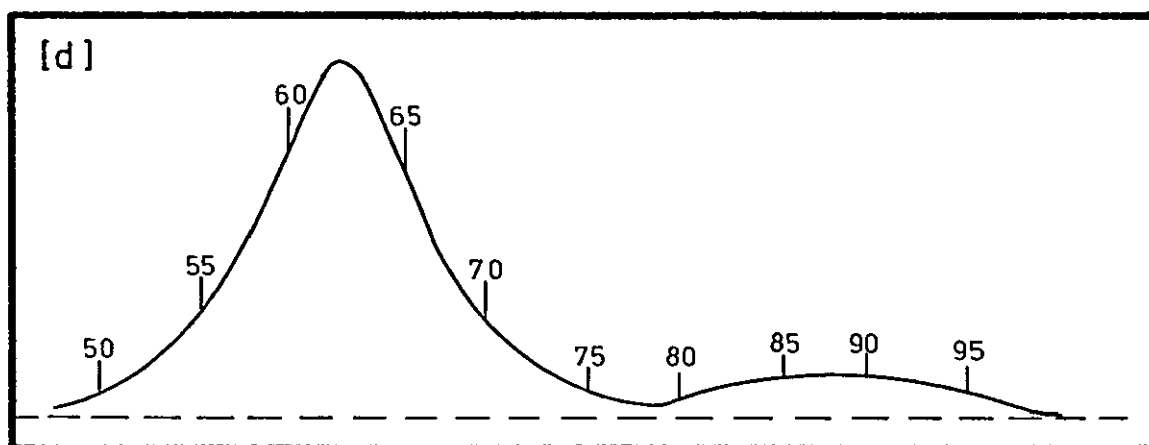
[d]   PS homopolymer A – block of   B7   ($\overline{M}_n$ = 95 300)
        prepared under N_2 blanket , showing low molecular
        weight impurity ($\overline{M}_n \sim 3\,000$).

an indication of the polydispersity ratio only, and a typical chromatogram is seen in figure 4.2(b). The PS homopolymer samples of polymers prepared under nitrogen blanket (B1-B7) all showed a small secondary peak due to low molecular weight PS impurity (figure 4.2(d)).

4.1.2 High Speed Membrane Osmometry

The number average molecular weight $\bar{M}_n$ was determined for products of $\bar{M}_n > 20\ 000$ by osmometry. Plots of π/c vs. c were linear over the range of concentrations used, for both block copolymers and homopolymers. Figure 4.3 shows a typical plot. The osmotic pressure and $\bar{M}_n$ are related according to the following virial expansion:

$$\frac{\pi}{c} = \frac{RT}{\bar{M}_n} + Bc + Cc^2 + \dots \qquad (4.1)$$

where π is the osmotic pressure

  c is the polymer concentration $[g.dl^{-1}]$

  R is the Gas Constant

  T is absolute temperature

  B and C are the second and third virial coefficients.

  As c approaches zero:

$$\lim_{c \to 0} \frac{\pi}{c} = \frac{RT}{\bar{M}_n} \qquad (4.2)$$

$\bar{M}_n$ was, therefore, obtained from the intercept of the above curve.

Osmometry gave absolute values of $\bar{M}_n$ for block copolymers, which agreed well with those obtained by summing $\bar{M}_n$ of the PS block (from G.P.C.) and $\bar{M}_n$ of the PDMS block (from G.P.C. and silicon analysis).
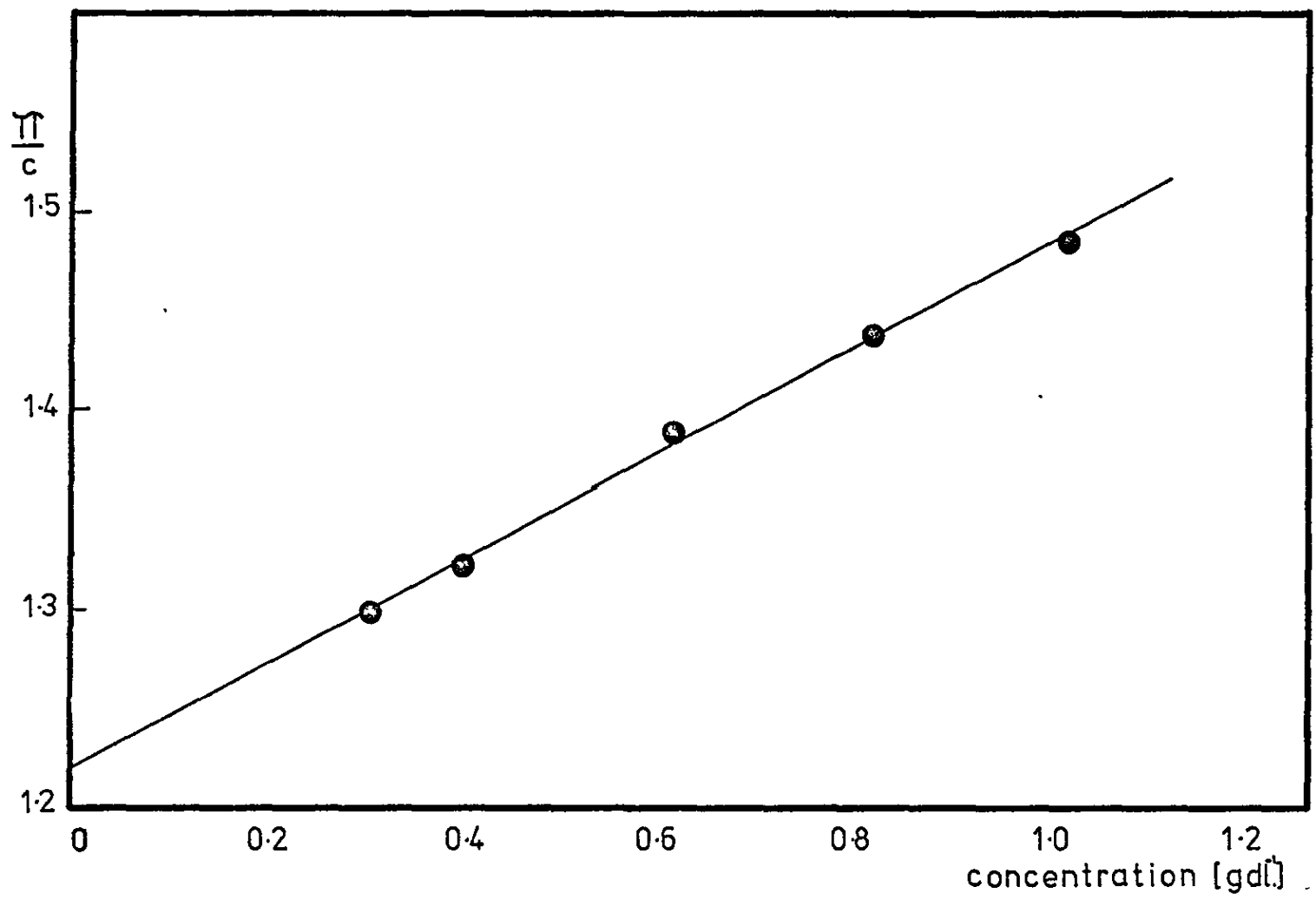
FIGURE 4.3

OSMOMETRY CURVE FOR STABILIZER B24

4.1.3 Silicon Analysis

From an analysis of the % Si present in a block copolymer, the PDMS content was calculated. This was combined with the value of $\bar{M}_n$ for the PS A block to calculate $\bar{M}_n$ for the PDMS block.

4.2 SOLUTION POLYMERIZATIONS

Samples of PDMS homopolymers S2, S4, S7 and S5 were characterized using G.P.C. and osmometry as described above. Owing to the similarity of the refractive indices of PDMS and THF (~ 1.4), higher concentrations ($\sim 1\%$ w/v) of PDMS were used in G.P.C. analysis. Although the G.P.C. was calibrated for PS, the Dawkins' method [130] gives a very comparable calibration curve for PDMS. Therefore, whilst the molecular weight averages quoted are actually PS equivalent molecular weights, these are very close to the actual molecular weights for PDMS. Values of $\bar{M}_n$ were corrected for peak broadening as before. Results of the characterization are presented in table 4.2.

Anionic solution polymerizations of styrene (S3, S8 and S9) were performed in the presence of block copolymer stabilizer. Table 4.3 gives the conversion of monomer achieved for each polymerization. The extent of monomer conversion was seen to increase with decreasing PDMS concentration.

The conversion of styrene with time was followed in the anionic solution polymerization S6. The resulting curve is presented along with an equivalent dispersion polymerization (D73) in figure 4.5.

Table 4.2

Characterization of POMS Homopolymers

Sample Number	$\bar{M}_n$ from GPC	$\bar{M}_w/\bar{M}_n$ from GPC	$\bar{M}_n$ from Osmometry
S2	33 500	< 1.42	33 000
S4	10 600	< 1.09	–
S7	23 300	< 1.29	–
S5	267 300	< 2.56	218 000*

* As determined by Dr. Tuminello [146].

Table 4.3

Extent of Monomer Conversion in Solution Polymerizations of Styrene

Polymerization Number	Block Copolymer	% POMS in Solution	Monomer Conversion [%]
S3	B15	1.12	5.0
S8	B24	0.71	19.5
S9	B20	0.46	68.3

4.3 DISPERSION POLYMERIZATIONS

4.3.1 Rate of Polymerization

The extent of monomer conversion was followed as a function of time for each of the dispersion polymerization systems studied. Figure 4.4 shows the curve for a radical dispersion polymerization of styrene [D67] and figure 4.5 shows the curve for an anionic dispersion polymerization of styrene [D73]. The curve for a radical dispersion polymerization of methyl methacrylate [D55] is given in figure 4.6. For comparison, figure 4.4 also shows the curve for a typical radical solution polymerization of styrene [131], and figure 4.6 likewise shows bulk and solution polymerization curves for methyl methacrylate [81]. The experimentally determined curve for an equivalent anionic solution polymerization of styrene [S6] is also given in figure 4.5.

4.3.2 Characterization of Dispersions

Tables 4.4 to 4.9 record the results of dispersion polymerizations for the three systems studied. The silicon content of the dispersedphase of several dispersions is given, from which the PDMS content could be estimated. The number average molecular weight, $\bar{M}_n$, of the dispersed phase was determined by G.P.C. for several products. Estimation of particle size and particle size distribution were by transmission electron microscopy, as described below.

Transmission electron microscopy [TEM]

Particle size was estimated by TEM, which also confirmed the sphericity of the particles in all the systems studied. Figures 4.7 to 4.9 show typical electron micrographs for both PS and PMMA particles. In general, at least 150 individual

FIGURE 4.4
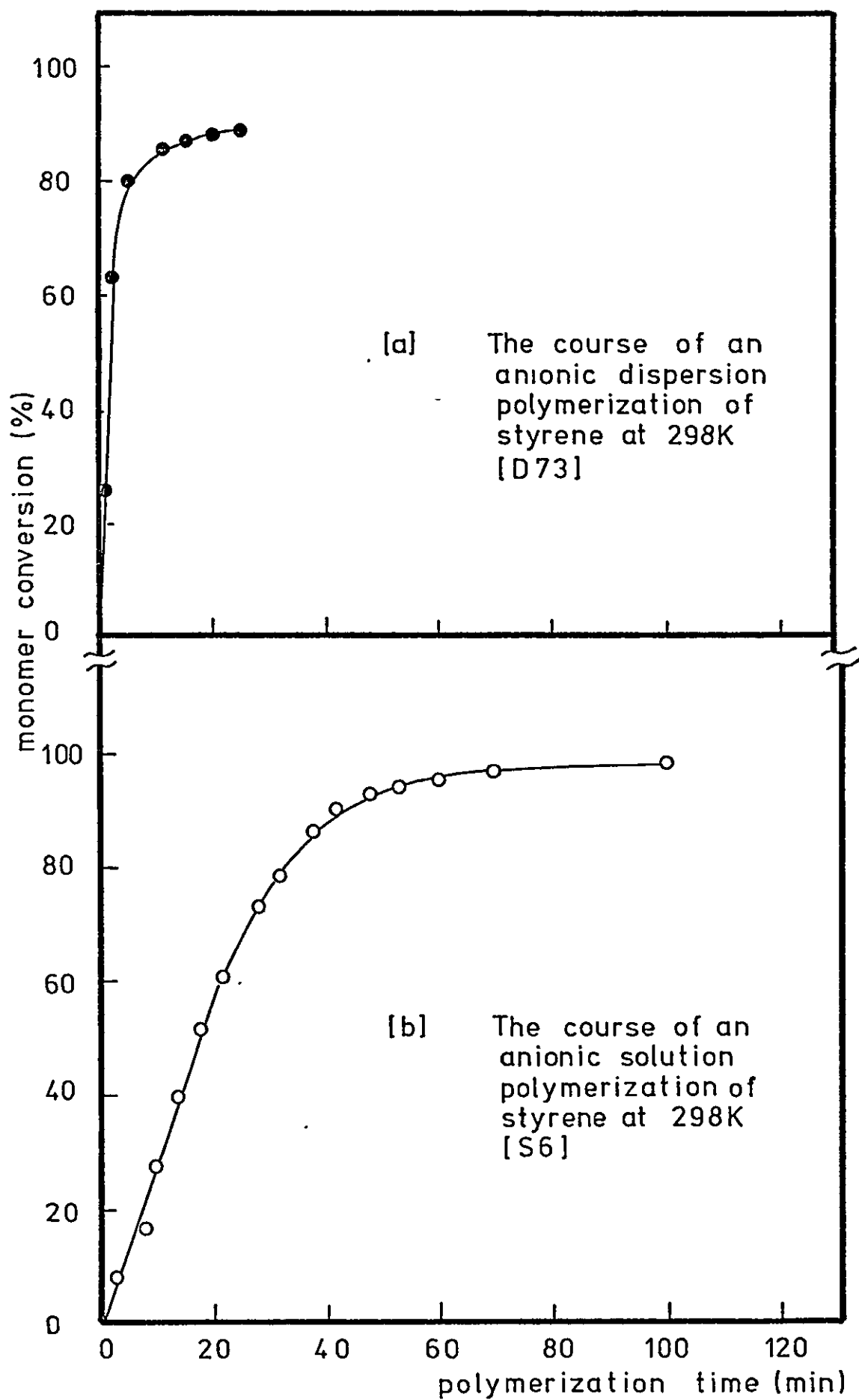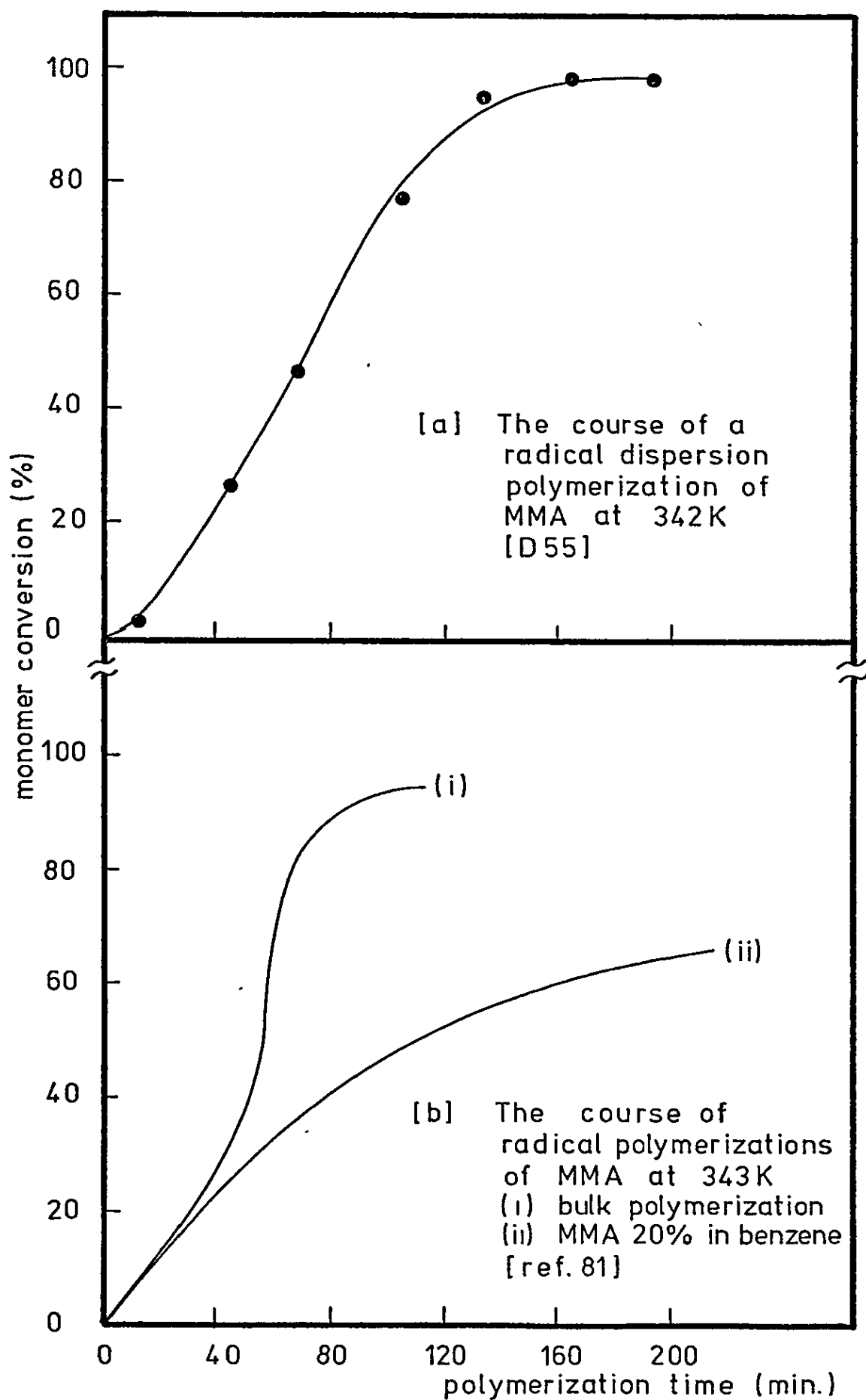
[a] The course of a radical dispersion polymerization of styrene at 343K (D 67)

[b] The course of a radical solution polymerization of styrene in toluene at 323 K (40% styrene; 0·083M benzoyl peroxide) [ref.131]

FIGURE 4.5

[a] The course of an anionic dispersion polymerization of styrene at 298K [D73]

[b] The course of an anionic solution polymerization of styrene at 298K [S6]

FIGURE 4.6

[a] The course of a radical dispersion polymerization of MMA at 342K [D 55]

[b] The course of radical polymerizations of MMA at 343K
(i) bulk polymerization
(ii) MMA 20% in benzene [ref. 81]

Results of the Radical Dispersion Polymerization of Styrene

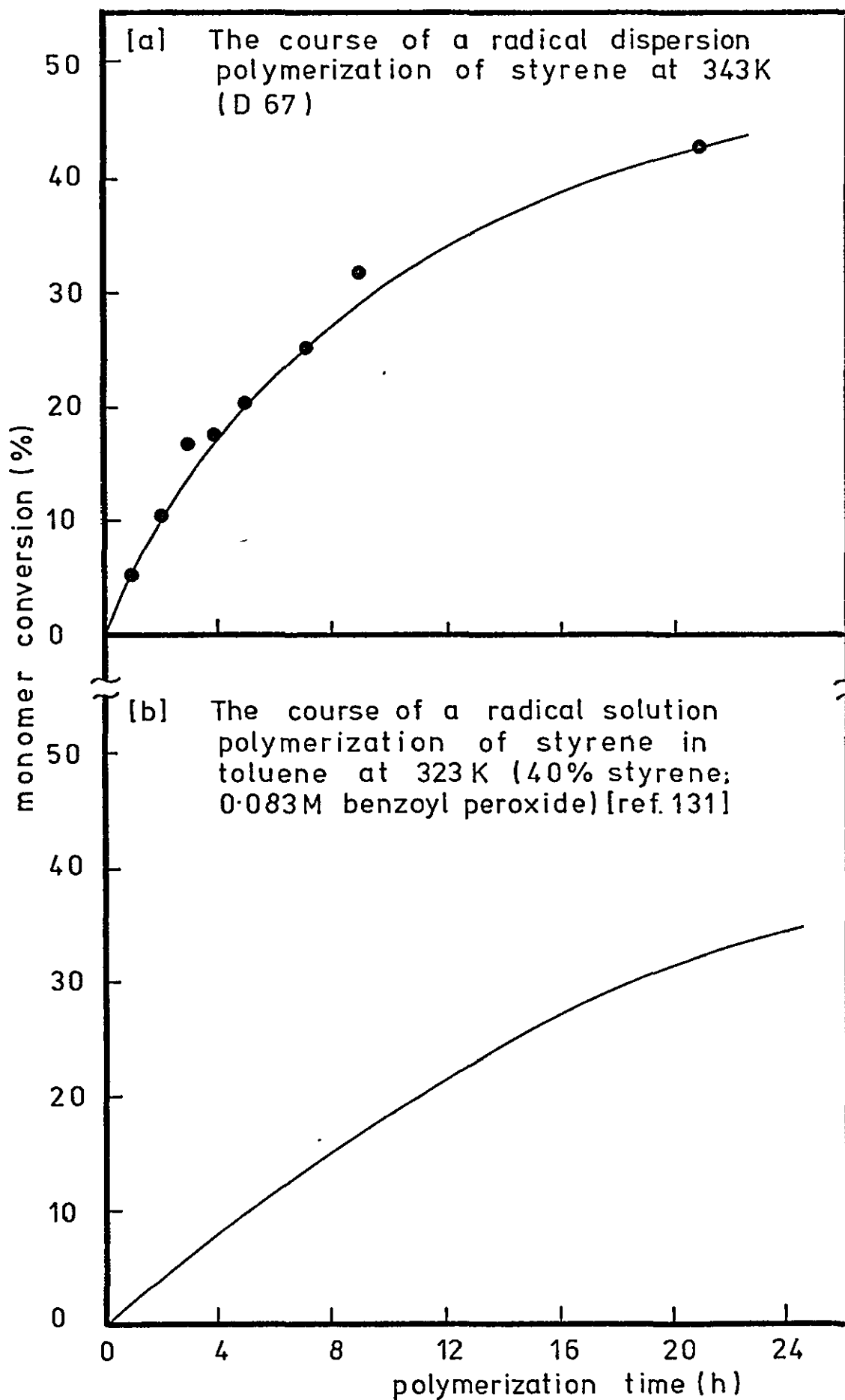| No.	Monomer Conversion [%]	Average Particle Size [μm]	Particle Size Distribution	$\bar{M}_n$ of Dispersed Phase
D1	55	>1	broad	18 000
D18	20	1.25	1.3	–
D19	47	0.58	1.2	8 600
D20	54	~1	–	–
D23	62	~1	–	–
D26	46	~0.4	1.8	5 000
D29	61	>1	–	–
D37	–	>1	broad	–
D48	43	>1	broad	–
D67	43	–	–	–
D94	57	>1	–	–

Table 4.4

Results of the Anionic Dispersion Polymerization of Styrene

No.	Monomer Conversion [%]	Average Particle Size [μm]	Particle Size Distribution	$\bar{M}_n$ of Dispersed Phase	% Si in Dispersed Phase	Remarks
D34	34	>1	-	-	-	Partially flocculated
D52	32	~0.3	broad	-	-	
D56	15	~1	-	-	-	
D57	30	>1	-	-	-	
D62	-	-	-	9 700	-	Particles dissolved to detect trapped anions
D64	81	0.21	1.08	17 500	0.70	
D72	-	>1	-	-	-	Partially flocculated
D73	89	0.2	1.1	-	-	Conversion/time followed
D77	72	>1	-	-	-	Partially flocculated
D95	33	~1	-	-	-	
D97	78	>1	-	10 000	-	Incremental initiator feed – flocculation at 78% conversion

Table 4.5

Results of the Anionic Dispersion Polymerization of Styrene (cont.)

No.	Monomer Conversion [%]	Average Particle Size [μm]	Particle Size Distribution	% Si in Dispersed Phase
D98	65	>1	-	-
D99	89	>1	-	-
D100	47	0.32	1.07	0.69
D103	71	>1	-	-
D104	13	>1	-	-
D106	62	>1	-	-
D107	30	0.36	1.00	0.94
D108	56	>1	-	-
D110	48	>1	-	0.64
D112	62	-	-	-

Table 4.6

Results of the Radical Dispersion Polymerization of Methyl Methacrylate

No.	Monomer Conversion [%]	Average Particle Size [μm]	Particle Size Distribution	% Si in Dispersed Phase	$\bar{M}_n$ Dispersed Phase
043	~80	0.54	1.16	-	-
044	80	0.25	1.01	1.16	130 000
049	70	0.39	1.02	0.60	-
051	60	~0.3	-	-	-
055	98	0.48	1.01	0.56	300 000
066	66	-	-	-	15 800
074	91	0.069	1.16	3.09	-
075	98	~0.07	-	-	-
076	90	0.096	1.03	3.17	-
078	dispersion flocculated	-	-	-	-
079	96	0.11	1.01	1.39	-
080	95	0.074	1.02	2.87	-
084	93	0.13	1.01	2.16	430 000
088	95	0.095	1.01	3.12	-
089	83	0.67	1.14	3.36	-

Table 4.7

Results of the Radical Dispersion Polymerization of Methyl Methacrylate (cont.)

No.	Monomer Conversion [%]	Average Particle Size (μm)	Particle Size Distribution	% Si in Dispersed Phase	$\bar{M}_n$ Dispersed Phase
D90	95	0.35	1.01	0.71	–
D91	97	0.22	1.00	1.46	–
D101	90	0.33	1.01	0.62	–

Table 4.8

Characterization of Micellar Dispersions

No.	Average Particle Size (μm)	Particle Size Distribution	% Si in Dispersed Phase
085	very coarse	wide	2.72
086	0.044	1.01	14.06
087	0.044	1.01	14.06
0102	0.044	1.01	14.06
0113	0.11	1.01	8.09
0114	0.044	1.01	14.06
0115	0.17	1.00	5.26
0116	> 3	wide	4.39

Table 4.9

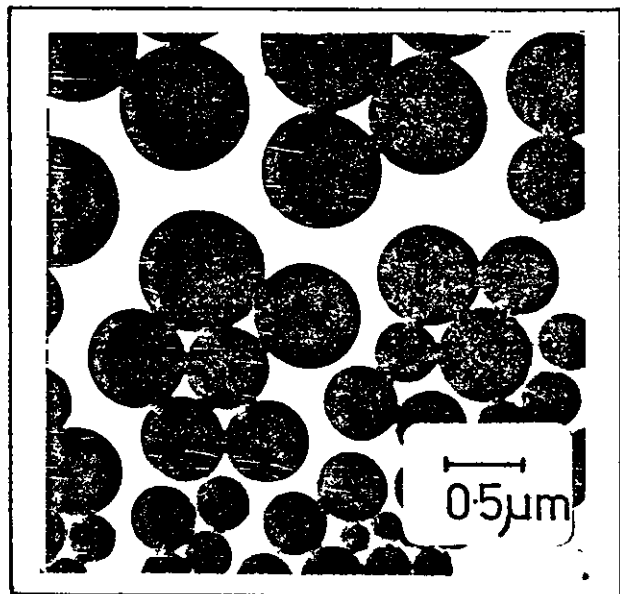# FIGURE 4.7

TRANSMISSION ELECTRON MICROGRAPHS

[a] one-stage PS
     dispersion
     polymerization
     (D18)
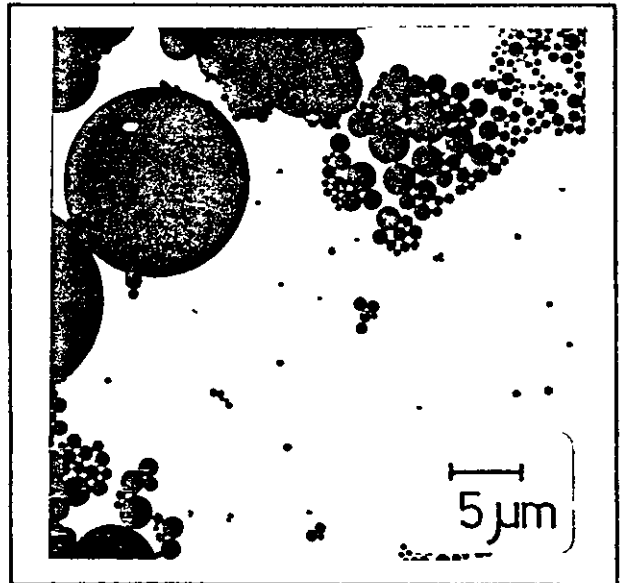
[b] seeded PS
     dispersion
     polymerization
     (D19)

[c] as [b] after
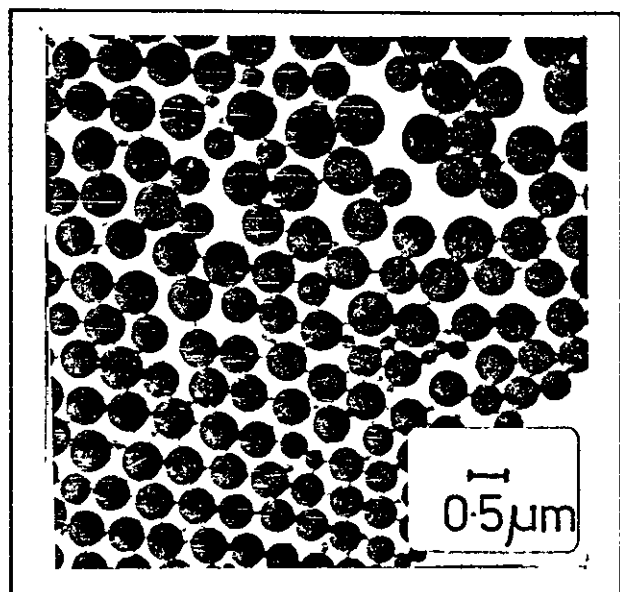   several
     redispersion
     cycles

FIGURE 4.8

TRANSMISSION ELECTRON MICROGRAPH
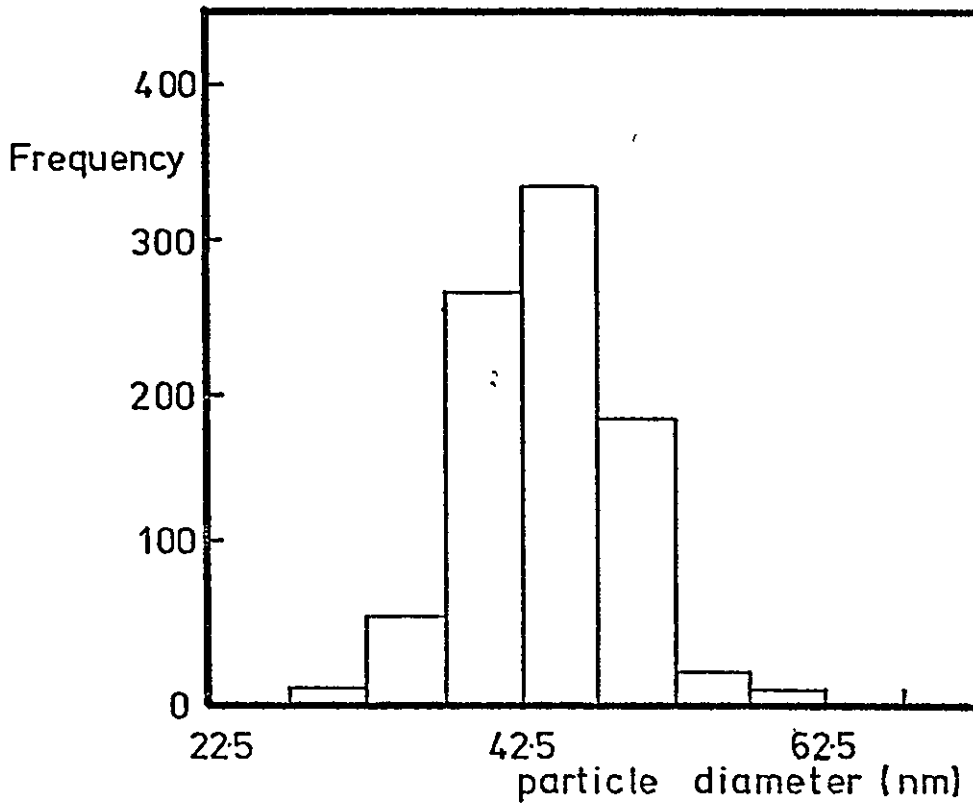AND PARTICLE SIZE DISTRIBUTION OF
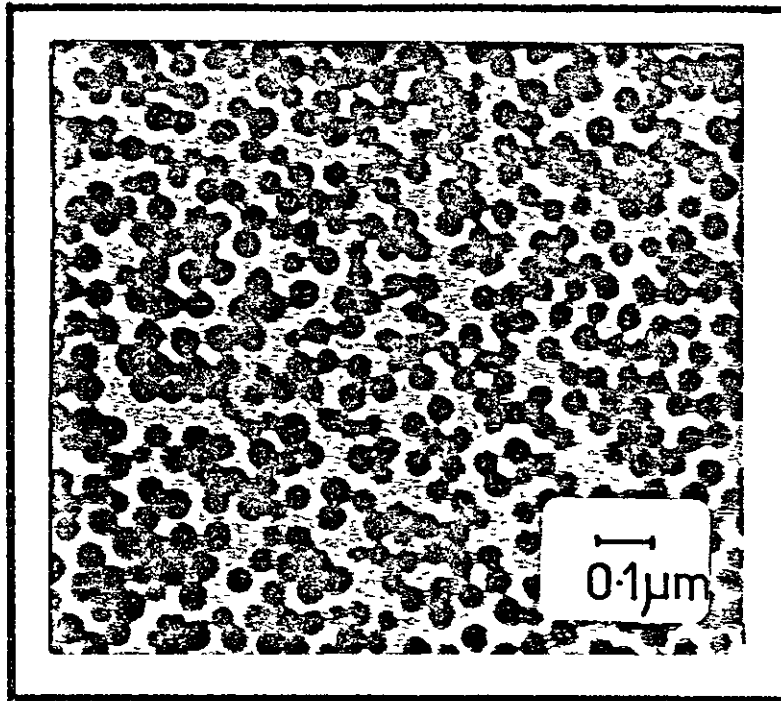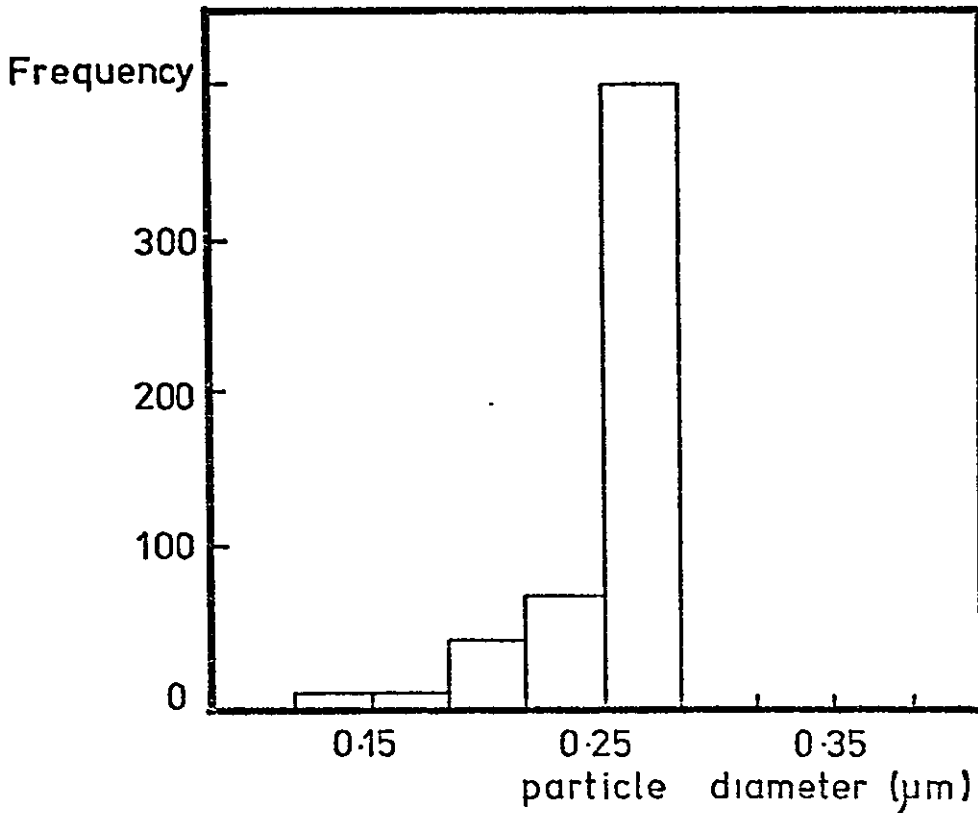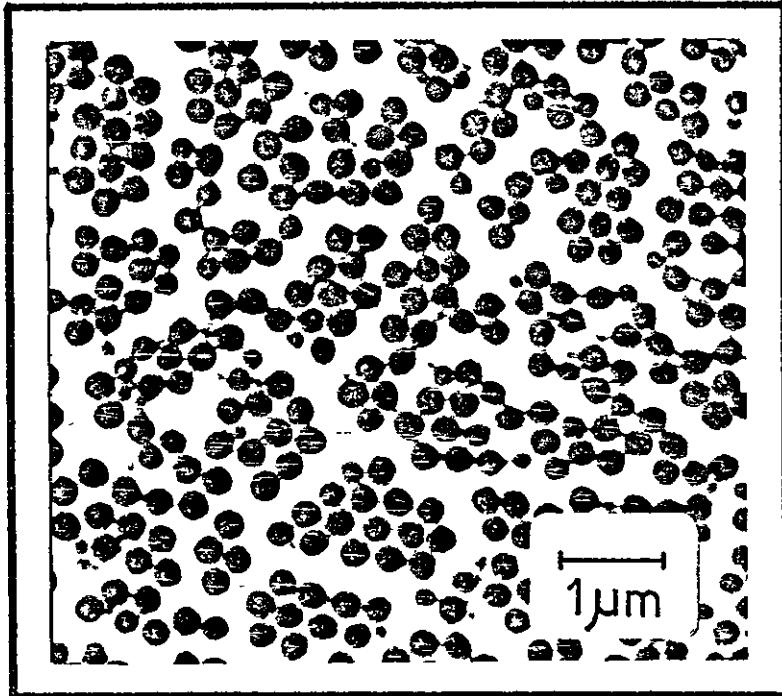MICELLAR DISPERSION D 86

FIGURE 4.9

TRANSMISSION ELECTRON MICROGRAPH
AND PARTICLE SIZE DISTRIBUTION OF
PMMA DISPERSION D 44

particle diameters were measured and histograms constructed as shown. The average particle diameters quoted are the number average $[\bar{D}_n]$ given by

$$\bar{D}_n = \frac{\sum N_i D_i}{\sum N_i} \qquad (4.3)$$

where N_i is the number of particles of diameter D_i. This average represents the ratio of the first and zeroth moments of the distribution. An indication of the breadth of the particle size distribution was given by the ratio $\bar{D}_s/\bar{D}_n$, where $\bar{D}_s$ is given by

$$\bar{D}_s = \frac{\sum N_i D^2_i}{\sum N_i D_i} \qquad (4.4)$$

$\bar{D}_s$ represents the ratio of the second to the first moment of distribution.

Light Scattering

An estimate of the particle size of two dispersions, D84 and D74, was made using dissymmetry methods. Each sample was studied dispersed in Freon 113, of measured refractive index 1.356, and a mixture of n-dodecane and n-heptane of measured refractive index 1.404. The refractive index of three samples of PDMS homopolymer [S2, S4 and S7] was found to be 1.404.

For each dispersion, the intensity [I] at various angles was measured, and the background intensity of the pure dispersion medium $[I_B]$ was subtracted. The dissymmetry $[I_\theta/I_{180^\circ - \theta}]$ was calculated at each angle. From equation 2.45 and figure 2.11 [Section 2.4.2], D/λ' was obtained from the dissymmetry The wavelength of light in the medium $[\lambda']$ was given by 546/refractive index of the dispersion medium, and hence D was calculated.

Tables 4.10 and 4.11 summarize these results.

Results of Dissymmetry Measurements for D84

System	Angle	40°	50°	60°	70°	80°	100°	110°	120°	130°	140°
D84 in alkane mixture concentration 4×10^{-4} g dl^{-1}	$I - I_b$	0.498	0.368	0.249	0.193	0.156	0.110	0.095	0.094	0.094	0.099
	$I_\theta / I_{180^{\circ} - \theta}$	5.03	3.92	2.65	2.03	1.42	Average $D/\lambda' = 0.478$				
	D/λ'	0.480	0.495	0.468	0.475	0.470	Hence $\underline{D = 192 \text{ nm}}$				

System	Angle	50°	60°	70°	80°	100°	110°	120°	130°
D84 in Freon 113 concentration 5×10^{-4} g dl^{-1}	$I - I_b$	1.23	0.725	0.506	0.360	0.251	0.213	0.211	0.229
	$I_\theta / I_{180^{\circ} - \theta}$	5.35	3.43	2.38	1.56	Average $D/\lambda' = 0.521$			
	D/λ'	0.520	0.530	0.520	0.515	Hence $\underline{D = 210 \text{ nm}}$			

Table 4.10

Table 4.11

Results of Dissymmetry Measurements for D74

System	Angle	$50°$	$60°$	$70°$	$80°$	$100°$	$110°$	$120°$	$130°$
D74 in alkane mixture concentration 7×10^{-4} g dl^{-1}	$I-I_b$	0.535	0.445	0.403	0.371	0.328	0.290	0.278	0.291
	$I_\theta/I_{180°-\theta}$	1.84	1.60	1.39	1.16	Average D/λ' = 0.335			
	D/λ'	0.330	0.330	0.335	0.345	Hence D = 131 nm			

System	Angle	$40°$	$50°$	$60°$	$70°$	$80°$	$100°$	$110°$	$120°$	$130°$	$140°$
D74 in Freon 113 concentration 6×10^{-5} g dl^{-1}	$I-I_b$	3.35	1.95	1.38	1.01	0.77	0.55	0.52	0.51	0.55	0.63
	$I_\theta/I_{180°-\theta}$	5.32	3.55	2.71	1.94	1.40	Average D/λ' = 0.472				
	D/λ'	0.480	0.475	0.473	0.460	0.470	Hence D = 190 nm				

Small-Angle X-ray Scattering

Small-angle X-ray scattering from samples of D84 and D87 was used to estimate particle size. Manual smoothing of the scattering curve compensated for statistical counting fluctuations, and the data were desmeared using a computer program written by Dijkstra, Kortleve and Vonk [132]. The method of Guinier was used to calculate the radius of gyration of the particles. From a plot of log(desmeared intensity I) vs. ε^2 (where ε is the scattering angle) the radius of gyration (R_o)·could be found from the slope, using Guinier's equation (equation 2.47 in Section 2.4.3). Hence the radius (R) of the particles was found,since for a sphere

$$R_o = (\tfrac{3}{5})^{\frac{1}{2}}R \qquad\qquad (4.5)$$

Figures 4.10 and 4.11 show Guinier plots for D87 and D84 respectively. For D84 the plot was curved, and therefore the limiting slope was taken [113].

Values obtained for diameter of the particles were as follows

    D87 dispersed in dodecane   D = 44 nm

    D84 dispersed in n-heptane   D = 133 nm

    D84 dried disperse phase   D = 119 nm

4.3.3 Stabilizer Anchoring Mechanism

A sample of the stabilizer [B15] adsorbed onto low molecular weight PMMA particles [D66] was isolated as described in Section 3.7.3. G.P.C. analysis of the isolated stabilizer gave a PS equivalent $\bar{M}_n$ value of 19 300 and polydispersity ratio of 1.26. These values are comparable with those obtained from a G.P.C. analysis of the original
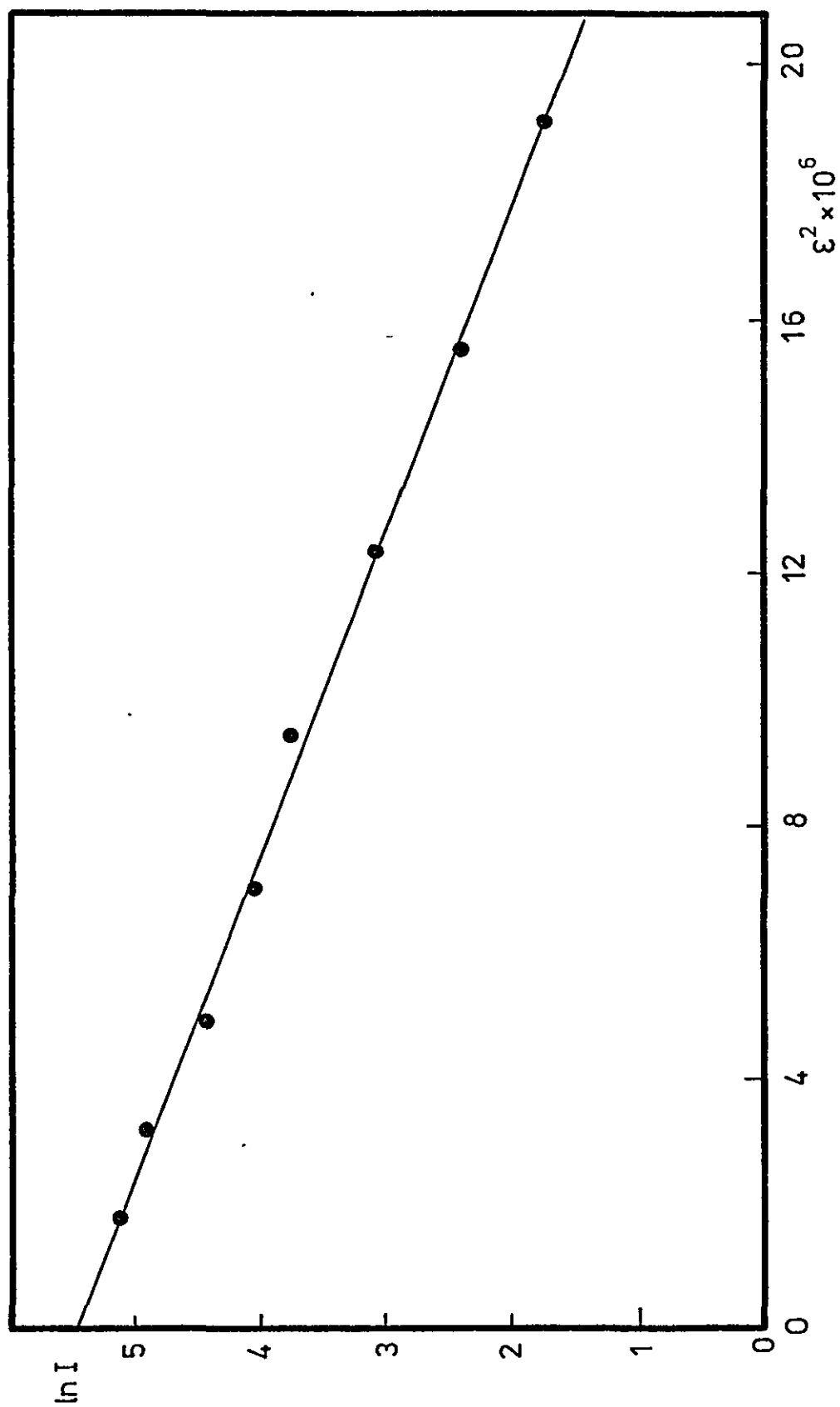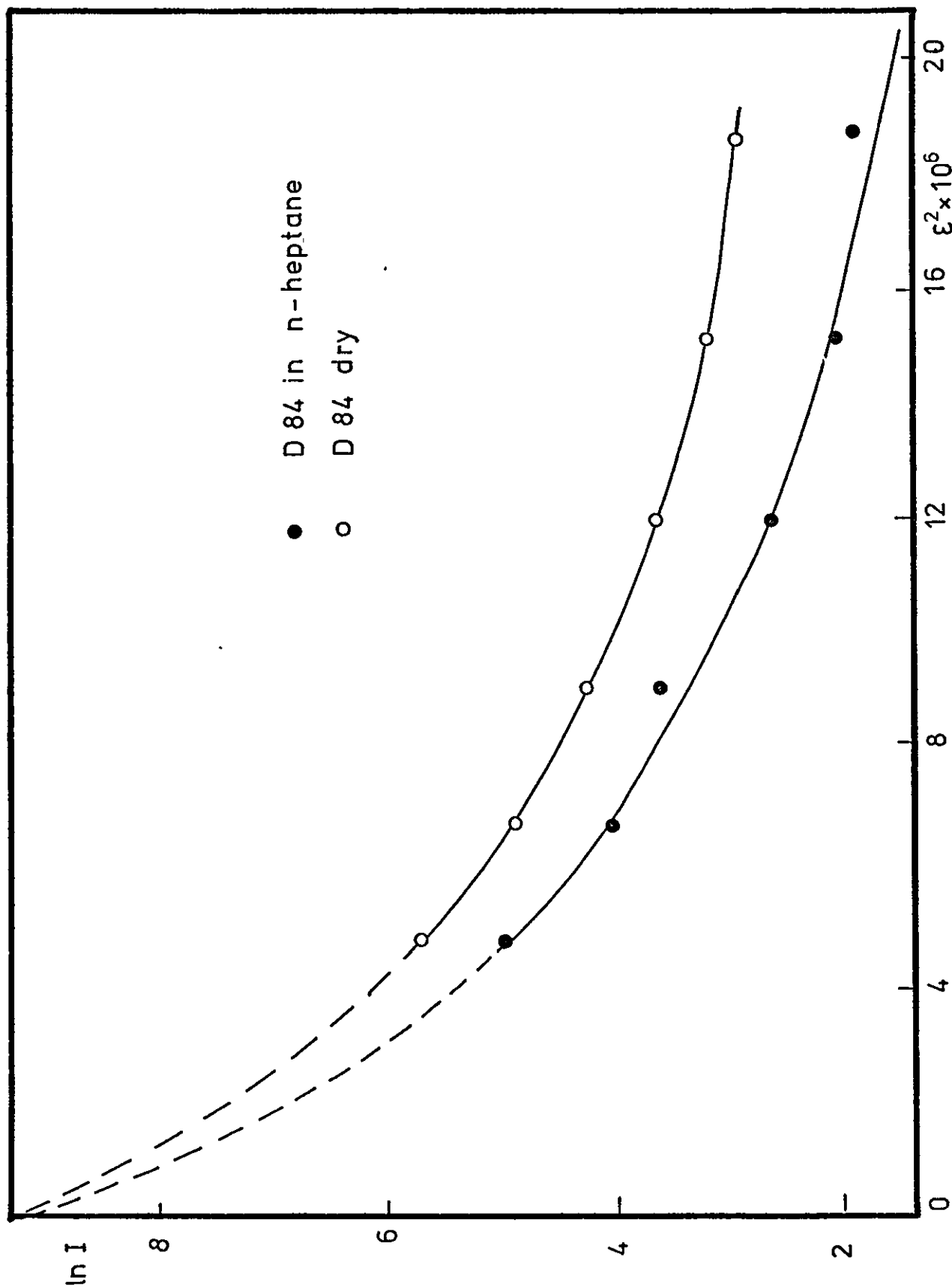
FIGURE 4.10

GUINIER PLOT FOR D87 IN n-DODECANE

FIGURE 4.11

GUINIER PLOT FOR D 84

stabilizer [$\bar{M}_n$ = 22 600, $\bar{M}_w/\bar{M}_n$ = 1.18]. The small decrease in $\bar{M}_n$ and increase in the polydispersity ratio are consistent with the presence of a small amount of residual PMMA. The conclusion is, therefore, that grafting of the stabilizer onto the PMMA particle core does not occur, since if this were the case, an apparent increase in the molecular weight of the isolated stabilizer would have resulted.

The efficiency of the anchoring mechanism of the stabilizer onto the particle surface was confirmed by redispersing samples of PMMA dispersions [D44 and D55] in cyclohexane. Such dispersions remained stable at 298 K, and even after 60 h at 333 K, only slight flocculation was noted, implied by a slightly faster rate of sedimentation. When such a dispersion was cooled to 298 K, the dispersion returned to its original state, showing that the flocculation was reversible.

Dispersions of PMMA were invariably unaffected by ultrasonic vibration. Whilst most PS dispersions also behaved in this way, D100 quickly flocculated when subject to ultrasonic vibration.

4.4   PROPERTIES OF NON-AQUEOUS DISPERSIONS

4.4.1   Rheology

All rheological studies were performed using an Ostwalde-Fenske type viscometer at 298 ± 0.02 K. Flow times for the pure dispersion medium were of the order 200 s and reproducibility was better than ± 1%. Relative viscosities [η_r] for dispersions at various volume fractions of polymer were measured, and converted to absolute viscosities using literature values [133] for the viscosities of the dispersion

media used. The volume fraction of the polymer particle cores
(ϕ_o) was calculated from a knowledge of the total polymer
content of the dispersion, the PDMS content and the density
of the core. The core density was taken as that of the
appropriate bulk polymer (1.19 g cc^{-1} for PMMA and 1.04 g cc^{-1}
for PS (17)), and allowance was made for the swelling of the
low molecular weight PS core of micellar dispersions D102 and
D11 4. This swelling behaviour, estimated by Pléstil and
Baldrian(134) to correspond to about a 6% increase in
diameter, is discussed further in Section 5.2.1.

Figure 4.12 shows the plot of viscosity vs. ϕ_o for PMMA
particles of various diameter (D) in heptane, stabilized by
the same block copolymer (B15). Several points determined at
low ϕ_o values have been omitted for clarity. The viscosity
of the dispersion is seen to increase with decreasing particle
diameter. Waters and Walbridge (6) have determined the
thickness of the soluble layer (δ in equation 2.41) from the
slope of such a curve at $\phi_o = 0$. The errors which can arise
from such a method are large, and so for the present work the
method of Barsted et al. (124) was adopted. $\phi_o/\ln \eta_r$ was
plotted against ϕ_o, and the method of least squares was used
to determine the best straight line through the points
(figure 4.13).' From equation 2.42 the intercept of such a
curve is the reciprocal of the effective Einstein coefficient
$(\alpha_o f)$ and the crowding factor, k, can be obtained from the
slope (k/α_o). A plot of $(\alpha_o f)^{1/3}$ vs. D^{-1} was linear, as seen
in figure 4.14. From equation 2.44 the ratio of the slope to
the intercept of this curve gave a value of 8.9 nm for δ.
From the intercept, a value of 2.49 ± 0.08 was found for α_o
which is in good agreement with the Einstein coefficient of

FIGURE 4.12

VARIATION OF VISCOSITY [η] OF DISPERSIONS OF DIFFERING PARTICLE DIAMETER [D] WITH PARTICLE PHASE VOLUME FRACTION [ϕ_o]
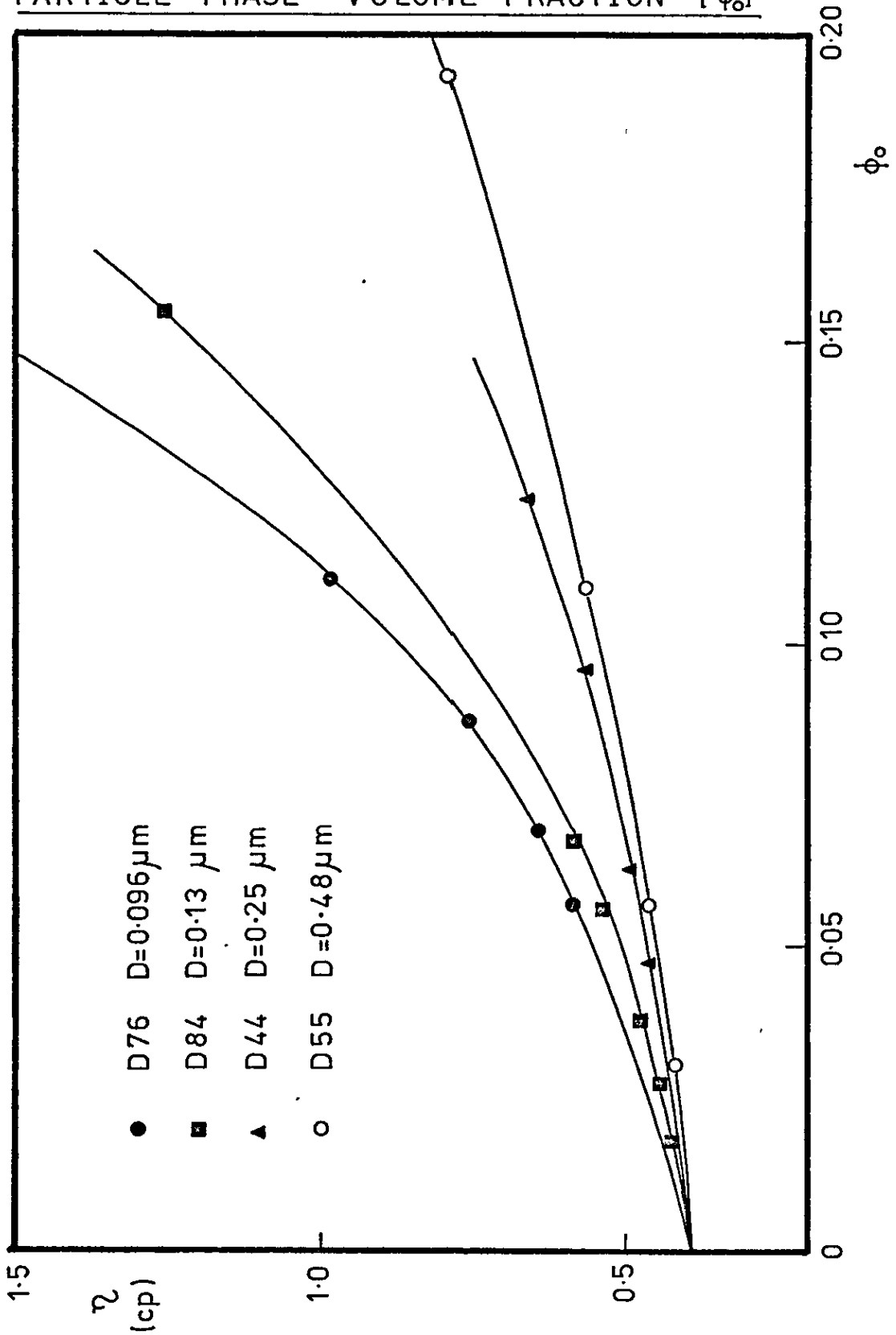
FIGURE 4.13

$\dfrac{\phi_\circ}{\ln\eta_r}$ vs $\phi_\circ$ FOR PMMA DISPERSIONS OF
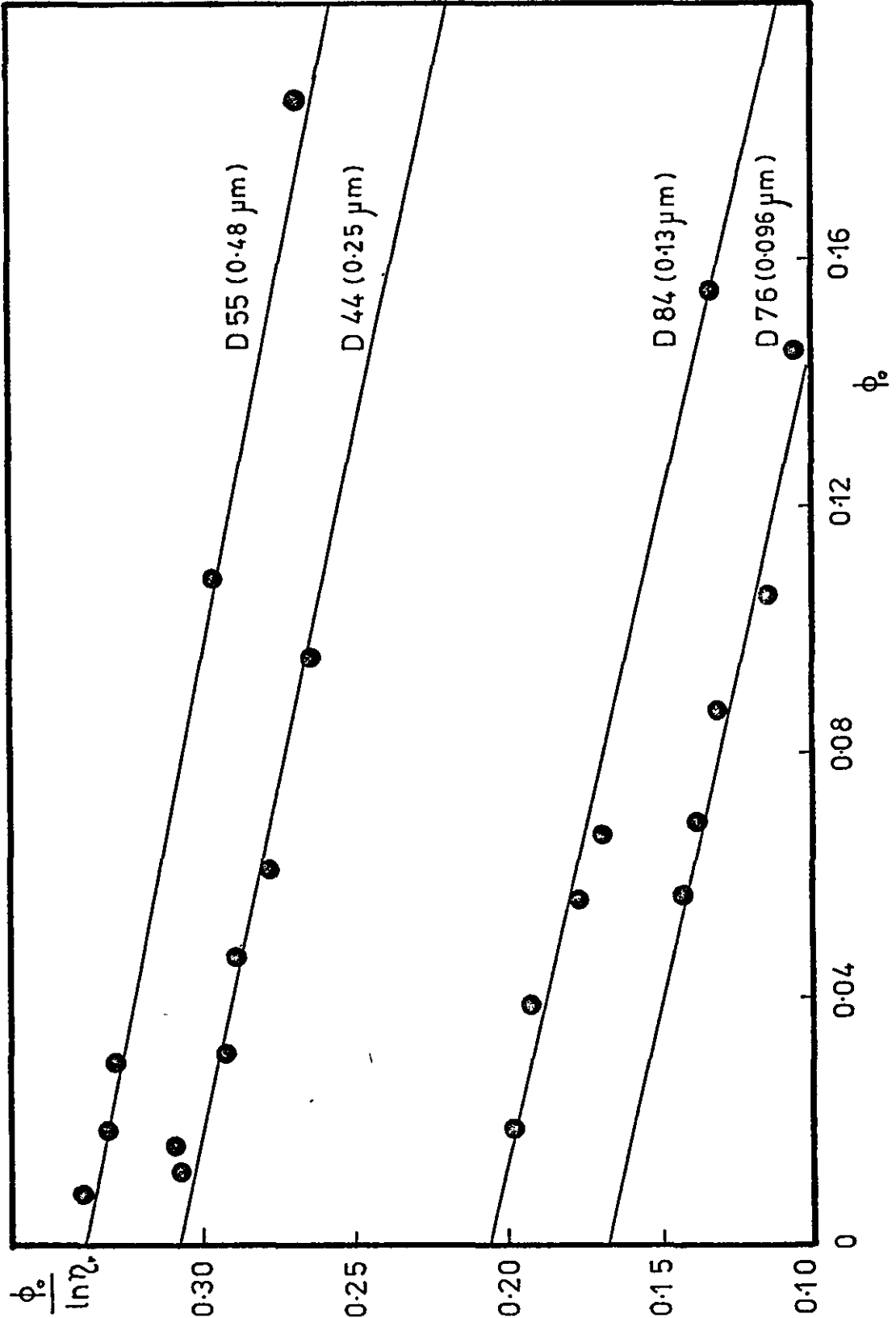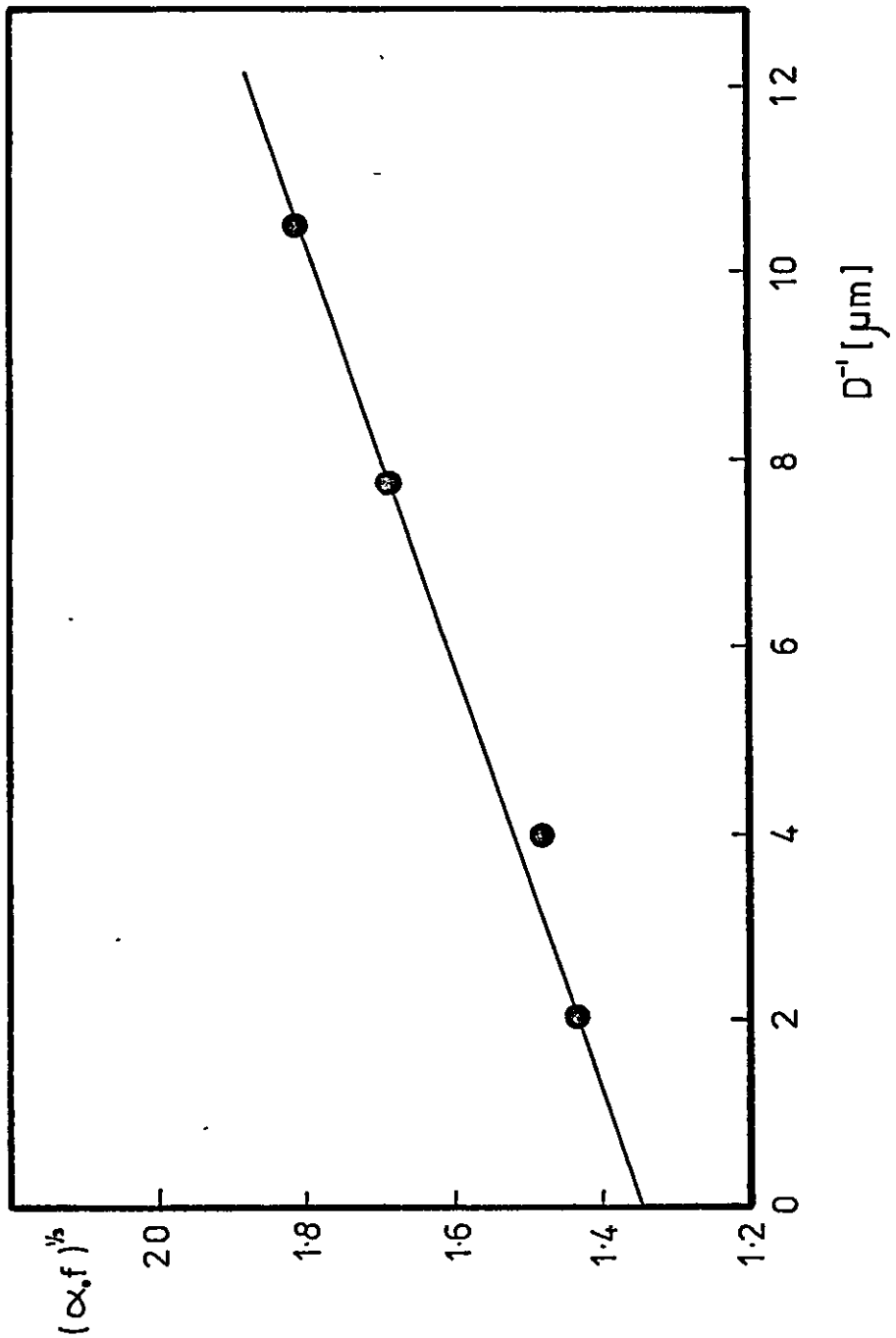
DIFFERING PARTICLE DIAMETER

FIGURE 4.14

$(\alpha_\circ f)^{1/3}$ vs. D^{-1} FOR PMMA PARTICLES
- D 76 , D 84 , D 44 , D 55

2.50. Figures 4.15 and 4.16 show the equivalent curves for PS dispersions each stabilized by PDMS of similar molecular weight. Again the intercept confirms a value for α_o (2.54 ± 0.09) which is close to 2.50.

Dispersions stabilized by a range of stabilizer compositions and molecular weights were studied, with both PS and PMMA particle cores. Figure 4.17 shows the increase in viscosity which resulted from increasing the molecular weight of the PDMS block of the stabilizer, for three dispersions of similar particle size. Plots of $\phi_o/\ln\eta_r$ vs. ϕ_o are given in figures 4.15, 4.18 and 4.19. Values for δ were calculated directly from equation 2.44 taking values of D from electron microscopy and 2.5 for α_o. An error of 6% was estimated on values of δ. The crowding factor k was found from the slope of the curves, and the results are summarized in tables 4.12 to 4.14.

Figures 4.20 and 4.21 show the variation of δ with the molecular weight of the PDMS block of the stabilizer. For comparison, the fully extended end-to-end length and diameter of gyration $(2\langle s^2 \rangle^{\frac{1}{2}})$ for PDMS in heptane are plotted as a function of molecular weight. These molecular dimensions were calculated as described in the Appendix.

4.4.2 Flocculation Studies

The critical flocculation volume (c.f.v.) and critical flocculation temperature (c.f.t.) for dispersions of PMMA particles of differing particle size are given in table 4.15. The stabilizer was the same for all these dispersions.

Table 4.15 shows that the flocculation points were independent of the particle size. It was also noted that

FIGURE 4.15

$$\frac{\phi_o}{\ln \eta_r} \text{ vs. } \phi_o \quad \text{FOR MICELLAR DISPERSIONS}$$

$$- \quad D\,102 \text{ , } D\,113 \text{ , } D\,114 \text{ , } D\,115$$
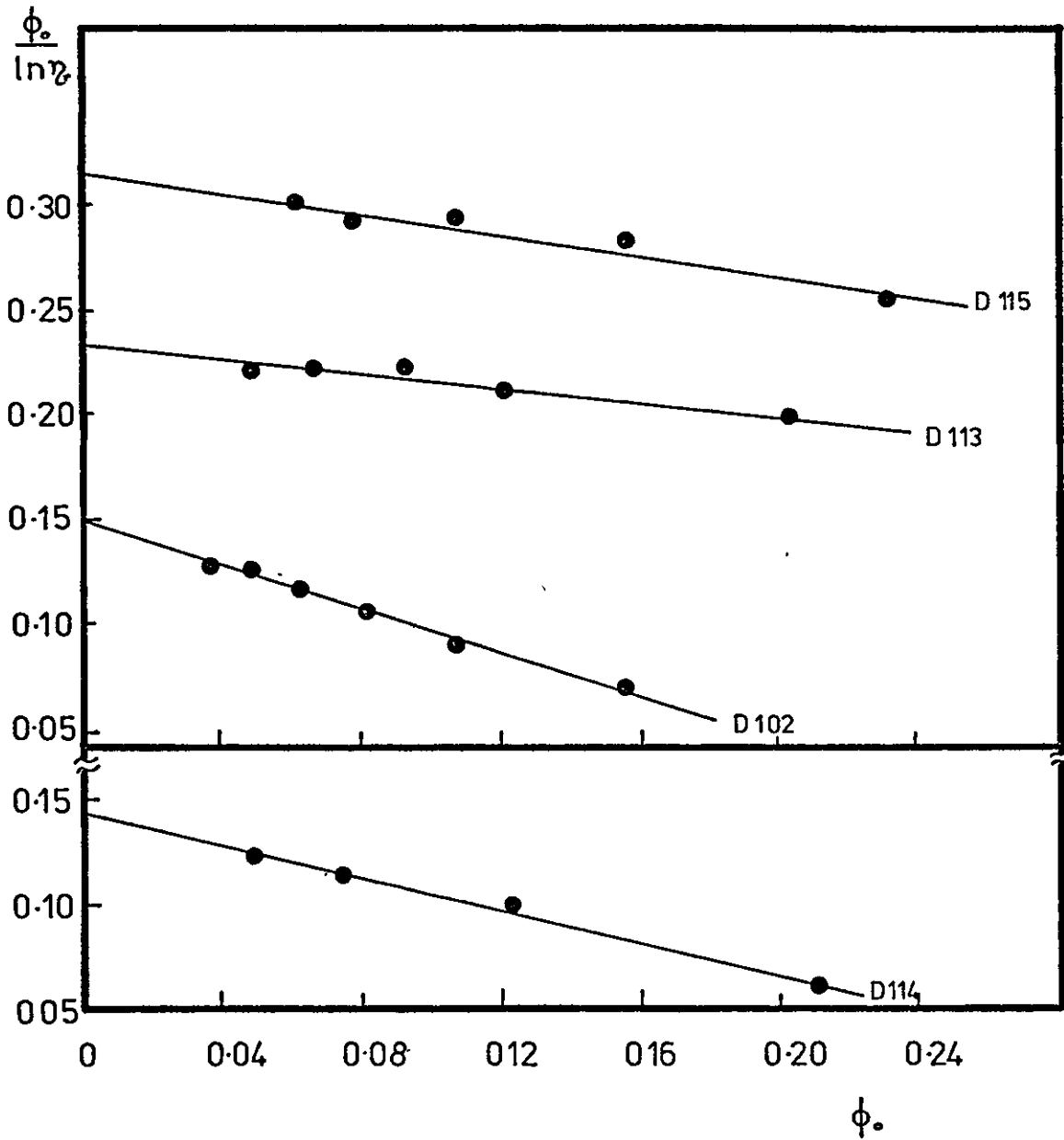
FIGURE 4.16

$(\alpha . f)^{1/3}$ vs. D^{-1} FOR MICELLAR & PS PARTICLES — D64, D102, D113, D114, D115.

FIGURE 4.17

VARIATION OF η WITH ϕ. FOR PMMA
DISPERSIONS OF SIMILAR PARTICLE SIZE
AND DIFFERING PDMS MOLECULAR WEIGHT
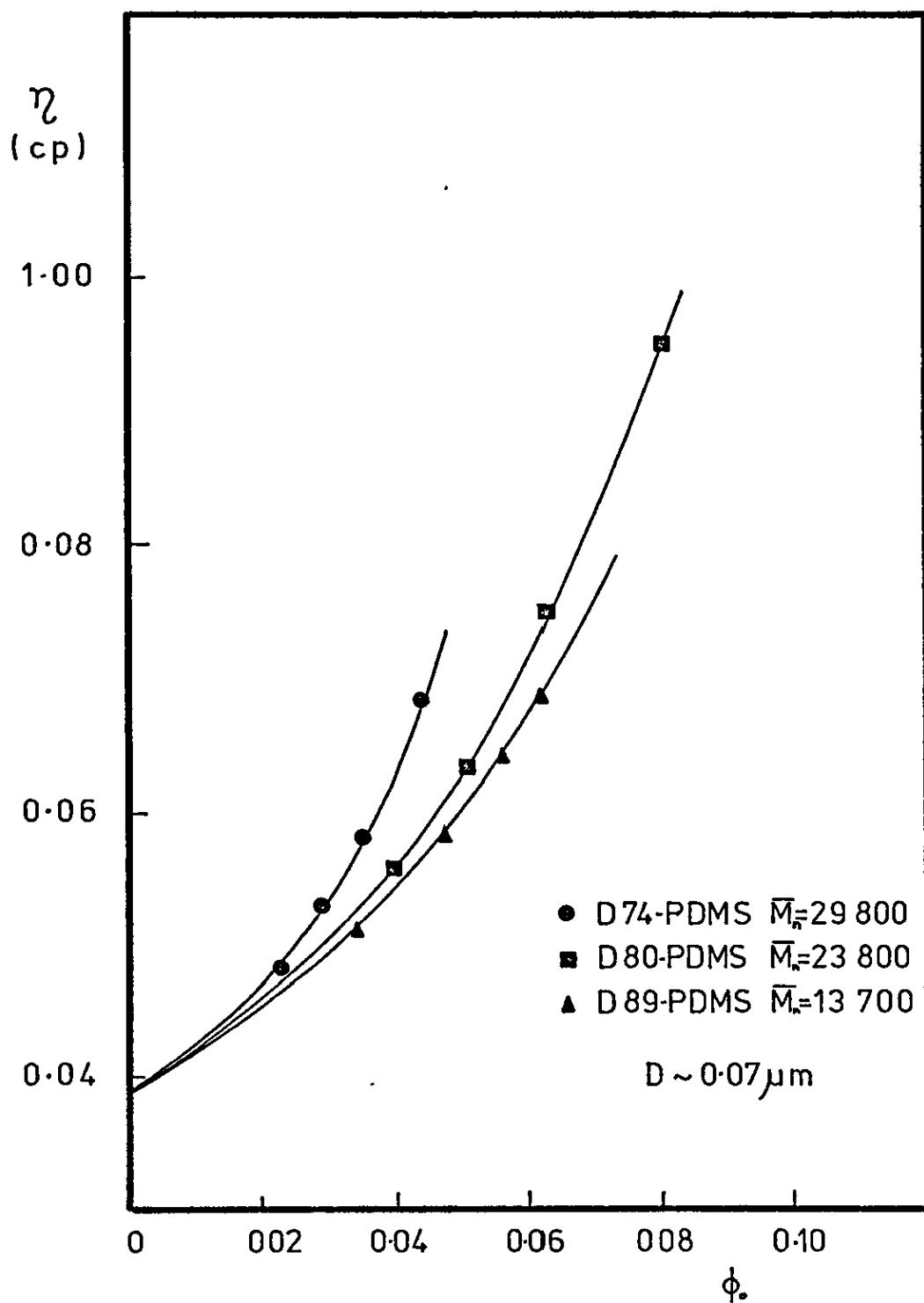
FIGURE 4.18

$\frac{\phi_o}{\ln \eta_r}$ vs. ϕ_o FOR PMMA DISPERSIONS

— D 49 , D74 , D79 , D80 , D88 , D89.
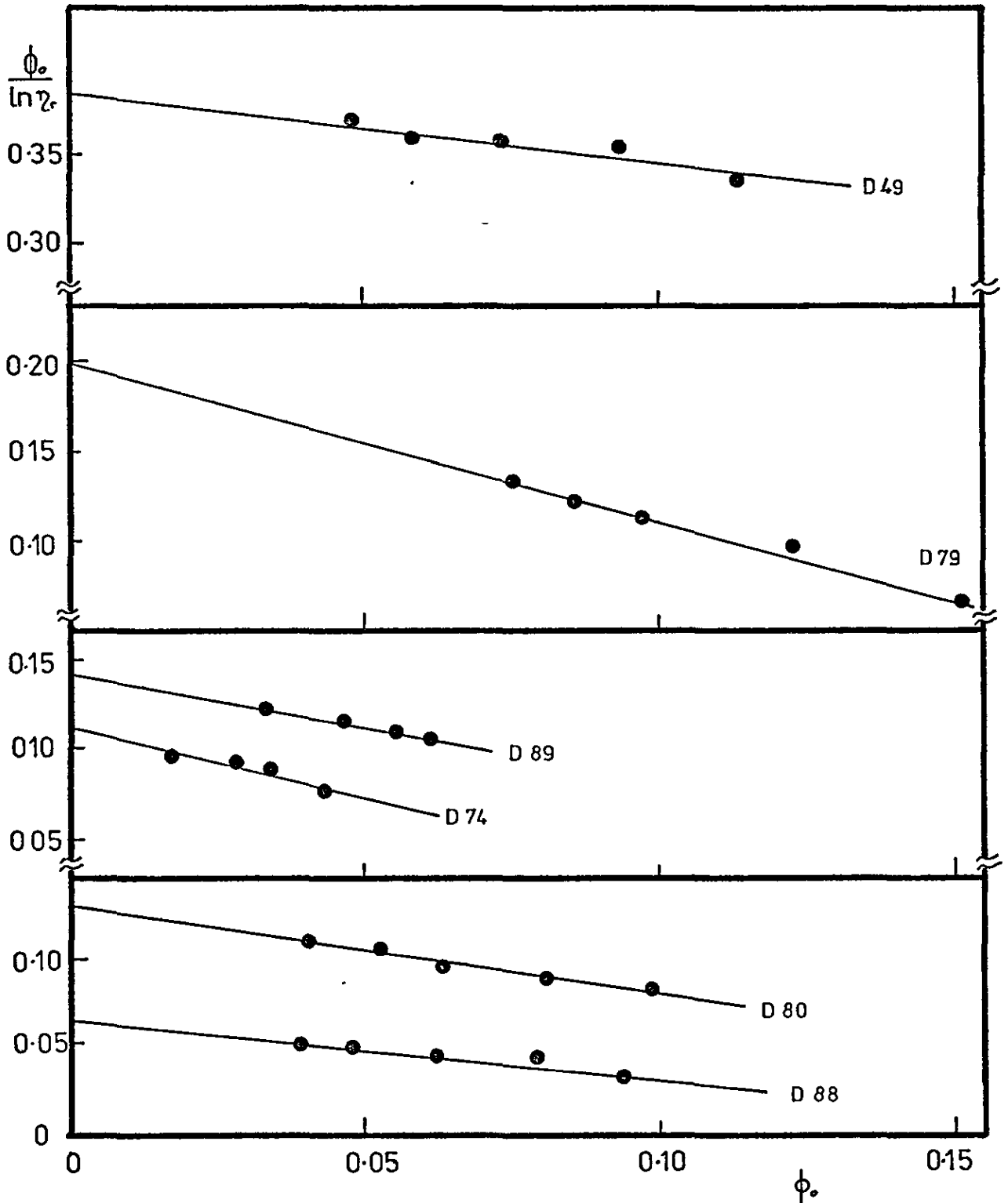
FIGURE 4.19

$$\frac{\phi_o}{\ln \eta_r} \text{ vs } \phi_o \quad \text{FOR PS DISPERSIONS}$$

— D 64 , D 100 , D 107.
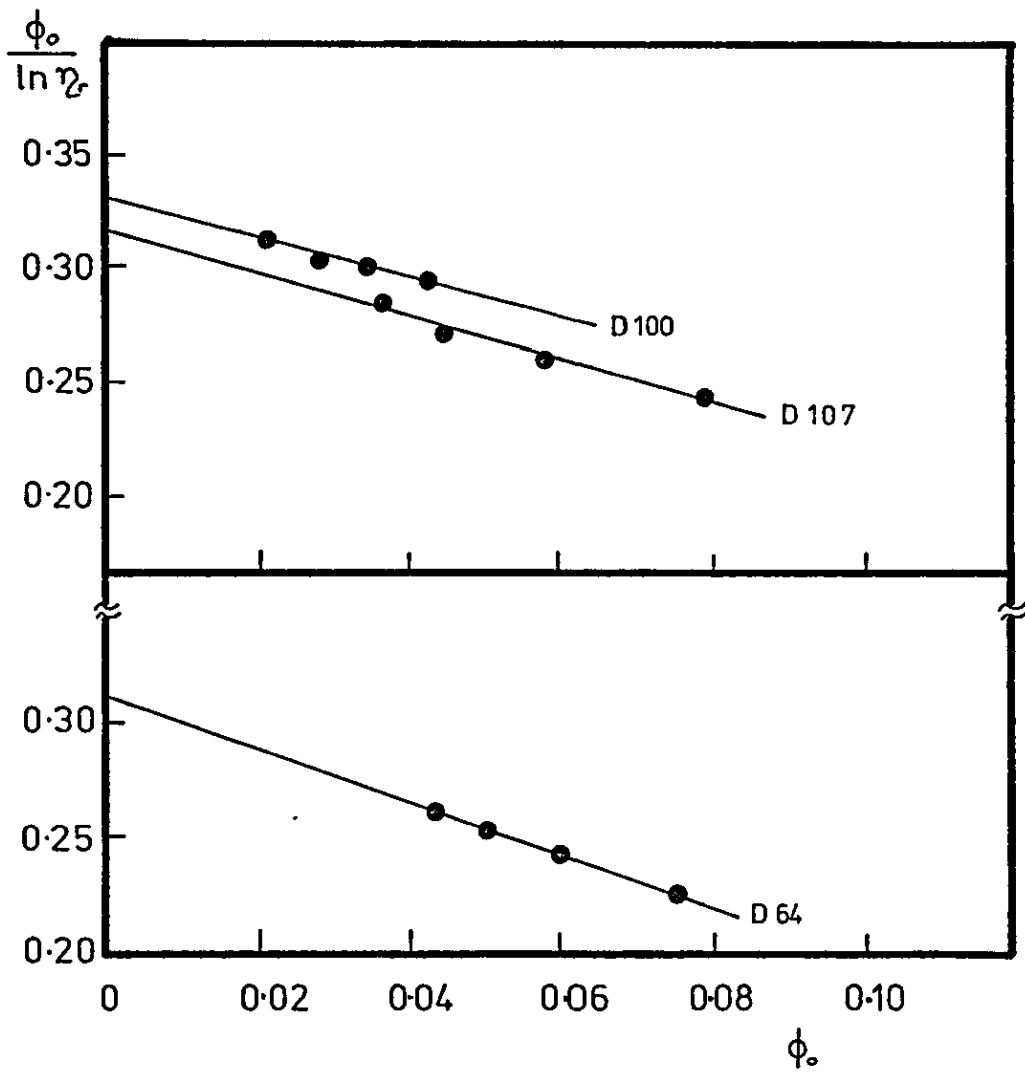
Table 4.12

Rheology of PMMA Dispersion in n-heptane

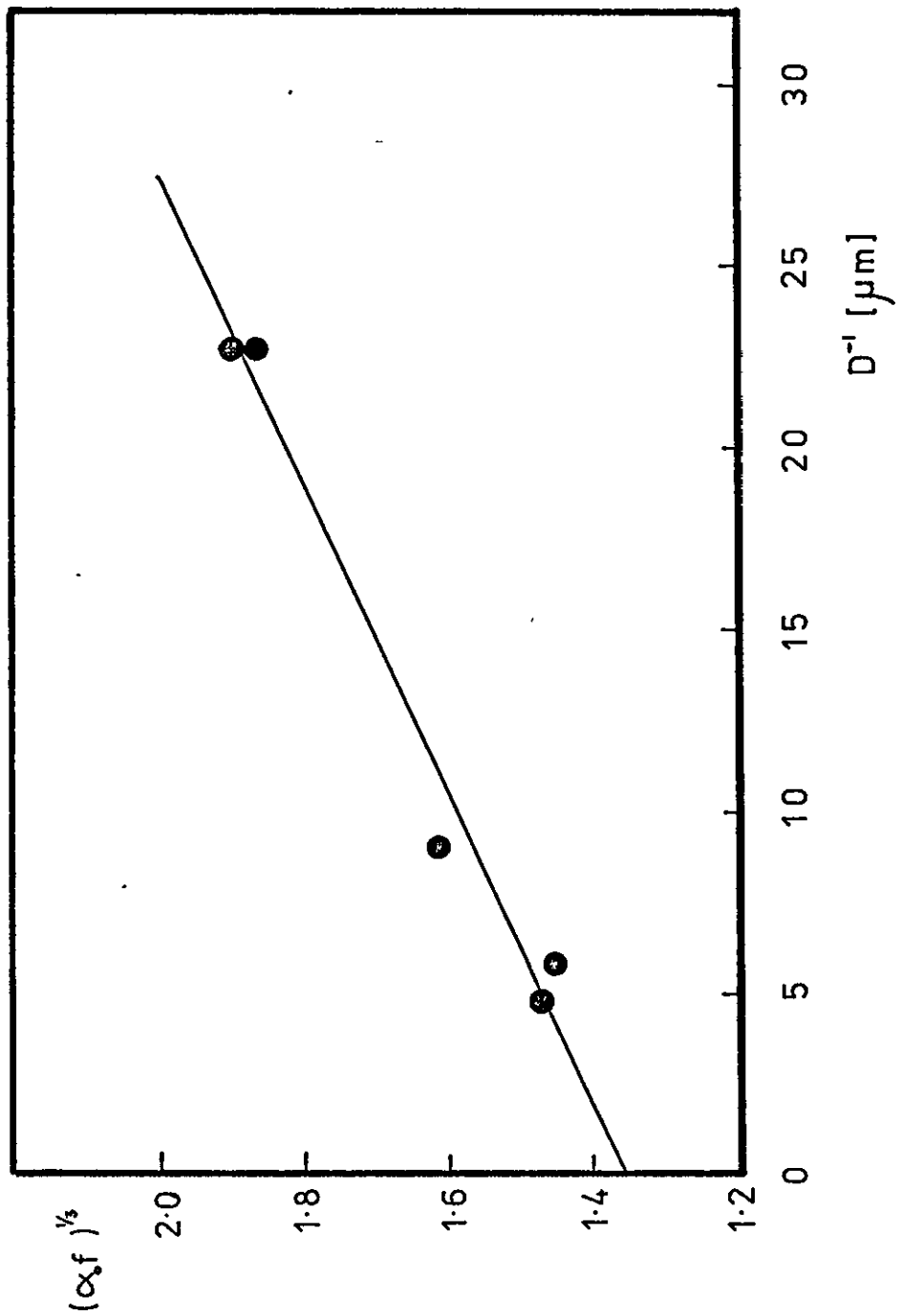| Dispersion Number	Stabilizer	$\bar{M}_n$ PDMS block	Particle Diameter D [μm]	δ [nm]
D79	B20	3 200	0.114	15.1
D49	B14	7 000	0.390	4.0
D76	B15	11 200	0.099	8.9
D84	B15	11 200	0.130	8.9
D44	B15	11 200	0.254	8.9
D55	B15	11 200	0.478	8.9
D89	B16	13 700	0.067	13.6
D80	B21	23 800	0.074	17.0
D74	B17	29 800	0.069	18.2
D88	B23	48 000	0.095	40.2

Table 4.13

Variation of the Crowding Factor (k) with Particle Size

Dispersion Number	Total Particle Diameter D + 2 [μm]	k
D89	0.094	1.48
D74	0.105	1.72
D80	0.108	1.26
D76	0.117	1.11
D79	0.144	1.30
D84	0.148	1.12
D88	0.175	0.72
D44	0.272	1.09
D49	0.398	0.88
D55	0.496	1.00

Table 4.14

Rheology of PS Dispersions

Dispersion Number	Stabilizer	$\bar{M}_n$ PDMS Block	Particle Diameter [μm]	δ [nm]	Dispersion Medium
D102	B1	3 300	0.044	6.6	n-heptane
D114	B1	3 300	0.044	7.2	n-dodecane
D115	B4	4 000	0.172	7.0	n-dodecane
D113	B3	5 000	0.113	11.2	n-dodecane
D64	B1	3 300	0.213	9.1	n-heptane
D100	B24	7 600	0.319	10.6	n-heptane
D107	B16	13 700	0.360	15.1	n-heptane

FIGURE 4.20

VARIATION OF δ WITH $\overline{M}_n$ PDMS BLOCK

OF PS-PDMS STABILIZER-PMMA PARTICLES
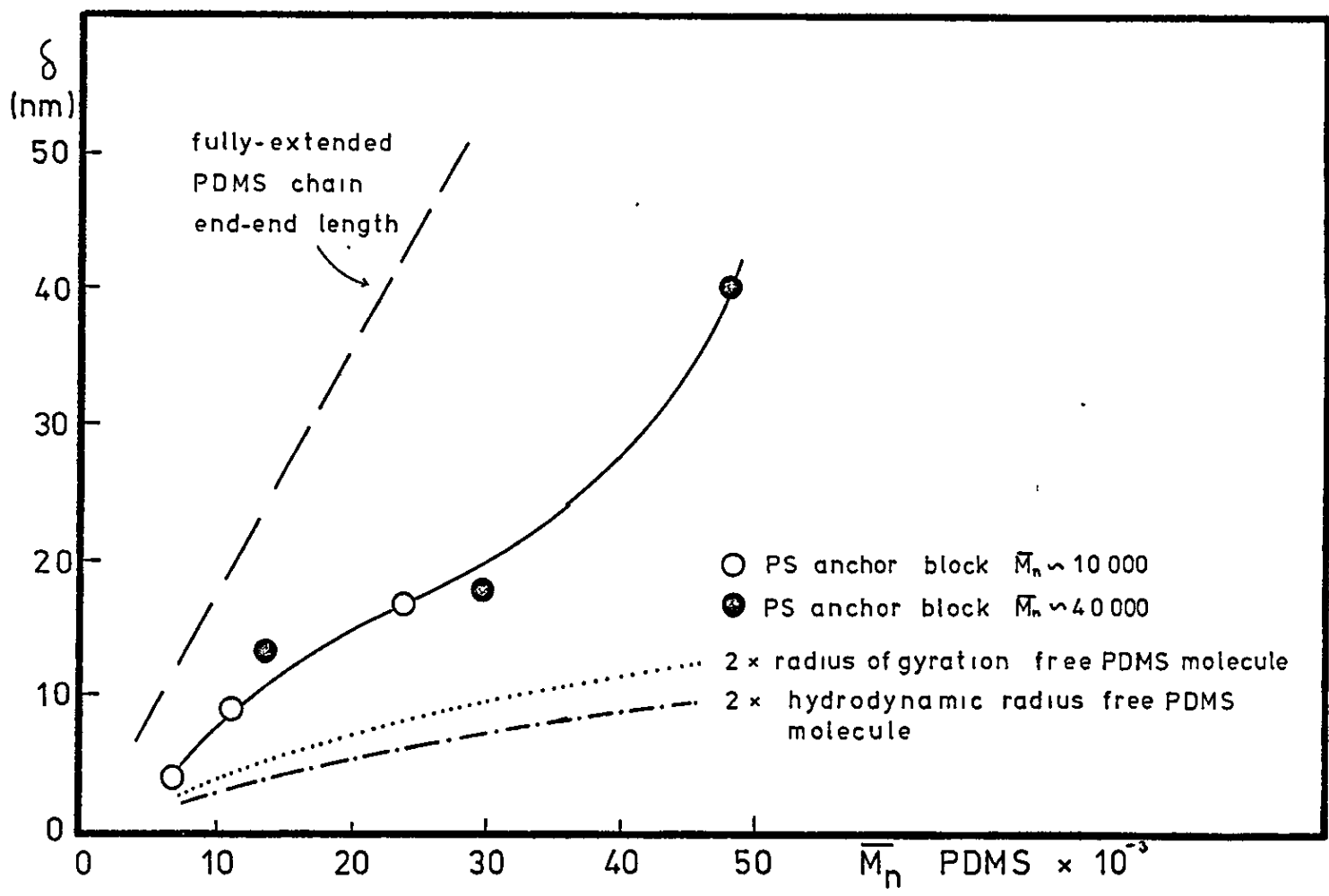
VARIATION OF δ WITH $\overline{M_n}$ PDMS BLOCK

OF PS-PDMS STABILIZER — PS PARTICLES
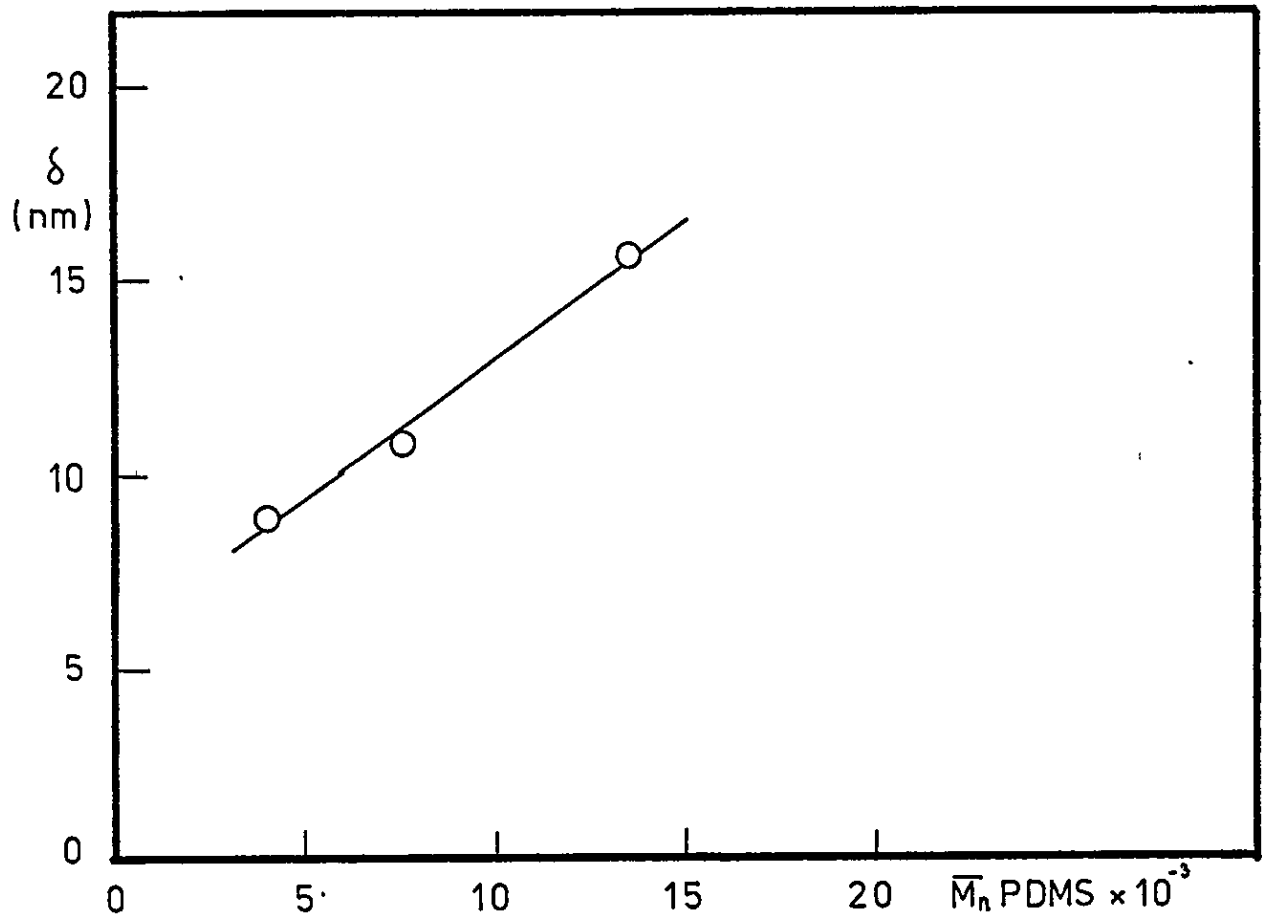
Table 4.15

Dispersion Number	Particle Diameter (μm)	c.f.v. at 298 K	c.f.t. K
D76	0.096	43.2%	340.0
D84	0.13	43.2%	340.0
D44	0.25	43.6%	340.1
D55	0.48	43.6%	340.2

there was no variation with the polymer content of the dispersions, at least up to 10^{-1} g dl^{-1}. The effect of varying $\bar{M}_n$ of the PDMS block of the stabilizer on c.f.v. and c.f.t. is shown in table 4.16.

4.5 PHASE SEPARATION STUDIES

4.5.1 Determination of the θ-Composition for PDMS in a Heptane/Ethanol Mixture

The θ-composition for PDMS in a heptane/ethanol mixture was determined at 298 K according to the method of Suh and Clarke [125]. Plots of the square of the volume fraction of added ethanol vs. log[volume fraction PDMS] were linear, and extrapolation to pure polymer gave the θ-composition. Figure 4.22 shows this plot for the three molecular weights of PDMS studied. The common intercept gave a value of 38.7% added ethanol for the θ-composition.

4.5.2 Determination of the θ-Temperature for PDMS in a Heptane/Ethanol Mixture

Again following Suh and Clarke, the θ-temperature was obtained from the intercept of a plot of [temperature]$^{-2}$ vs. log[volume fraction PDMS] [Figure 4.23]. A value of 339.0 ±

Determination of c.f.v. and c.f.t. for PMMA Dispersions

Dispersion Number	$\bar{M}_n$ PS anchor block	$\bar{M}_n$ PDMS stabilizing block	c.f.v. (volume fraction of added ethanol as %)	c.f.t. [K]
D79	12 700	3·200	38.6	339.6
D44	8 800	11 200	43.6	340.1
D89	44 000	13 700	47.9	339.0
D101	16 400	16 100	46.1	340.4
D80	12 700	23 800	38.9	340.5
D74	44 000	29 800	42.3	340.4
D88	33 400	48 000	42.6	338.2

Table 4.16

FIGURE 4.22
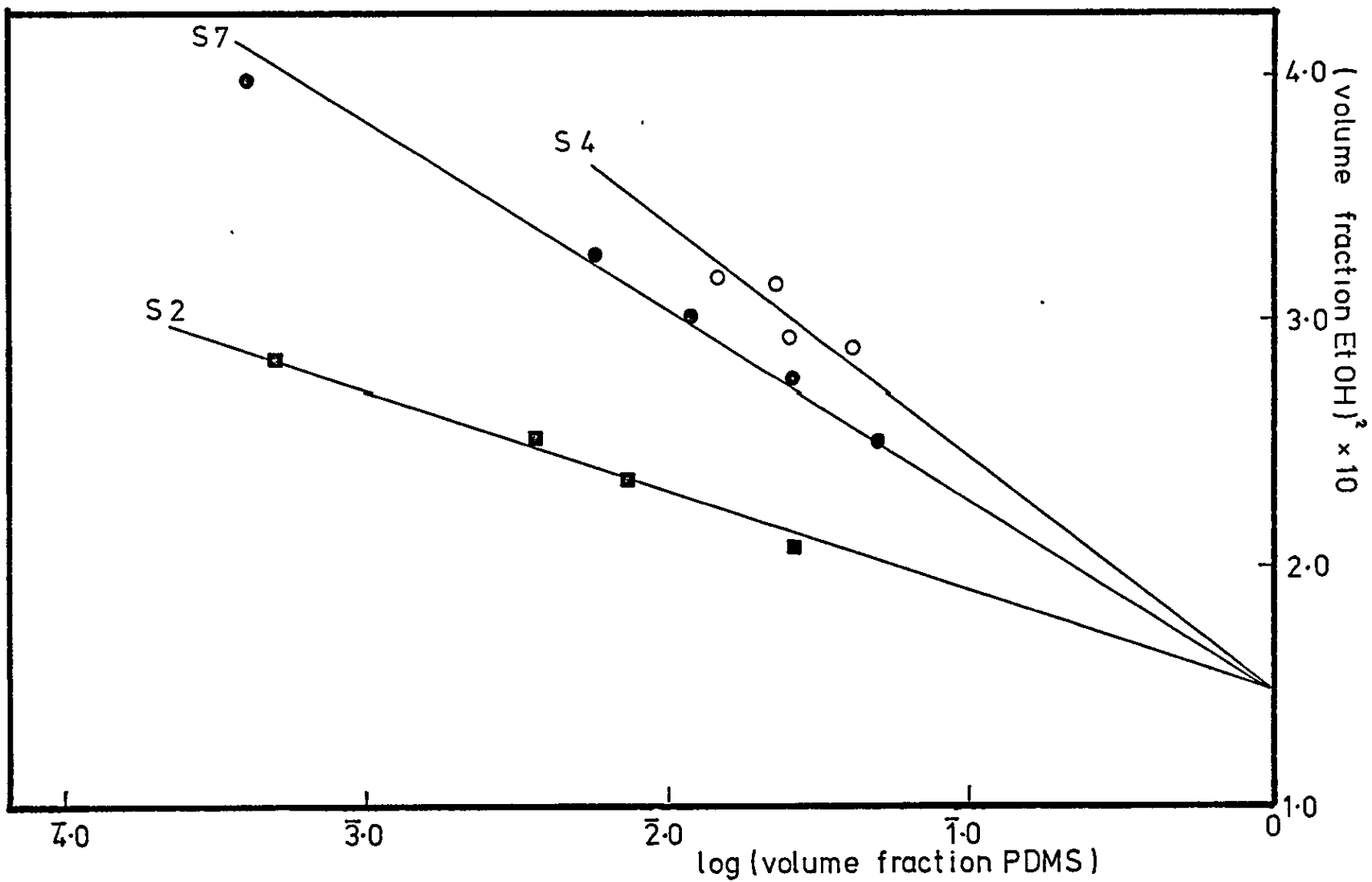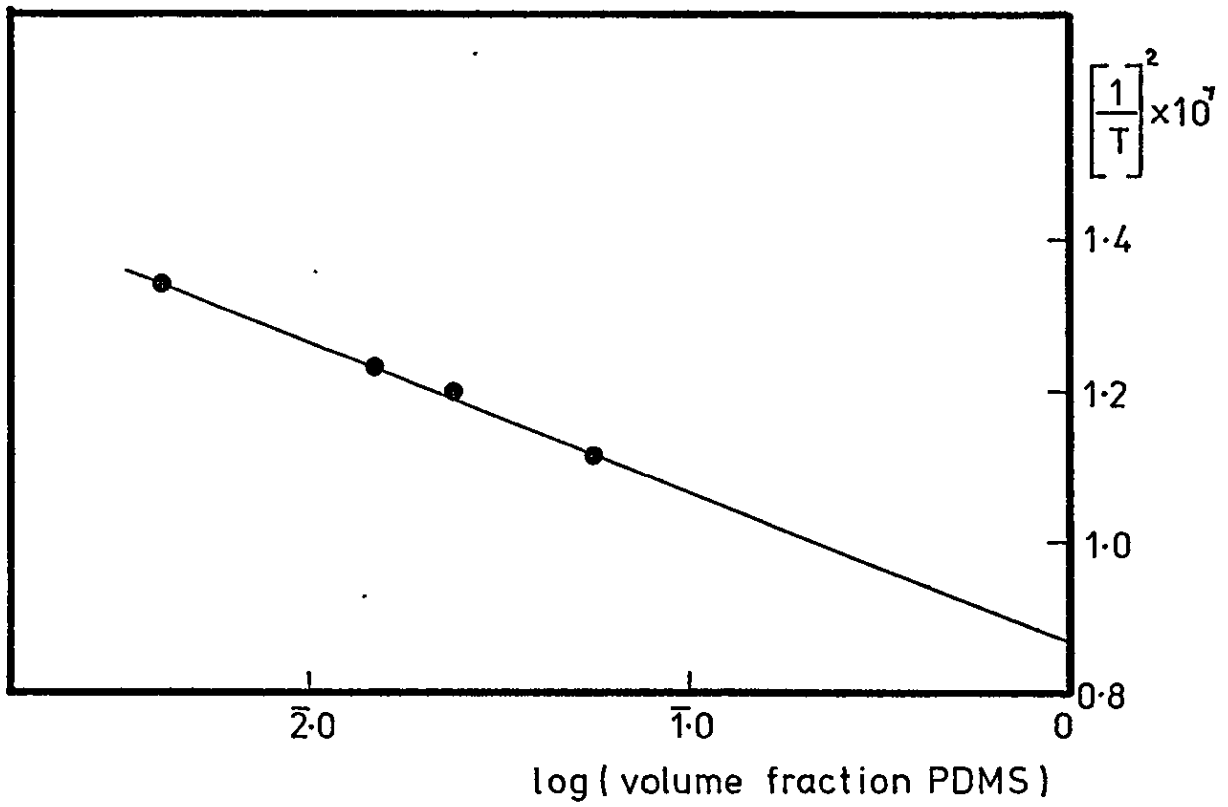
DETERMINATION OF θ-COMPOSITION FOR PDMS

FIGURE   4.23

DETERMINATION OF   θ-TEMPERATURE   FOR   PDMS
— SUH   AND   CLARKE   METHOD

1 K was obtained for the θ-temperature.

As a check on the above method, a second method of obtaining the θ-temperature was compared. This method, due to Talamini and Vidotto [126], involved plotting [temperature]$^{-1}$ against [degree of polymerization (DP)]$^{-0.6}$ and extrapolating to an infinite degree of polymerization [figure 4.24]. A value of 341.2 ± 2 K was obtained by this method, which is in agreement with that obtained using Suh and Clarke's method.

4.5.3 Determination of the Threshold Molecular Weight for Precipitation of PS under Various Conditions

The solubility of PS in alkanes and Freon 113

The phase separation curves of temperature vs. molecular weight for PS in various solvents were determined. Figure 4.25 shows the results for n-heptane, n-dodecane and Freon 113.

The solubility of PS in heptane/styrene mixtures

Figure 4.26 shows the phase separation curves for the solubility of PS in a mixture of heptane and styrene. Results were also obtained for the phase separation in the presence of block copolymer stabilizer, and these are also shown in figure 4.26.

4.6 SOLUTION VISCOSITY STUDIES OF PDMS

The intrinsic viscosity $[\eta]$ for PDMS (S2) in various solvents was obtained from the common intercept of plots of η_{sp}/c and $\ln \eta_r/c$ vs. c. η_{sp} is the specific viscosity, and was obtained from the relative viscosity (η_r) minus unity, and c is the concentration [g dl^{-1}]. Figures 4.27 a,b and c show plots of PDMS in n-heptane, n-dodecane and Freon 113.

FIGURE 4.24

DETERMINATION OF θ-TEMPERATURE FOR PDMS
— TALAMINI AND VIDOTTO METHOD
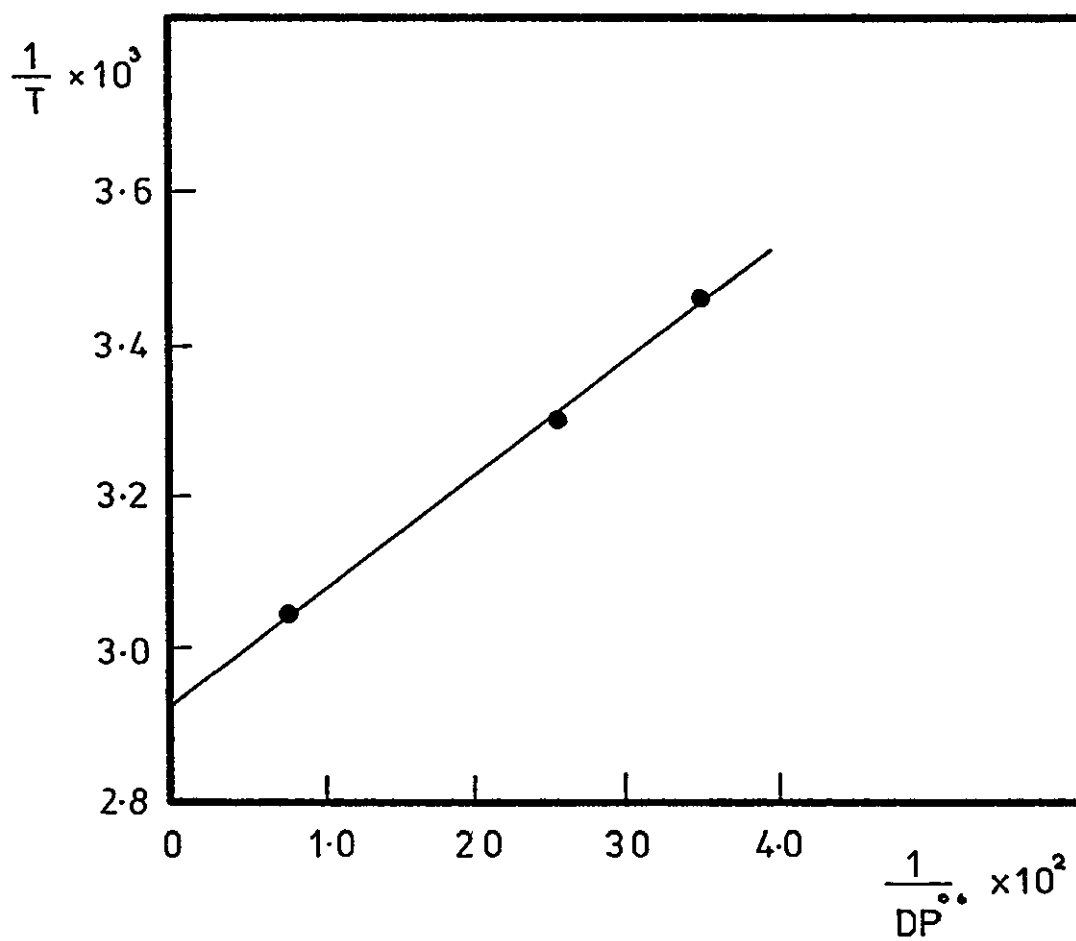
FIGURE 4.25

PHASE SEPARATION STUDIES FOR PS
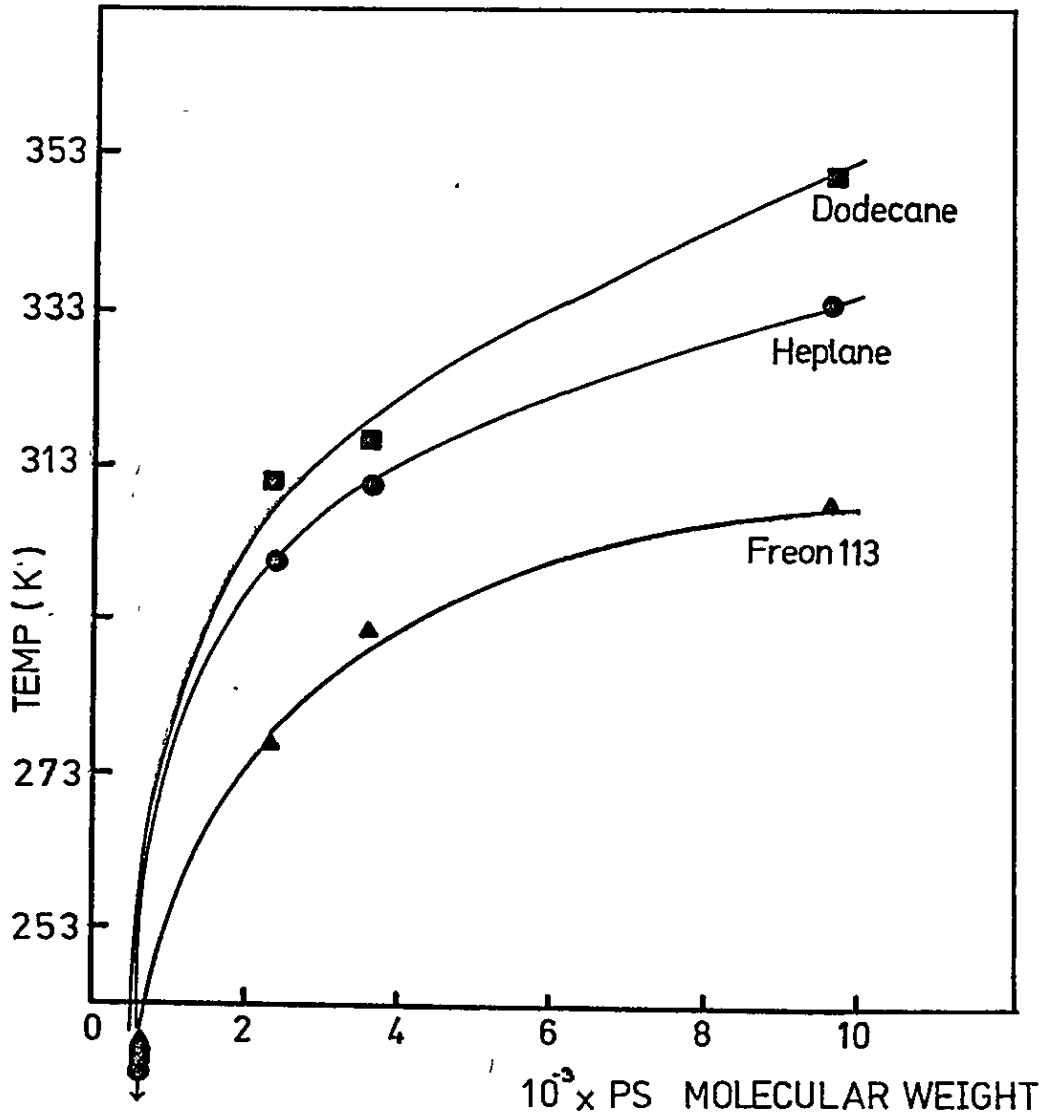
FIGURE 4.26

THRESHOLD MOLECULAR WEIGHT FOR PRECIPITATION
OF PS   UNDER DISPERSION POLYMERIZATION CONDITIONS
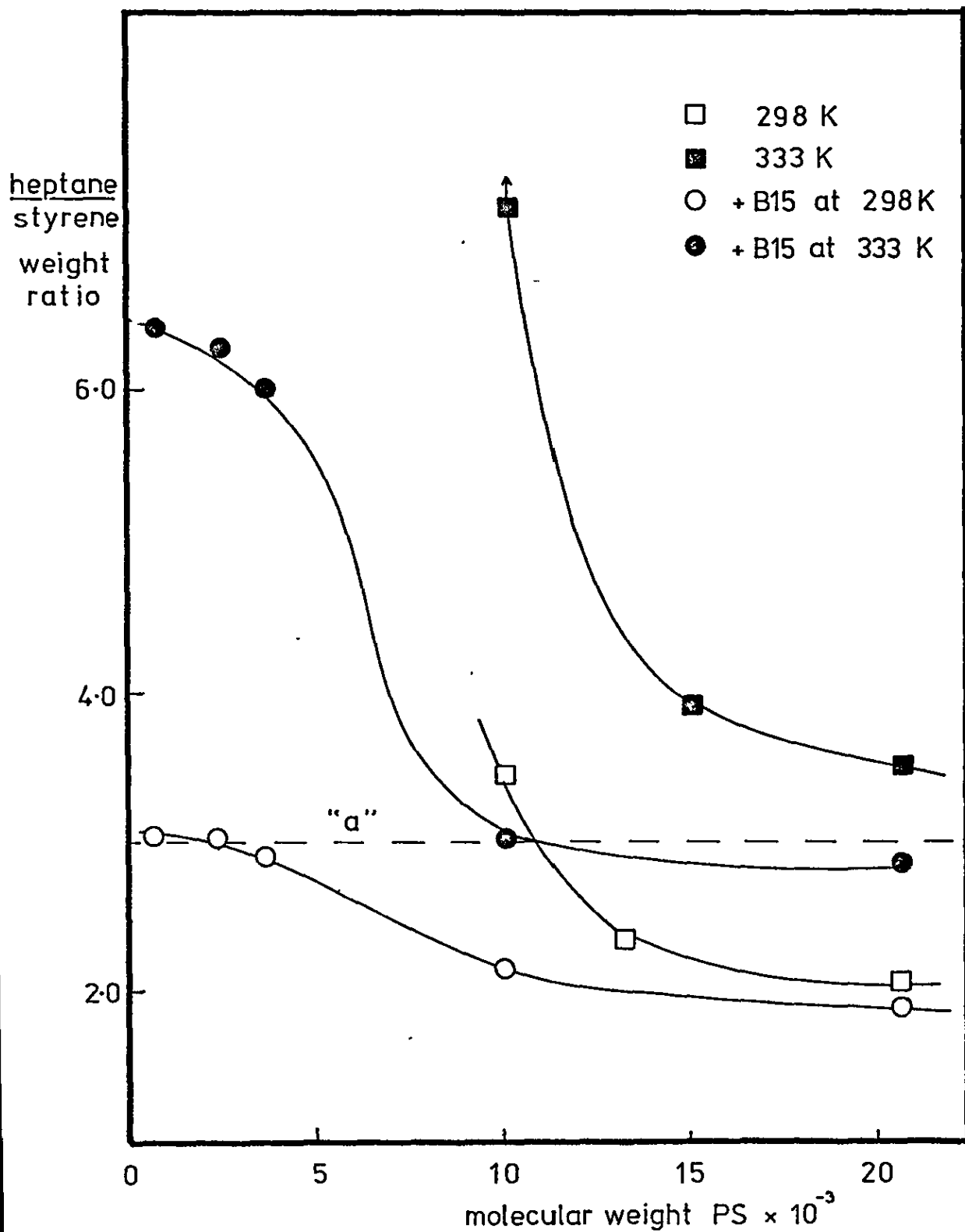
FIGURE 4.27

DETERMINATION OF THE INTRINSIC VISCOSITY OF PDMS IN VARIOUS SOLVENTS
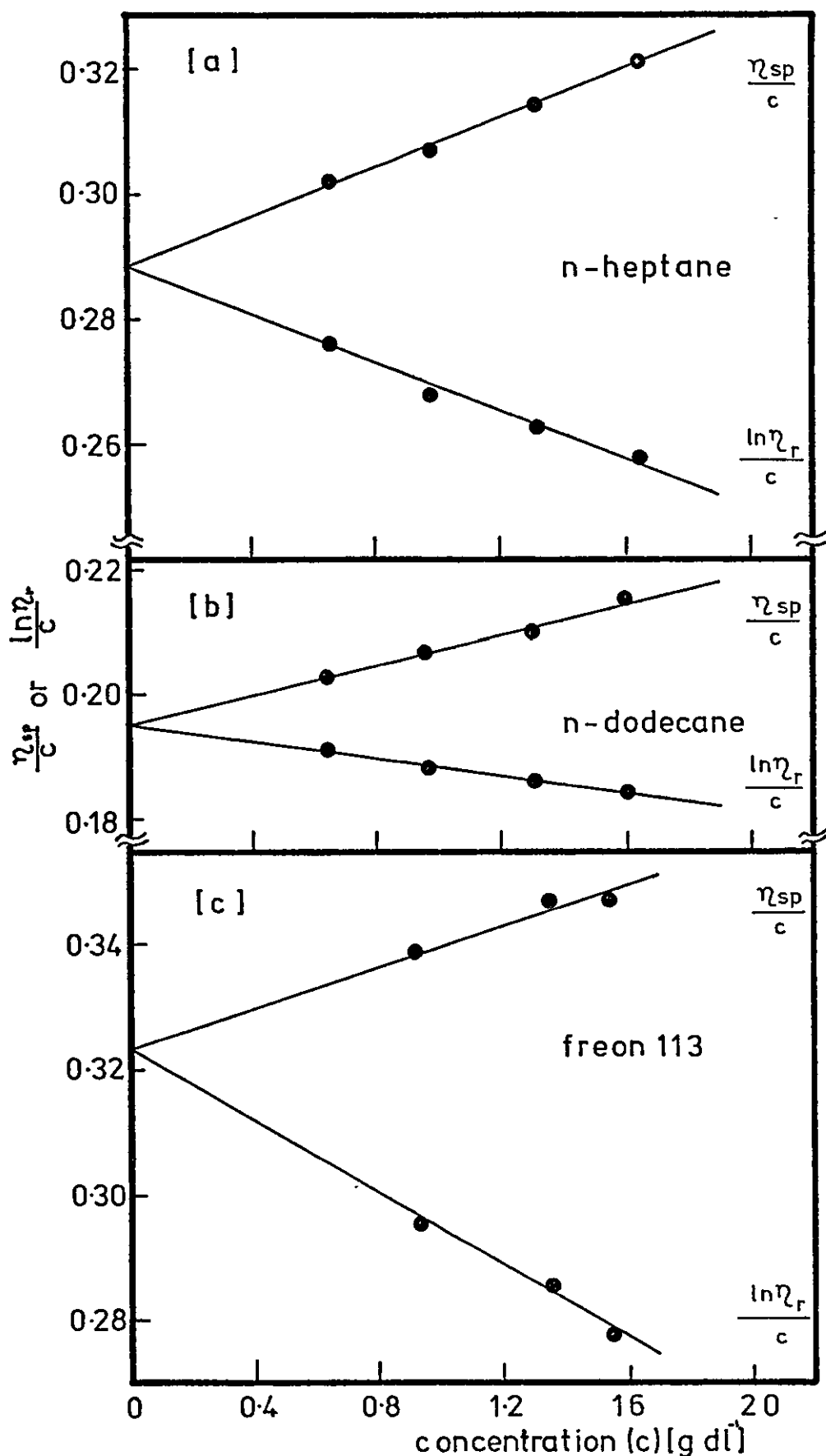
The intrinsic viscosities $[\eta]$ are recorded in table 4.17.
The extension parameter α was obtained from the relationship
[32]

$$\alpha^3 = \frac{[\eta]}{[\eta]_\Theta} \qquad\qquad (4.6)$$

$[\eta]_\Theta$, the intrinsic viscosity in a theta-solvent, was calcu-
lated for PDMS in bromocyclohexane at 301 K from the Mark
Houwink relationship

$$[\eta] = K M^a \qquad\qquad (4.7)$$

where K is 7.8×10^{-4} dl g^{-1} [135]
and   a is 0.5.

Table 4.17 suggests the following order of solvent power:

Freon 113 $>$ n-heptane $>$ n-dodecane

4.7 MONOMER PARTITION STUDIES

The partition of styrene between n-heptane and the
dispersed phase of D86 was studied as described in Section 3.11
and the results are given below.

Initial concentration of styrene in the
dispersion medium   = 1.56% w/v

Refractive index of supernatant dispersion
medium after centrifuging   = 1.388

From calibration curve, concentration of
styrene in supernatant   = 1.50% w/v

Hence wt. styrene adsorbed per gramme of
the disperse phase   = 8.16×10^{-2} g

Assume swelling of the particle core produces a 19.1% increase

in volume

Table 4.17

Values For $[\eta]$ and α for FDMS in Various Solvents

Solvent	$[\eta]$ $dl\ g^{-1}$	α
n-heptane	0.288	1.27
n-dodecane	0.195	1.11
Freon 113	0.323	1.32
Bromocyclohexane [θ-solvent]	0.142	1

Therefore, concentration of monomer within
PS particles   .   = 3.9% w/v

and concentration of monomer in the
dispersion medium   = 1.5% w/v

and monomer partition coefficient $= \dfrac{3.9}{1.5} = 2.6$

CHAPTER 5

DISCUSSION

5.1   PREPARATION OF STABILIZERS

Well-defined AB block copolymers were prepared using
anionic polymerization techniques under conditions of high
purity.   Two methods of achieving such conditions have been
compared, namely polymerization under an inert gas blanket
and polymerization under high vacuum.

A series of stabilizers (B1-B7) were prepared under a
dry nitrogen blanket.   The PS anchor blocks of these
stabilizers were of a much higher molecular weight than the
soluble PDMS stabilizing blocks, with ASB values in the range
6 - 36.   The experimental techniques described in Section
3.1.1 provided a relatively quick synthesis of the block
copolymers, and the products were of acceptably narrow
molecular weight distribution ($\bar{M}_w/\bar{M}_n$ was typically < 1.2).
Invariably, however, such products contained a significant
amount of low molecular weight polymer (up to 10%), as can be
seen in the GPC trace in figure 4.2.d.   This low molecular
weight material ($\bar{M}_n$ of order 10^3) was in fact PS homopolymer,
and its presence suggests that the system was not sufficiently
free from impurities.   These impurities terminated growing
polystyryl   anions during the early stages of the
polymerization.   The presence of small amounts of PS homo-
polymer is, however, not too detrimental when the copolymers
are used as stabilizers for dispersion polymerization.   Low
molecular weight PS is often soluble in the dispersion medium

or can be solubilized by the block copolymers themselves, as will be discussed below.

Most of the block copolymer stabilizers (B8-B25) were synthesized using high vacuum techniques as a method of improving the purity of the system. Products prepared in this way (B8-B25) showed no PS homopolymer contaminant in GPC analysis, and were again of acceptably narrow molecular weight distribution. Using similar experimental techniques other workers (61 ,64) have reported the presence of small amounts (< 2%) of PS homopolymer and PDMS homopolymer. As mentioned above, the presence of PS homopolymer can be tolerated in the subsequent use of the copolymers as stabili- zers, and a   PDMS impurity also causes no problem, since it is completely soluble in the dispersion medium.

The molecular weight distribution of the PS block was usually narrower than that of the copolymer, owing to a broadening of the PDMS molecular weight distribution caused by side reactions and randomization during polymerization. The molecular weights of the copolymers generally agreed to within 10% of the molecular weight predicted by equation 2.14.

Toluene proved to be a suitable solvent for this polymerizing system, since the propagation rate was reduced owing to association of anions. Thus,the initiation stage was virtually complete before any propagation occurred, and a narrow distribution of molecular weights resulted. Saam, Gordon and Lindsey (61) have suggested the use of cyclohexane as the polymerization solvent. Stabilizers B12 and B13 were prepared in cyclohexane, and the products were found to contain PS blocks of much higher molecular weight than predicted, and large amounts of PDMS homopolymer. This is

explained by the suggestion that the initiation of styrene
by n-butyl lithium in cyclohexane is slow relative to the rate
of propagation [136], and hence residual initiator remained
when all the styrene monomer had polymerized. Therefore, the
molecular weight of the PS block was higher than expected,
and the unreacted butyl lithium initiated the polymerization
of PDMS homopolymer upon addition of the second monomer.

Toluene was, therefore, the preferred polymerization
solvent and it would seem that in this solvent initiation must
be carried out at about .298 K. Stabilizers B18 and B19 were
prepared by initiating styrene at ~195 K, and both copolymer
products showed the characteristics of incomplete initiator
consumption described above.

5.2   THE PREPARATION OF NON-AQUEOUS DISPERSIONS

5.2.1   Micellar Dispersions

The ability of block and graft copolymers composed of
incompatible blocks to form micelles in solution was discussed
in Section 2.2.2. Block copolymers consisting of blocks of
similar molecular weight form reversibly associated aggregates
or micelles in equilibrium with free, unassociated copolymer
molecules. If a block copolymer is dissolved in a selective
solvent for one of the blocks, this equilibrium is moved
towards the aggregated form. As the molecular weight of the
insoluble block is increased relative to the soluble block,
the equilibrium increasingly favours the aggregated structure.
In the limit, at high ASB values, all the molecules are
present as irreversibly associated micelles. The size of
such micelles is governed by the molecular weight of the
insoluble block, and the surface area which the soluble block

is capable of stabilizing, according to equations 2.12 and 2.13 in Section 2.2.2.

Block copolymers of PS-PDMS with high ASB values (6 to 36) were used to prepare micellar dispersions as described in Section 3.4.1. In general the copolymer was dissolved in a hot alkane medium, and a micellar dispersion formed as the solution was allowed to cool. Micellar dispersions of B1 (ASB = 6) were prepared in n-heptane (D86), n-decane (D87) and n-dodecane (D114). Electron microscopy showed that the spherical particles produced in each dispersion medium were of narrow particle size distribution and of the same size (figure 4.8).

Micellar dispersions were also successfully prepared from B3 (ASB = 11) (D113) and B4 (ASB = 18) (D115). Attempts to prepare micellar dispersions using block copolymers of higher ASB values (22 - 36) resulted in coarse,irregular particles (D85, D116). This is a result of the short PDMS chains being unable to stabilize the large PS core produced by high molecular weight PS blocks.

The number of copolymer molecules involved in the formation of one micelle (micellization number) was calculated from equation 2.12. The core density was taken as that for bulk PS (1.04 g cc^{-1} [17]) and the area stabilized by each PDMS chain was obtained from the surface coverage data in figure 5.7. The radius, and hence the diameter of the particle core, was calculated from equation 2.13, and the result compared with the particle size estimated by electron microscopy in table 5.1.

Phase separation studies (Section 4.5.3) have shown that low molecular weight PS is soluble in n-heptane. The results

Table 5.1

Comparison of Predicted Micelle Size with Measured Size

Dispersion Number	Block Copolymer and $\bar{M}_n$			Predicted Micellization Number	Predicted Core Diameter (nm)	Measured Particle Diameter (nm)
D86	B1 PS PDMS	20 000 3 300		1 396	44	44 ± 4
D113	B3 PS PDMS	57 000 5 000		6 088	103	113 ± 11
D115	B4 PS PDMS	72 000 4 000		17 736	159	172 ± 17
D116	B5 PS PDMS	99 100 4 600		24 494	197	~ 3 000
D85	B6 PS PDMS	150 200 4 200		77 184	333	v. coarse

of such work, as seen in figure 4.25, show that the threshold molecular weight for precipitation of PS at 298 K is about 2 000. It would,therefore,be expected that PS of fairly low molecular weight would be swollen in heptane. Plĕstil and Baldriaň[134] have studied the micelles formed by an AB block copolymer of PS-polybutadiene in heptane by small-angle X-ray scattering techniques. These workers found that the PS block, of molecular weight 15 700, formed a core which was swollen by the heptane. The degree of swelling was estimated at temperatures in the range 291-323 K, and the swelling factor (ratio of swollen to unswollen core volume) was found to vary from 1.10 to 1.28. This represents an increase in core diameter due to swelling of only ~ 6% at room temperature.

The core diameters predicted in table 5.1 do not take into account any swelling behaviour. This additional factor will, however, only by slightly significant for D86, with a PS core of 20 000 molecular weight. The core diameters measured from electron micrographs are in good agreement with the diameters predicted by equation 2.13, which suggests that the micelles do approximate to the simple geometric model upon which this equation is based. Stacey and Kraus [47] have found that micelles formed by AB block copolymers of PS and polybutadiene in heptane can also be represented by this model.

5.2.2   Non-aqueous Radical Dispersion Polymerization of Styrene

Non-aqueous dispersions of PS stabilized by PS-POMS stabilizers were prepared by radical polymerization as described in Section 3.4.2. The reaction conditions and characteristics of the resulting dispersions are given in tables 3.2 and 4.4 respectively.

The rate of polymerization was found to be very slow in all cases, with typically only up to 50% conversion of monomer being achieved after 50 h polymerization. Figure 4.4 shows the conversion of monomer with time for 067. The form of this curve is very similar to that of a conventional solution radical polymerization of styrene as seen in figure 4.4.b. No increase in rate with conversion was observed, which would suggest that the gel effect was not occurring. The molecular weight of the PS polymerized in this way was relatively low $(5-18 \times 10^3)$, and this is, in fact, of the same order which would be expected from an equivalent solution polymerization. In order to explain this behaviour, the solubility of PS in the dispersion medium was studied. This has led to an estimation of the threshold molecular weight for precipitation.

Threshold conditions for precipitation of PS in a dispersion polymerization

The solubility of low molecular weight PS in alkanes was mentioned above. PS of molecular weight up to 2 000 was found to be soluble in heptane at 298 K (figure 4.25). At a typical dispersion polymerization temperature, 333 K, the threshold molecular weight for precipitation rose to 9 000. In a dispersion polymerization, the dispersion medium contains monomer and block copolymer stabilizer, which both affect the solvency of the medium for PS.

Styrene monomer is a solvent for PS, and hence the overall solvency of the dispersion medium is increased and thus the threshold molecular weight for precipitation increases. The effect of adding stabilizer to the dispersion medium is to lower the interfacial tension, which reduces

the energy required for phase separation and in turn the
threshold molecular weight for precipitation is reduced.
Thus,the addition of monomer and stabilizer to a dispersion
medium give opposing effects, and the threshold molecular
weight for precipitation would be expected to be similar to
that in the pure dispersion medium.

These effects are well illustrated in the phase separa-
tion studies recorded in Section 4.5.3, in which heptane was
added to a temperature-controlled solution of styrene monomer
and PS homopolymer of known molecular weight. The conditions
were chosen to simulate the very early stages of a typical
dispersion polymerization of styrene. The phase separation
point of PS over a range of molecular weights was recorded
as a function of the ratio of heptane to styrene present.
The latter parameter can be regarded as a measure of the
solubility of the PS, and this is plotted against PS mole-
cular weight in figure 4.26. The study was also repeated in
the presence of stabilizer. The horizontal line "a" in figure
4.26 represents the conditions of a typical dispersion poly-
merization of styrene [e.g. D1]. The addition of stabilizer
is seen to lower the threshold molecular weight for precipita-
tion. Increasing the temperature increased the overall
solvency of the system, and an upward shift in the curves
resulted,which leads to an increase in the threshold mole-
cular weight for precipitation. For reaction conditions "a",
therefore, at a polymerization temperature of 333 K, the
threshold molecular weight for the precipitation of PS is
about 10 000. This is very similar to the phase separation
of PS in pure heptane at this temperature.

The solubility of low molecular weight PS in heptane

must be considered when designing the block copolymer stabilizer. The indication is that a PS block of molecular weight less than about 10^4 would not act effectively as an anchor.

An appreciation of the relatively high threshold molecular weight for precipitation now makes it possible to describe a model for the dispersion polymerization of styrene. Radical chains are initiated in solution, where they grow until reaching the threshold molecular weight for precipitation (say, ~ 10 000). Since the molecular weight of the PS produced by such a polymerization is low, termination by combination must have occurred almost immediately after the growing chains precipitated. The high solvency of the dispersion medium for the growing chains decreases the tendency for the chains to be adsorbed onto existing particles. A broad particle size distribution would, therefore, be predicted, because significant nucleation will occur throughout the course of the polymerization.

Since the polymer chains exist for the majority of their growing lifetime in solution, it is reasonable to expect a similar kinetic behaviour to that of a conventional solution polymerization. This was in fact observed experimentally, as noted above. The broad particle size distribution predicted as a result of the high solvency of the dispersion medium was also seen in practice. Figure 4.7.a shows an electron micrograph of the particles of a typical radically-polymerized PS dispersion [D18]. The problem of high solvency has been greatly reduced using a "seeding" technique.

Seeded polymerizations

By initially polymerizing a seed portion of monomer as described in Section 3.4.2 and feeding in further monomer and stabilizer, the overall solvency of the dispersion medium was held at a lower value than that in a simple one-stage polymerization. The particle size distribution from such a seeding procedure was found to be considerably narrower, as shown by the electron micrograph of D19 in figure 4.7.b. The molecular weight of the PS dispersedphase was also significantly lower, e.g. D19 and D26. In seeded polymerizations the threshold molecular weight for precipitation was reduced, and again it would seem that termination occurred very soon after precipitation.

All dispersions were washed with fresh dispersion medium by several redispersion cycles, as described in Section 3.6. Successive redispersion operations reduced the particle size distribution even further by a simple fractionation mechanism, but this was of course accompanied by a significant loss of product.

Several parameters were varied in the dispersion polymerization of styrene in an attempt to improve both the rate of polymerization and the particle size distribution. Each variable will now be discussed.

Type of initiator

Three radical-producing initiators were compared, namely benzoyl peroxide, azobisisobutyronitrile (AZBN) and bis(4 - tert.butylcyclohexyl)peroxydicarbonate ("Perkadox 16"). The effectiveness of each initiator was estimated by a comparison of the degree of conversion of monomer in a given time.

Results obtained using benzoyl peroxide were very comparable to those of AZBN-initiated systems, as may be seen in a comparison of D19 and D20. Comparison of the rate constants for each initiator [17] suggests a slightly faster rate of initiation for an AZBN polymerization, but this was not detected in the present work.

Barrett [10] reports the use of diisopropylperoxydicarbonate as an initiator for the dispersion polymerization of styrene at 303 K. This initiator was no longer commercially available, and,therefore,the efficiency of another peroxydicarbonate initiator, "Perkadox 16", was investigated. Dispersion polymerization D48 showed that this initiator was not significantly more efficient than either of the other two initiators, although there was the advantage of a lower polymerization temperature.

Initiator concentration

Whilst no rigorous kinetic studies have been performed on these systems, the effect of increasing the initiator concentration $[I]$ in a given polymerization has been shown to give an increased rate of polymerization. Comparing the degree of monomer conversion at a given time gave an indication of the rate of polymerization, and a plot of $\log_{10}$[conversion] vs. $\log_{10}$ $[I]$ was linear [figure 5.1].

Effect of temperature

Increasing the polymerization temperature gave a faster rate of polymerization as a result of an increased rate of initiation. It should be noted, however, that PS swells considerably in the hydrocarbon dispersion medium at higher temperatures, and therefore a practical limit of 343 K was

FIGURE 5.1

EFFECT OF INITIATOR CONCENTRATION [I]
ON CONVERSION AT A GIVEN TIME
— D20 , D23 , D29 , D94.
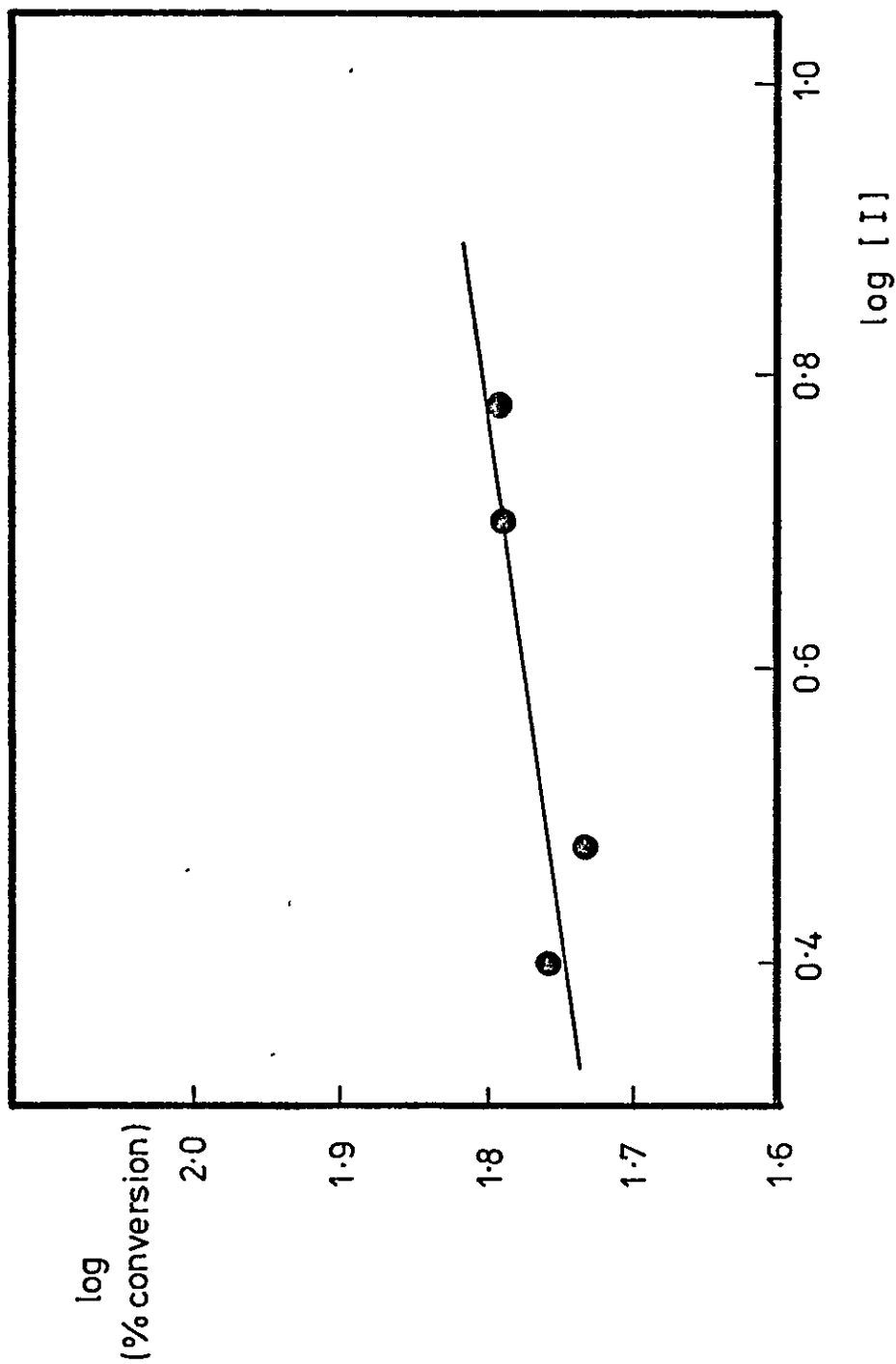
set for dispersion polymerizations of styrene.

Effect of varying stabilizer type

Dispersions of PS stabilized by copolymers B1-B7 have been prepared radically (D18, D19, D20, D23, D94). The particle size distributions of the dispersions were broad, and seeding techniques produced no improvement. Stabilizers B1-B7 were composed of large PS blocks and small PDMS blocks, and form irreversibly associated micelles which might be regarded as particles, as discussed above. Thus, in a dispersion polymerization such as a stabilizer acts as a "seed", and if further stabilizer is fed into a polymerization, new nuclei are effectively being added. This effect broadens the particle size distribution and compensates any advantage gained from seeding techniques.

Vincent [13] has suggested that the most efficient stabilizers have an ASB value within the range 0.33 to 3. Dispersions D1, D26, D29, D37, D48 and D67 were prepared in the presence of stabilizers with ASB values within this range. The particle size distribution was again fairly broad owing to the relatively high solubility of PS in the dispersion media.

Effect of stabilizer concentration

The average particle size of a PS dispersion decreased with increasing stabilizer concentration. This effect has been studied more closely for dispersions of PMMA, and will be discussed in Section 5.2.4.

5.2.3 <u>Non-aqueous anionic dispersion polymerization of styrene</u>

The sluggish nature of radical polymerizations of styrene prompted consideration of a different polymerization mechanism, namely anionic polymerization. The rate of anionic polymerization is known to be much faster than a similar radical polymerization.[136]. As a model polymerizing system, anionic dispersion polymerization would seem an ideal choice. In such a polymerization, under the correct conditions, all growing polymer chains will be of a similar molecular weight, having been initiated virtually simultaneously. The formation of incipient particle nuclei would,therefore,be expected as a sharp transition, after which subsequent polymerization would occur within the particles only, as monomer diffused in.

Attempts were made to prepare dispersions of PS anionically, stabilized by copolymers from the series B9-B25 [i.e. those with ASB < 3]. The results are summarized in tables 4.5 and 4.6. Initiator [e.g. n-butyl lithium] was added to a clear colourless solution of monomer, stabilizer, promotor and dispersion medium, and the orange colour characteristic of polystyryl anions was seen to develop immediately. The clear orange solution rapidly became opaque orange as PS particles precipitated to form a "living" dispersion. The orange colour, however, soon faded to give a white dispersion, and a conversion of monomer of only up to 40%.

Anionic polymerizations require conditions of rigorous purity, as discussed in Section 2.2.3. The purity of the present system was shown to be adequate by performing a conventional solution polymerization of styrene in benzene, under exactly the same conditions [96]. Such a polymerization retained the characteristic orange colour of a "living" system

for many hours. The colour associated with a "living" PS solution is due to the anions at the ends of the PS chains. The possibility that these coloured ends could be buried within the matrix of the PS particles of a dispersion was considered. This behaviour was shown not to occur by preparing a PS dispersion anionically under high vacuum (D62), and distilling highly-purified toluene into the reactor after the orange colour had faded. The toluene dissolved the PS particles, so that any trapped polystyryl anions would once more have given rise to an orange-coloured solution. No colouration was observed and it was, therefore, concluded that the anions had been prematurely terminated.

Anionic solution polymerizations of styrene in toluene were performed (S3, S8 and S9) in the presence of equivalent concentrations of block copolymer to that in D62. The fading of the orange colour was even more rapid, and the conversion of monomer was correspondingly low (table 4.3). Block copolymers with $-SiMe_3$ end groups (in S8) produced a similar effect to those with hydroxyl end groups (in S3 and S9). The extent of conversion before termination was governed by the concentration of PDMS in solution, as seen in figure 5.2. The extent of monomer conversion in several anionic dispersion polymerizations is also given in this figure. It is seen that a dispersion polymerization achieves a higher conversion for a given PDMS concentration than a solution polymerization.

Premature termination is thus clearly a result of inter-action between polystyryl anions and PDMS chains. Papirer and Nguyen [137] report the grafting of polystyryl anions onto a heat-treated aerosil silica. The following reaction scheme was proposed:

FIGURE 5.2

THE EFFECT OF THE CONCENTRATION OF PDMS IN SOLUTION ON THE EXTENT OF CONVERSION OF ANIONIC SOLUTION AND DISPERSION POLYMERIZATIONS OF STYRENE
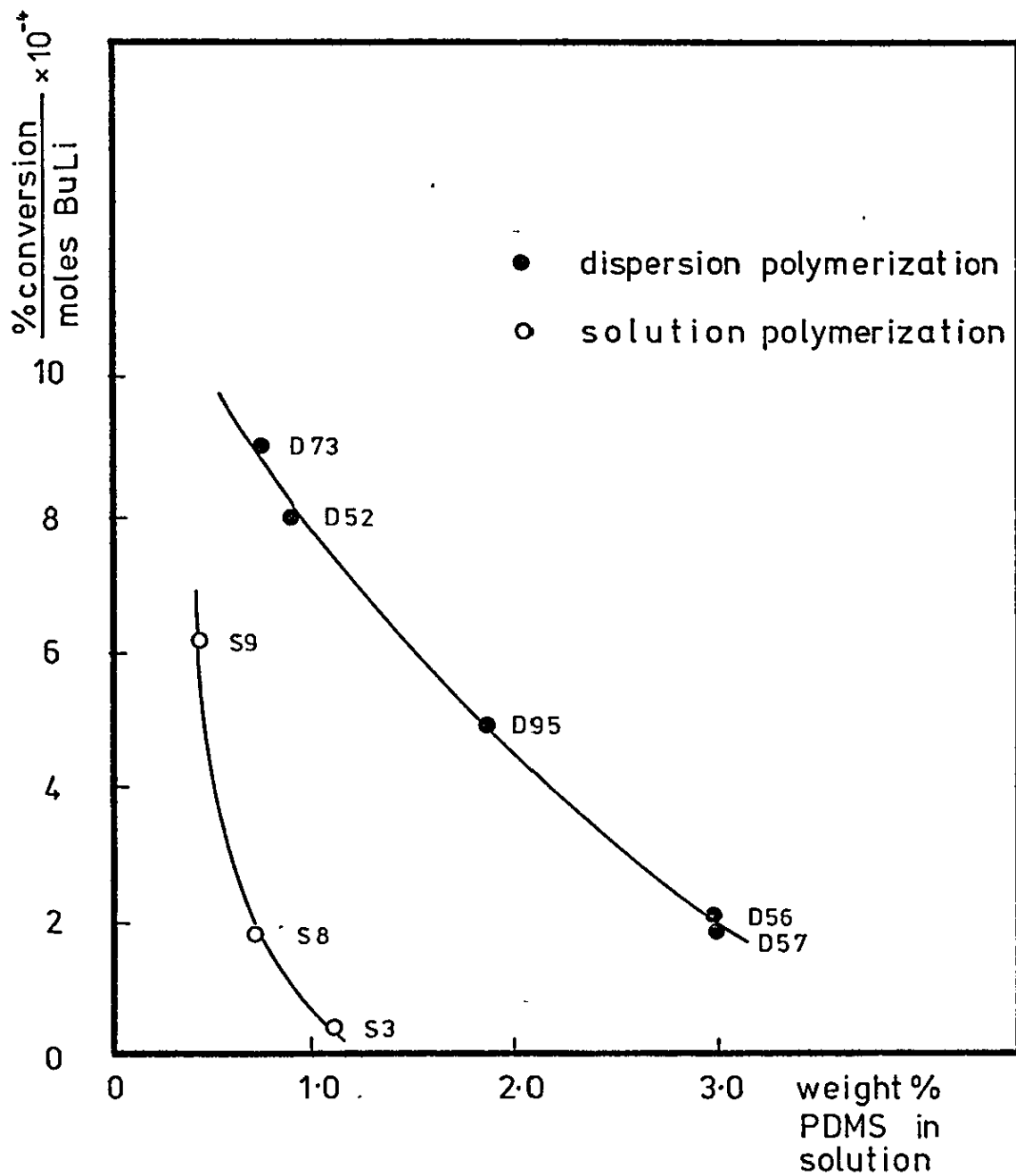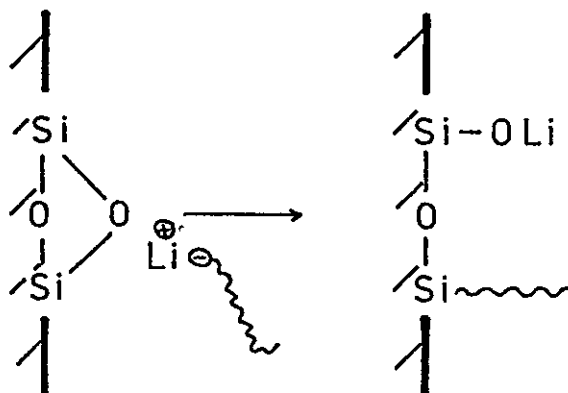
The attack of polystyryl anions on PDMS is thought to be similar to that above. This reaction gives a dimethylsilano-late anion, which is unreactive towards styrene monomer, as discussed in Section 2.2.3. Thus, whilst the system remains "living", such a reaction stops further propagation of styrene polymerization, and, therefore, polymerization is effectively terminated. The lower conversion of the solution polymerizations in figure 5.2 suggests that the PDMS is to some extent protected from the polystyryl anions in a dispersion polymerization.

The problem of this detrimental mechanism of premature "termination" could, however, be minimised. Initiator has been added as an incremental feed to an anionic dispersion polymerization [D97]. Each increment was added upon fading of the orange colour. Using this method, up to 80% conversion of monomer was achieved, but above this, flocculation occurred. This was due to the breakdown of the stabilizing PDMS layer by PS anions. Figure 5.3 shows the extent of monomer conversion

FIGURE 5.3

COURSE OF AN ANIONIC DISPERSION POLYMERIZATION
OF STYRENE WITH INCREMENTAL INITIATOR FEED (D95)
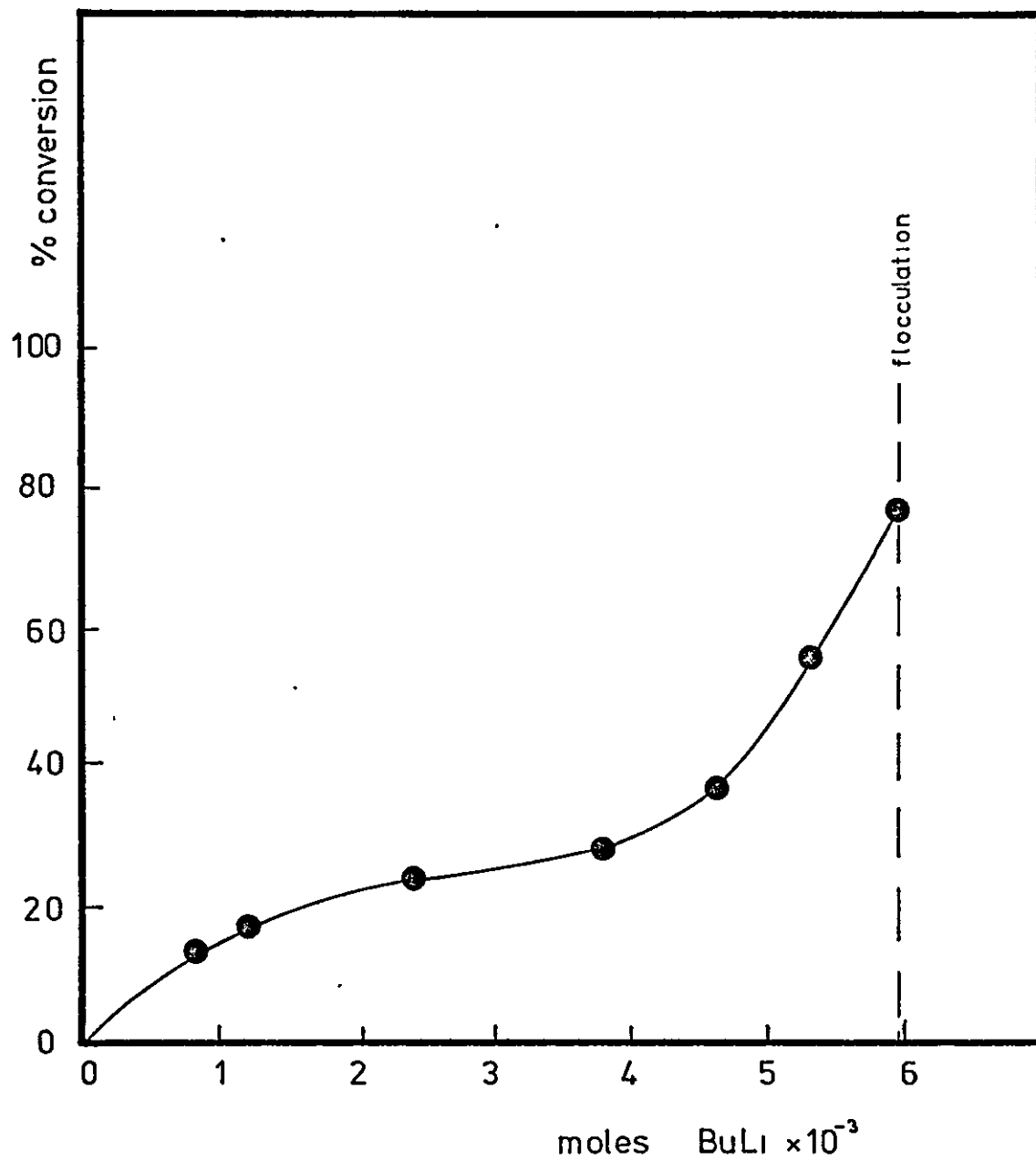
with added initiator. Whilst a high degree of conversion is desirable, the above system does not give a model dispersion with well defined PDMS surface layers.

A better method of minimising premature termination of the polymerization was developed, which involved essentially protecting the PDMS chains from growing anions. This has been achieved in two ways. Anions are largely removed from the presence of PDMS chains when they become a part of a particle nucleus. Two methods of reducing the time which a polystyryl anion spends in solution were, therefore, developed.

Dispersions were initially "seeded" with a micellar dispersion. Growing polystyryl chains then adsorbed into these particles, where growth continued as monomer diffused into the core. Using such a method, dispersions stabilized by B1 (D64, D73), B2 (D72) and B3 (D77) have been prepared with up to 90% monomer conversion, and narrow particle size distribution. The conversion of such an anionic dispersion polymerization was followed as a function of time, and the result is seen in figure 4.5. The rate of polymerization is seen to be much more rapid than in a radical polymerization. Stampa [9] reports a very similar curve for the anionic dispersion polymerization of α-methyl styrene. Styrene was also polymerized in benzene solution (S6) under similar conditions to D73, and the conversion vs. time curve is shown for comparison in figure 4.5.b. The rate of dispersion polymerization was higher than that of an equivalent solution polymerization. This is probably a result of the somewhat higher concentration of monomer within the particles of a PS dispersion (Section 4.7).

A second method of minimising premature "termination"

was to polymerize for a short period of time in a medium which was a worse solvent for PS, such as n-dodecane. Using this technique, up to 71% conversion of monomer was achieved in a 4 minute polymerization (e.g. D103). A comparison of the conversion of heptane-based D95 (33%) with dodecane-based D98 (65%) shows the significant improvement which was gained when a higher alkane was used as the dispersion medium.

The attack of the PDMS by polystyryl anions is thought to be a slower reaction than the propagation of styrene polymerization. Indeed, when anionic polymerization techniques were used to prepare the stabilizers, the cross-over reaction between polystyryl anions and D_3 was observed to be much slower than the propagation of the styrene polymerization. If, therefore, an anionic dispersion polymerization is deliberately terminated after a short time, very little reaction with the PDMS should have occurred. The PDMS layer could, therefore, still be regarded as well-defined.

Effect of stabilizer composition and concentration

The ASB value of the stabilizer greatly influenced the size of the particles produced. Stabilizers of ASB values in the range 0.53-1.47 produced large particles ($>0.8 \mu$m) (D103, D104, D106, D108, D110). Stabilizers of larger ASB value (2.05-6.7) gave dispersions of smaller particle size (0.2-0.4 μm) (D98, D99, D100, D107, D112). Although stabilizers of higher ASB values exist as irreversibly associated micelles in the dispersion medium, stable dispersions were produced. As the particles grow, "bald spots" will develop on the particle surfaces. In the absence of free stabilizer molecules which could be adsorbed onto the

surface, the system retains its stability by a limited agglomeration process. It has been calculated that each particle of dispersion D64 contains the equivalent of 17 original stabilizer micelles.

Increasing the concentration of stabilizer present in solution produced smaller particles for two reasons. Smaller incipient nuclei were produced, as discussed in Section 5.2.2, which in turn gave rise to smaller particles. Premature "termination" problems also increased with increasing PDMS concentration, and therefore conversion, and hence particle size, were reduced (cf. D98 and D99). In general, similar concentrations of stabilizer were used as for radical dispersion polymerization (i.e. 2-5% w/v).

5.2.4   Non-aqueous radical dispersion polymerization of MMA

Dispersions of PMMA were prepared radically as described in Section 3.5, and the results are recorded in tables 4.7 and 4.8. The dispersion polymerization of MMA in the presence of graft copolymer stabilizers has been extensively reported in the literature (e.g. see [10]). Stabilization of PMMA dispersions by adsorbed block copolymers represents a novel system, although many of the characteristics of such a poly- merization are similar to those of graft copolymer-stabilized systems.

The rate of dispersion polymerization was found in all cases to be much faster than that of an equivalent styrene polymerization. Near complete conversion of monomer was usually achieved within 5 h polymerization time. A comparison of the ratio $k_p/k_t^{0.5}$ for styrene and MMA [17] would imply about a 40-fold faster rate of polymerization for MMA over

that for styrene.   This was reflected in the relative rates
of dispersion polymerization observed, and also the relative
molecular weights of the polymers formed.

The solubility of PMMA in aliphatic hydrocarbon is
almost negligible.   Swelling of the particles was,therefore,
not a problem   as was the case for PS particles, and the
polymerization temperature could be increased.   In practice,
the temperature of polymerization was often chosen as the
refluxing temperature of the dispersion medium [e.g. 342 K
for hexane].   .

Figure 4.6 shows the conversion of monomer with time for
a typical MMA dispersion polymerization.   The curve is of a
sigmoidal form, in common with similar work reported in the
literature [7].   The increase in the rate of polymerization
at about 10% conversion was a result of the gel effect,
described in Section 2.3.2.   For comparison, the corresponding
bulk and solution polymerization curves are presented in
figure 4.6.b.   The curve for the dispersion polymerization
of MMA is of a similar form to that for a bulk polymerization,
in which the increased rate due to the gel effect is also
noted.

The molecular weight of the PMMA produced in a dispersion
polymerization was high, of order $1-5 \times 10^5$.   The molecular
weight was significantly reduced by polymerizing in the
presence of a chain transfer agent.   Dispersion polymerization
D66 was performed in the presence of carbon tetrabromide, and
the PMMA produced had a number average molecular weight of
15 800.

Electron microscopy has shown that the particles of PMMA
produced were spherical and of narrow particle size distribu-

tion. As with the dispersion polymerization of styrene, both one-stage and seeding techniques were compared. Since this dispersion polymerization system produced better defined particles, a more rigorous study of the influence of various reaction conditions could be made. These effects will be discussed individually.

Polymerization technique

MMA is a solvent for PMMA, and so a seeding technique was often used to produce smaller particles of a narrow size distribution. The rapid rate of the polymerization, coupled with the insolubility of PMMA in the dispersion medium, gave particles of an acceptably narrow size distribution even with a simple one-stage polymerization. The amount of monomer polymerized in a seed stage did, however, have a marked effect on the final particle size. Figure 5.4 shows the variation of particle size of dispersions [D76, D84, D44, D55] prepared with an increasing proportion of the monomer in the seed stage. When less than 30% of the total monomer was polymerized in the seed stage, the lower limit of particle size [0.1 μm for this particular system] was reached. Increasing the monomer content of the seed stage increased the overall solubility of the dispersion medium. Thus increasing particle sizes were produced, until in the limit, when all the monomer is in the seed stage [i.e. a one-stage polymerization], particles of 0.48 μm were produced.

Effect of stabilizer concentration

In general, somewhat higher concentrations of stabilizer were needed than for dispersion polymerizations of styrene. At a stabilizer concentration comparable with that of a

FIGURE 5.4

VARIATION OF PARTICLE DIAMETER OF PMMA DISPERSIONS WITH % TOTAL MONOMER IN SEED STAGE
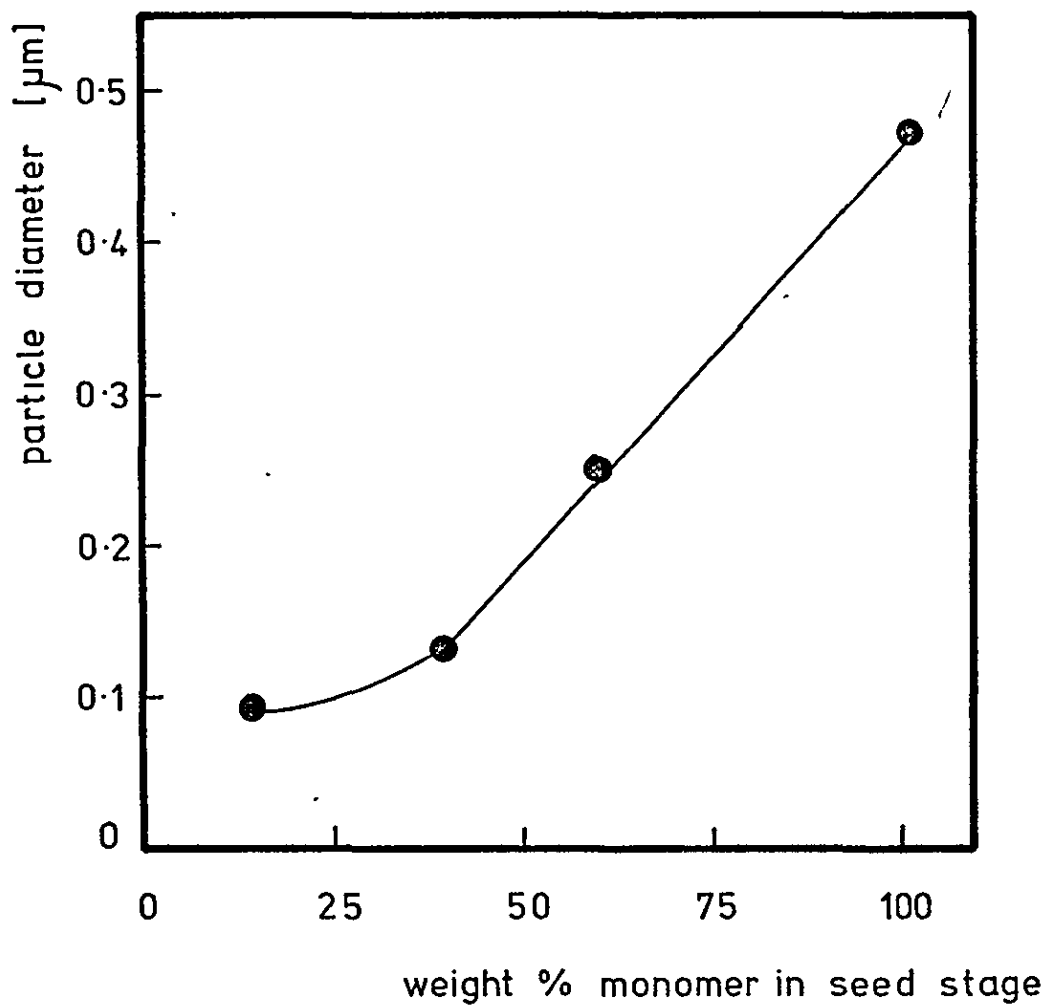
typical styrene polymerization (~2%), a dispersion polymer-
ization of MMA (D43) produced coarse particles of a wide
particle size range (0.3-1 μm).

Figure 5.5 shows the variation of average particle size
of dispersions (D43, D44, D90, D91) prepared in the presence
of differing concentrations of stabilizer. Increasing the
stabilizer concentration produced smaller particles, as pre-
dicted by the theories of particle formation (Section 2.3.3).
Replotting the above curve on logarithmic axes gave a straight
line, which obeyed the relationship

$$D \propto c^{-0.77}$$

in which D is the particle diameter

and c is the concentration of stabilizer in solution.

Barrett [10] has reported a similar relationship for
dispersions of PMMA stabilized by graft copolymers. These
systems have a concentration coefficient in the range -0.5
to -0.6.

Dispersion polymerizations of MMA were usually performed
in the presence of about 5% stabilizer in solution. It should
be noted that despite this relatively high concentration, only
up to 20% of the stabilizer was actually incorporated into
the PMMA particles. Higher concentrations were required
since the adsorption of the block copolymer stabilizer onto
the particle surface occurs less readily than a chemical
reaction grafting a stabilizer onto the surface. Dispersions
of PMMA required a higher stabilizer concentration in solution
than PS dispersions owing to the incompatibility of PMMA and
the PS anchor block, as will be discussed in Section 5.3.3.
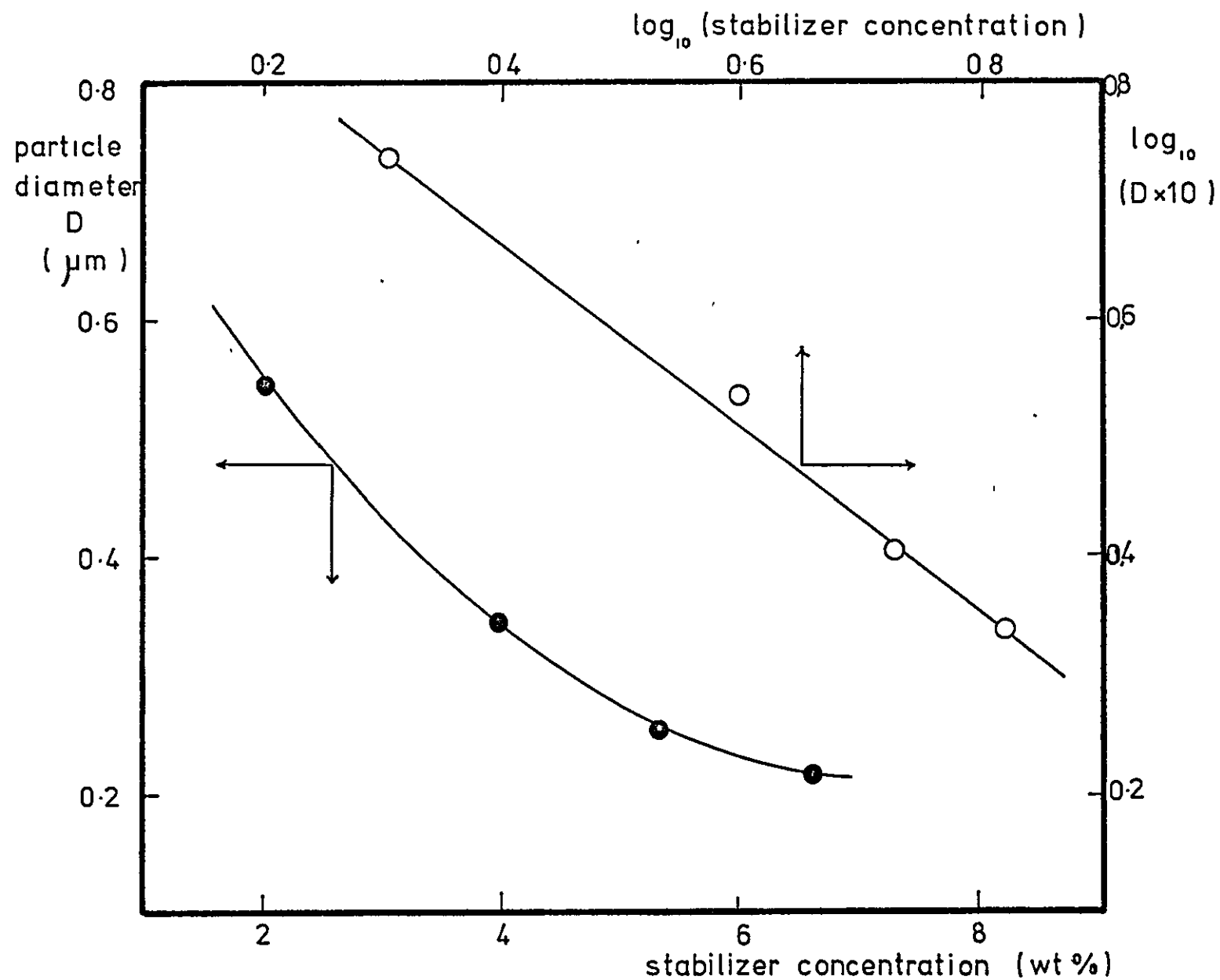
THE EFFECT OF STABILIZER CONCENTRATION

ON PARTICLE SIZE

FIGURE 5.5

Effect of FDMS molecular weight

The use of stabilizers containing higher molecular weight FDMS blocks led to smaller particles. This was because the larger FDMS chains were capable of stabilizing a larger surface area of the particle surface. Figure 5.6 shows the effect on particle size of varying the molecular weight of the FDMS block of the stabilizer. The dispersions considered (D49, D44, D74, D51 and D80) were all prepared in the presence of similar concentrations of FDMS.

Effect of the stabilizer's ASB value

It was found impossible to produce dispersions of PMMA in the presence of stabilizers of ASB value greater than 4.4. Such stabilizers irreversibly micellize in the dispersion medium as discussed in Section 2.2.2. Whilst these stabilizers were successfully used as a seed for a styrene dispersion polymerization, they could not be used in this way in a MMA polymerization. This is a result of the incompatibility of PMMA and PS. A growing PMMA radical cannot enter into the PS core of a micelle, and so upon reaching its threshold molecular weight for precipitation, particles are formed in the dispersion medium. The stabilizer is not free to diffuse to and be adsorbed on these incipient nuclei, and so floccula- tion quickly occurs. The gross flocculation observed in D78 is thus explained. Successful dispersions have, however, been prepared in the presence of stabilizers of ASB value in the range 0.53 to 3.97 (e.g. D44, D49, D51, D74, D75, D79, D80 and D88).

FIGURE 5.6

VARIATION OF PARTICLE DIAMETER (D) WITH MOLECULAR WEIGHT PDMS AT CONSTANT PDMS CONCENTRATION
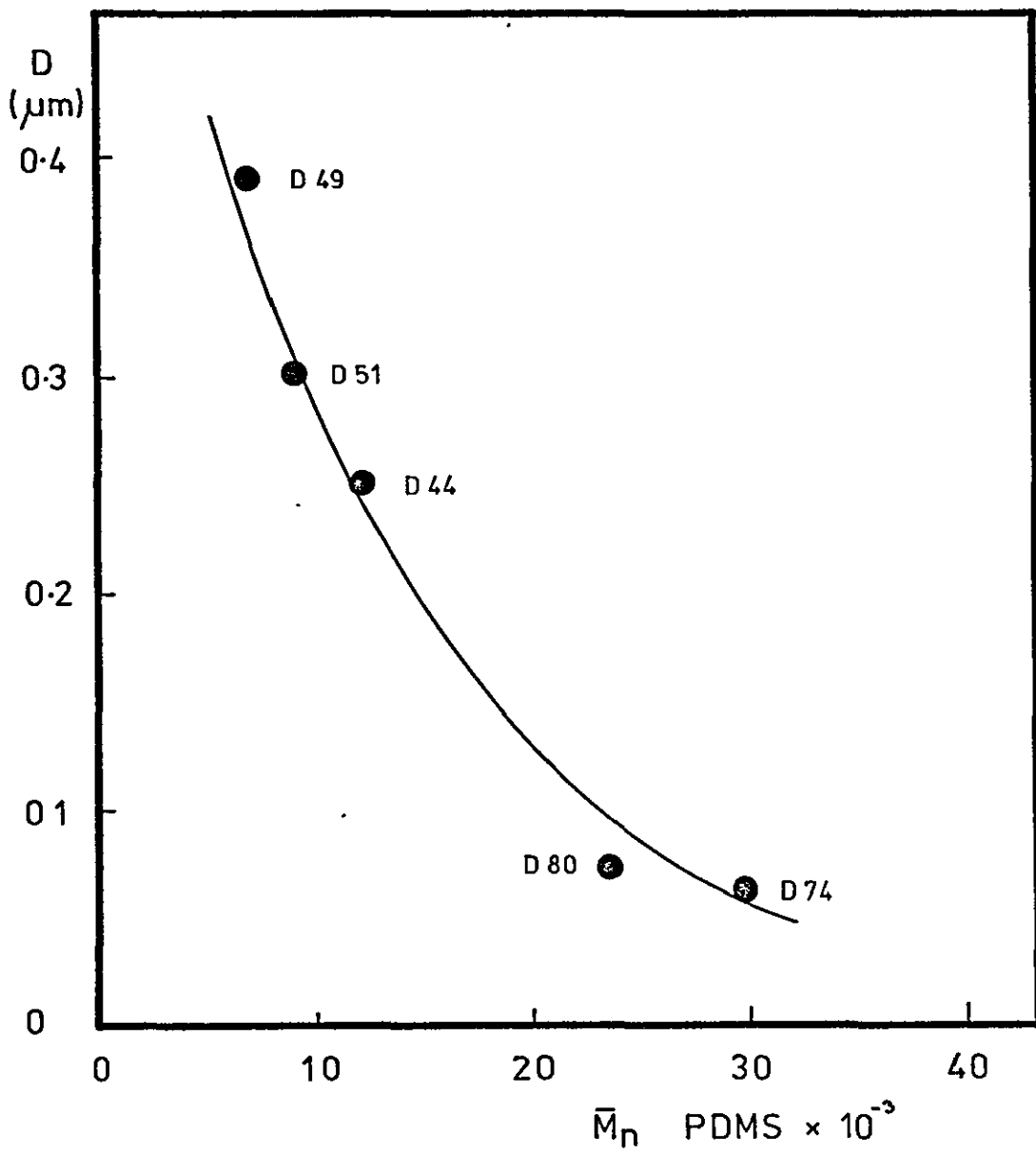
5.3 CHARACTERIZATION OF NON-AQUEOUS DISPERSIONS

5.3.1 Particle Size and Shape

Transmission electron microscopy (TEM)

Transmission electron microscopy was used as the principle method of determining particle size and shape. The soluble PDMS stabilizing layer which surrounds the particles, collapses onto the particle surface when the dispersion medium is removed. The thickness of this collapsed layer on a dry particle was calculated to be only of the order 2 nm, which represents less than a 3% increase in the diameter of the smallest particles. Thus, the collapsed layer could be neglected, and the particle diameter measured from electron micrographs was taken as the core diameter.

Although the instrument was calibrated with a replica of a diffraction grating, electrical fluctuations can generate up to 10% error in the recorded magnifications. A more fundamental source of error might result from a change in the sample during preparation of the microscope grids. If the particles were significantly swollen in the dispersion medium, removal of the medium might be expected to change the particle size. Depolymerization of polymer particles has also been reported under the rather hostile conditions of high vacuum and electron bombardment within an electron microscope [78].

In the present work, damage to the particles in the electron beam was only noted occasionally with very small particles (order 50 nm). In this situation, exposure times were kept to a minimum, such that beam damage was negligible. The swelling of the PS core of a micellar dispersion particle was discussed in Section 5.2.1. It was suggested that

swelling by the dispersion medium would only increase the core
diameter by 6%, which is within the limits of error of TEM.
Hence, the good agreement between the predicted micellar core
radius and the radius measured by TEM in Section 5.2.1 was
reasonable.

In order to confirm that there was little change in a
particle during TEM sample preparation, two referee techniques
were considered. These both involved radiation scattering
studies, which gave a measurement of a particle in an
essentially undisturbed state.

Small-angle X-ray scattering

The method of Guinier [113] was used to determine the
radius of gyration of the particles of a micellar dispersion
(D87) and a PMMA dispersion (D84). The results are given in
Section 4.3.2.

The scattering from D87 gave a good straight line
Guinier plot (figure 4.10) from which the particle diameter
was calculated as 48 nm. The core diameter estimated by TEM
was 44 ± 4 nm. The scattering of X-rays was due not only to
the particle core, but also to the silicone layer at the
surface. Therefore, a larger value of the apparent particle
diameter would be expected from SAXS measurements than from
TEM. This would be particularly true for PDMS of higher
molecular weight, which would form a thicker layer at the
surface. SAXS would not, however, be expected to define the
total extent of the PDMS layer, since there will be some
distance from the surface at which the electron density
decreases such that no scattering occurs. This distance will
depend upon the configuration of the soluble chains. For D87,

the PDMS chains are short ($\bar{M}_n = 3\ 300$), and so the close
agreement between SAXS and TEM estimates of particle size
would be expected. This study confirmed the suggestion that
the swelling of the particle core is only slight.

SAXS studies on D84 have shown, at least qualitatively,
the presence of the silicone layer. SAXS from a sample of
the dried disperse phase was used to estimate the core
diameter. Scattering from a dispersed sample of D84 was
analysed to give the diameter of the core plus the PDMS layer.
As seen in figure 4.11, the Guinier plots for D84 were quite
strongly curved. Such behaviour is often characteristic of
a broad particle size distribution, but TEMs of D84 have
confirmed that the particle size distribution was narrow, and
quite comparable with that of D87.

An average particle size can still be calculated from a
curved Guinier plot by taking the limiting slope [113]. For
particles of this relatively large size, errors in extra-
polation were very large. The estimated diameter of the dry
particle core was 119 ± 24 nm and of the dispersed particle
133 ± 27 nm. These values are in fair agreement with the
core diameter of 130 ± 13 nm obtained from TEM. Whilst the
validity of the diameters estimated from such an extrapolation
procedure is rather dubious, the Guinier plots do show
qualitatively the presence of the PDMS layer. The greater
slope of the curve for the dispersed sample at all angles
suggests an apparently larger particle, which must be due to
the PDMS layer, assuming there was no swelling of the PMMA
core.

Small-angle X-ray scattering has,therefore,shown that
the particle diameters estimated from TEM are realistic within

the 10% limit of error. The presence of a surface layer, when the particles were present in a dispersion medium, was also detected.

Light scattering

The scattering of visible light from the dispersions provided a second referee technique for estimating the size of the particles in an essentially undisturbed state.

Some of the many techniques for determining the particle size of a dilute scattering system have been mentioned in Section 2.4.2. The size of the particles under present consideration lies within the Rayleigh-Gans region [92]. The particles were generally too small for analysis of the angular positions of maxima and minima in the polar scattering curve [95,96,97]. Since the particles were anisotropic, polarization studies of the scattering would be greatly complicated, if not invalidated. Dissymmetry measurements were chosen as a suitable method of determining the particle size of the non-aqueous dispersions. Since the refractive index of the particles was quite close to that of the dispersion medium, absolute refractive indices did not need to be known, which greatly simplified a consideration of such anisotropic particles.

Samples of PMMA dispersions were examined dispersed in Freon 113 and an alkane mixture. The alkane mixture was chosen to be isorefractive with the PDMS layer, so that scattering was due only to the PMMA core of the particles. Two PMMA dispersions were studied, one stabilized by PDMS of low molecular weight [D84] and the other stabilized by higher molecular weight PDMS [D74]. The results are summarized in tables 4.10 and 4.11.

Values obtained for the particle core diameter were in both cases somewhat higher than TEM measurements. These scattering systems obey the conditions described to satisfy equation 2.45, and swelling of the PMMA core could be neglected. To avoid multiple scattering effects, the dispersions were diluted with the dispersion medium until no change in dissymmetry with concentration was recorded. Napper and Ottewill [138] have suggested that multiple scattering between particles can be neglected if the interparticle separation is greater than 200 times the particle radius. At the dilutions used in the present study $(10^{-4} - 10^{-5}$ g dm$^{-3})$ this condition was fulfilled.

The overestimation of particle size could be a result of the particles being slightly flocculated. Rheology studies which will be discussed in Section 5.4.1, have shown that such systems were not flocculated under shear, but it is possible that in an undisturbed situation, weak flocculation may occur. The existence of a secondary minimum-type of attractive trough in the potential energy curve was suggested in Section 2.1.3 and illustrated in Figure 2.6. A limited, weak flocculation might also explain the curved Guinier plots obtained from SAXS of D84. Although the individual particles of the dispersion were monodisperse, weakly associated "flocs" would greatly broaden the particle size distribution. A polydisperse scattering system yields a characteristically curved Guinier plot. The linear Guinier plot given by D87 could then be taken to suggest that there was no flocculation in this micellar dispersion.

The apparent particle size of each dispersion was greater when measured dispersed in Freon 113 than when

measured dispersed in the alkane mixture. This again con-
firms the presence of the surface layer of PDMS around the
particles. Whilst the problem of the possibility of weak
flocculation greatly complicates an estimate of the absolute
size of the particles, it is of interest to compare the
relative sizes of the particle determined with and without
the PDMS layer. The apparent particle size of D84 was
increased by 9.2% due to the PDMS layer. Assuming a true
core diameter of 0.13 μm from TEM, this suggests a PDMS
optical layer thickness of 6.0 nm. The hydrodynamic thickness
(δ) from rheology for D84 was 8.9 nm, which is comparable with
the optical measurement. It should be noted that δ was deter-
mined with n-heptane as the dispersion medium. Measurement
of intrinsic viscosities (Section 4.6) has shown that a free
PDMS chain is slightly more extended in Freon 113 than in
n-heptane.

Similarly for D74, taking a true core diameter of
0.069 μm from TEM, the optical thickness of the PDMS layer
was calculated to be 15.6 nm. Again this was comparable with
the hydrodynamic thickness of 18.2 nm. As with SAXS studies,
optical methods would not detect the full extent of the PDMS
layer. The value obtained for the optical thickness would
depend upon the segment density distribution, i.e. the con-
figuration of the PDMS chains.

5.3.2 Surface Coverage

Analysis of the silicon content of samples of the dried
dispersed phase was combined with an estimate of the particle
size from TEM to give information about the surface coverage
by the PDMS chains. Surface coverage results are presented

as the surface area (A) occupied by each PDMS chain, and the mean separation (d) between adjacent chains in tables 5.2 and 5.3. The chain separation was calculated assuming each chain is terminally adsorbed in the centre of a regular hexagon of area A.

The area occupied, or stabilized, by a given PDMS chain was found to be constant over the range of particle sizes considered, for both PS and PMMA particles (table 5.2). This implies that "total" surface coverage may be assumed for all dispersions. Figure 5.7 shows the variation of A with the molecular weight of the PDMS chain. The area which one chain is capable of stabilizing increases with increasing molecular weight of the PDMS chain. It can also be seen that a given PDMS chain stabilizes the same area on both PS and PMMA particle cores, and the molecular weight of the PS anchor block has no influence on A. The suggestion is, therefore, that the PS anchor block does not extend significantly into the dispersion medium, and the PDMS chains may be thought of as being terminally adsorbed at the particle surface.

The radius of gyration $\langle s^2 \rangle^{1/2}$ of a free PDMS molecule in heptane was calculated as described in the Appendix, for the range of PDMS molecular weights under consideration. From these values, the root mean square (r.m.s.) volume occupied by each free molecule was calculated. Clayfield and Lumb [36] have used computer techniques to study the configuration of terminally adsorbed molecules using Monte Carlo methods, as discussed in Section 2.1.2. Whilst these workers were only able to simulate chains of up to 300 links, their findings suggested that the volume occupied by a terminally

Table 5.2

Area of core surface stabilized by one PDMS chain

(i) effect of core diameter

(a)   PMMA particles stabilized by PDMS $\bar{M}_n$ 11 200

No.	Particle core diameter (μm)	Area occupied per PDMS chain (nm^2)
D76	0.096	11.7
D84	0.13	12.6
D91	0.22	11.1
D44	0.25	12.0
D55	0.48	13.0

(b)   PS particles stabilized by PDMS $\bar{M}_n \sim$ 4 000

No.	Particle core diameter (μm)	Area occupied per PDMS chain (nm^2)
D86	0.044	5.1
D113	0.13	5.2
D115	0.17	4.2
D64	0.21	8.0

Table 5.3

Area of core surface stabilized by one PDMS chain

(ii) effect of $\bar{M}_n$ of PDMS

(a) PMMA particles

No.	$\bar{M}_n$ PDMS	Area occupied per PDMS chain $[nm^2]$	Mean PDMS chain separation (d) [nm]
D79	3 200	6.4	2.7
D49	7 000	9.5	3.3
D44	11 200	12.6	3.9
D89	13 700	19.4	4.7
D101	16 100	24.6	5.4
D80	23 800	35.4	6.5
D74	29 800	44.5	7.2
D88	48 000	51.3	7.4

(b) PS particles

No.	$\bar{M}_n$ PDMS	Area occupied per PDMS chain $[nm^2]$	Mean PDMS chain separation (d) [nm]
D86	3 300	5.1	2.5
D115	4 000	4.2	2.3
D113	5 000	5.2	2.5
D100	7 600	12.5	3.8
D107	13 700	14.7	4.1

FIGURE 5.7

SURFACE COVERAGE OF PS & PMMA PARTICLES vs MOLECULAR WEIGHT [$\overline{Mn}$] OF PDMS STABILIZING CHAINS
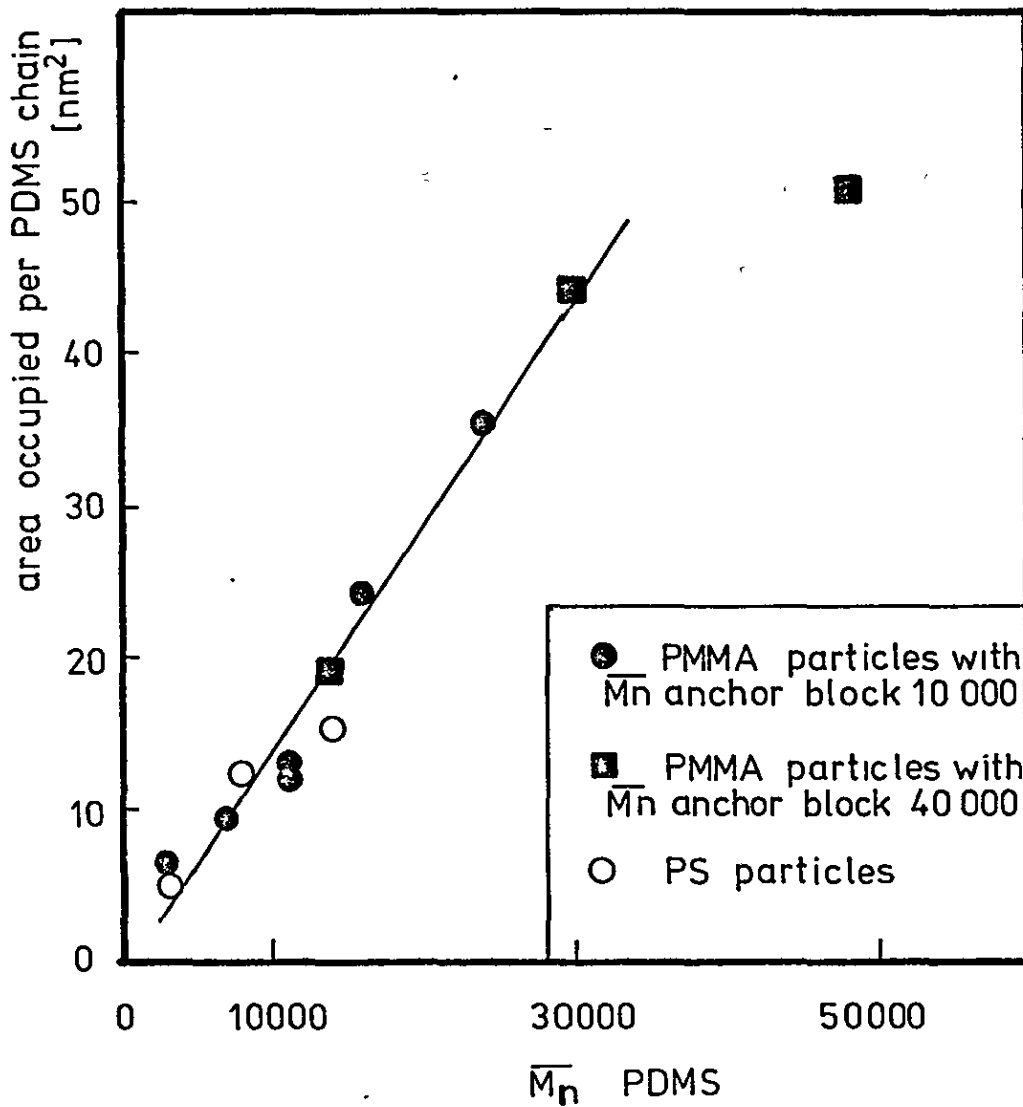
adsorbed chain was not significantly different to the volume of the free chain. Some very recent work by Tanaka [139] using random flight statistics also implies that there is little change in volume when a free molecule is terminally adsorbed onto a convex surface. In the present work, the r.m.s. volumes of a free and a terminally adsorbed molecule will be taken as being equal.

The mean separation of adsorbed PDMS chains (d) was plotted as a function of the radius of gyration $\langle s^2 \rangle^{\frac{1}{2}}$ of the free molecule in figure 5.8. The mean separation is seen to be slightly greater than the radius of gyration of the molecule over the range of molecular weights studied. If the mean separation between chains had been greater than twice the radius of gyration, no interaction between neighbouring chains would occur, as illustrated in figure 5.9(a). The thickness of the steric layer might in this case be expected to be equal to twice the radius of gyration of the stabilizing molecule. The separation was, however, found to be less than described above, and might be represented as in figure 5.9(b). Adjacent molecules can interact within the shaded region, and volume exclusion effects between segments will lead to an elongated volume. Assuming no overlap of neighbouring chains, this volume could be represented by figure 5.9(c). If the volume is held constant, the height which the chain attains (h) can be calculated. In a real situation, the molecule is adsorbed on the convex surface of a particle, and, therefore, the appropriate radius of curvature of the particle was considered in calculations of h. Figure 5.10 shows a plot of h against the molecular weight of the PDMS chains. Under conditions of no overlap, h might

FIGURE 5.8

MEAN   PDMS   CHAIN   SPACING   [d]   vs. $\langle s^2 \rangle^{1/2}$ OF
APPROPRIATE   FREE   PDMS   MOLECULE

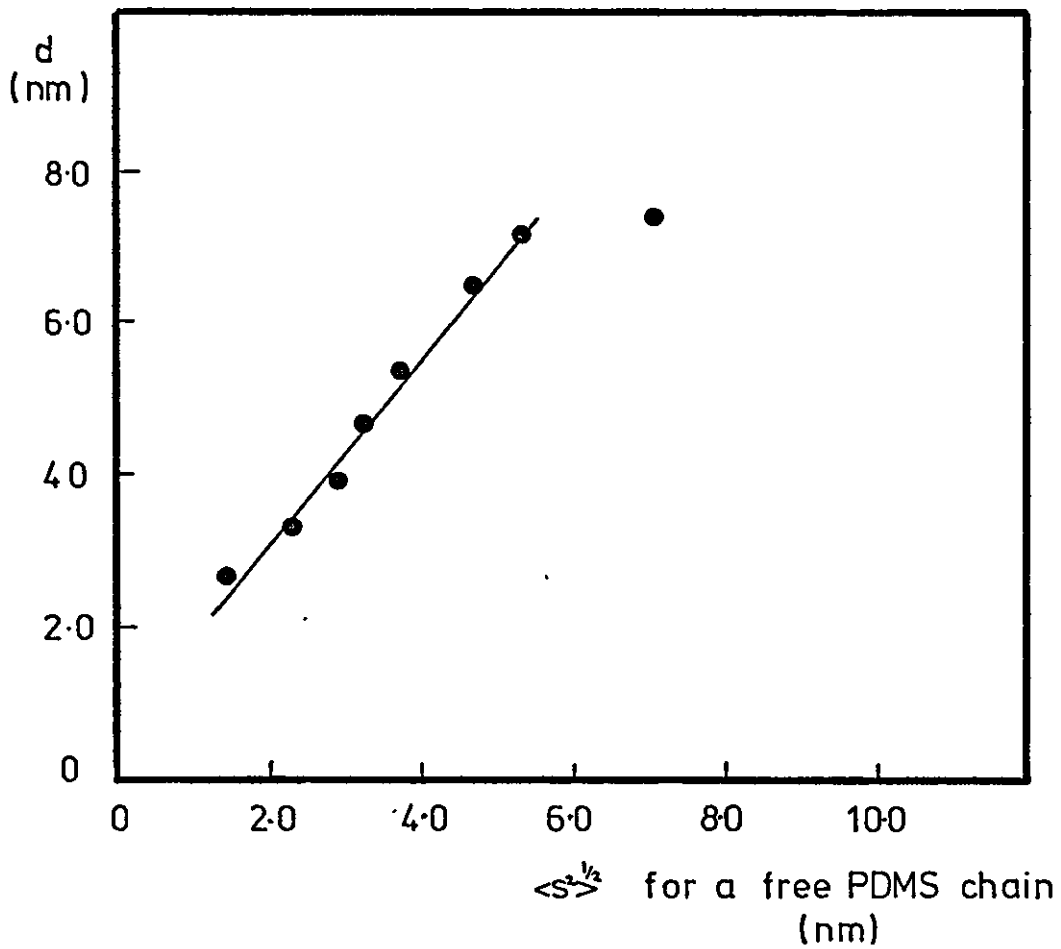— D 44 , D49 , D 74 , D 79 , D 80 , D 88 , D 89 , D101

FIGURE 5.9
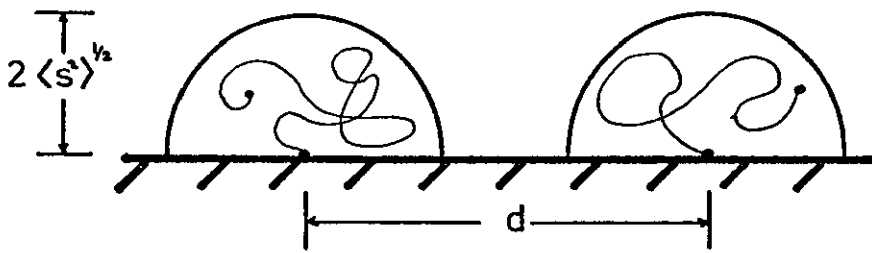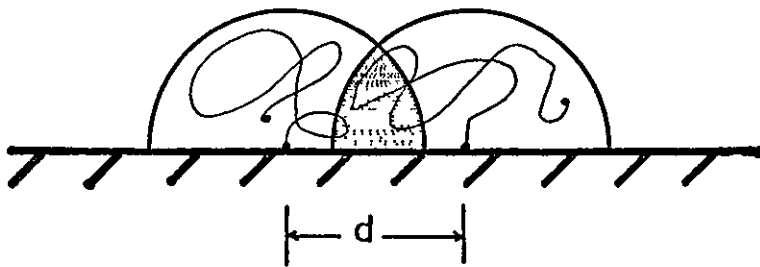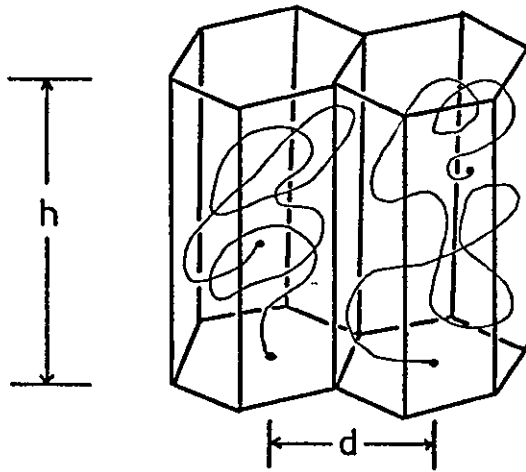
MODELS FOR TERMINALLY ADSORBED
POLYMER MOLECULES

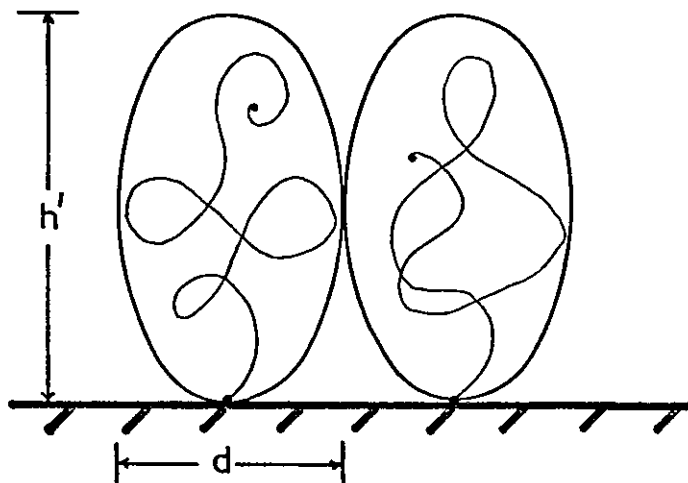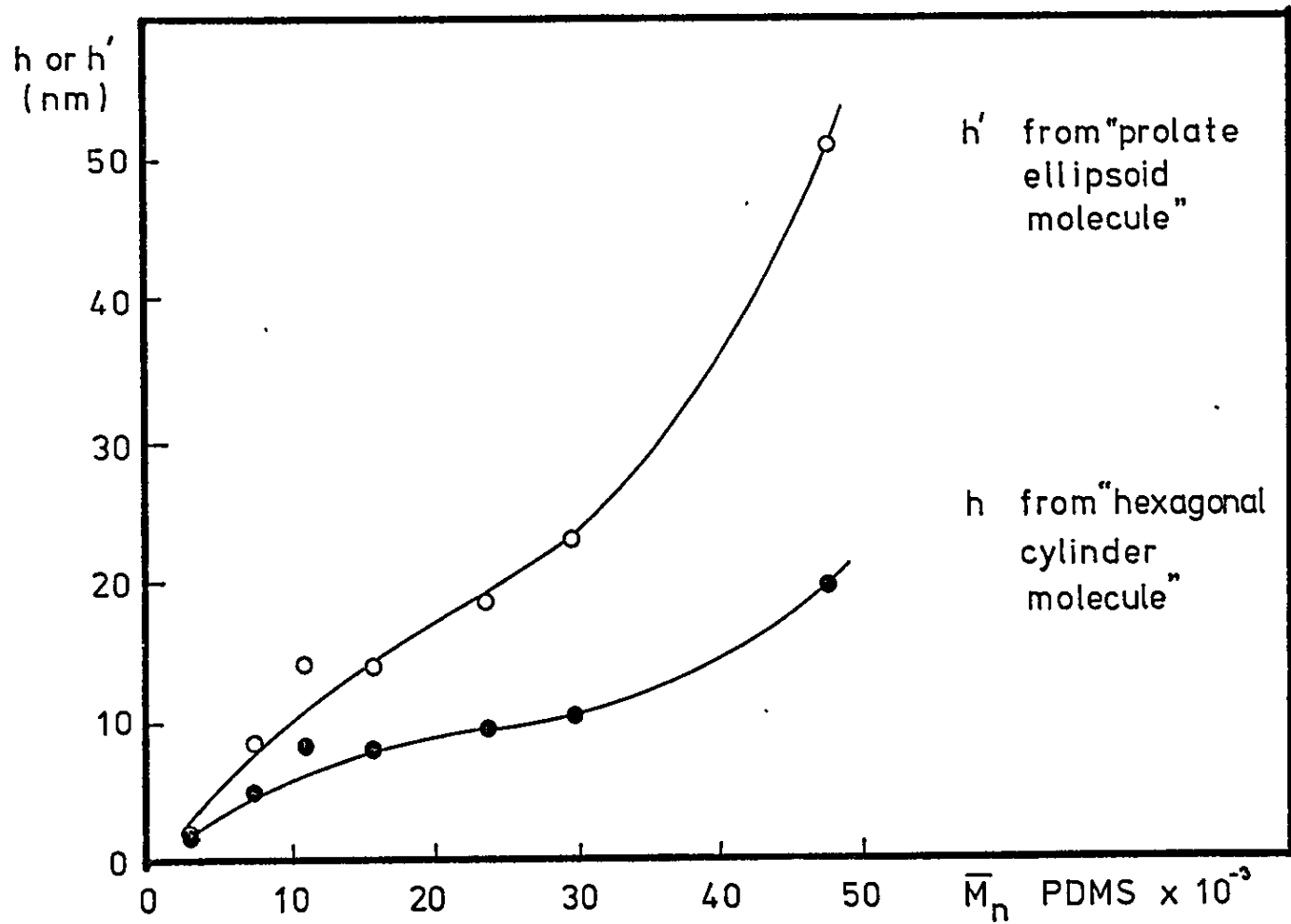
[a]

$d > 2\langle s^2 \rangle^{1/2}$

[b]

$d < 2\langle s^2 \rangle^{1/2}$

[c]

hexagonal
cylinder
model

[d]

prolate
ellipsoid
model

FIGURE 5.10

h and h' vs. MOLECULAR WEIGHT PDMS

be regarded as the effective thickness of the FDMS layer.

The value of h may be overestimated owing to the nature of PDMS chains. Such chains are very flexible and it would, therefore, not be unreasonable to expect some degree of over-lapping between neighbouring volumes. This would lead to lower values of h.

Clayfield and Lumb's work did not describe the segment density distribution of the adsorbed molecule, but did suggest that the segment density would be greatest near the centre of the molecular volume. Hesselink [29] has calculated the theoretical segment density distribution of the adsorbed molecule, and finds a near Gaussian distribution. Tanaka's recent work [139] confirms such a distribution, and suggests that an adsorbed molecule has an elongated volume at the interface. This gives rise to a second, and possibly more realistic model for such closely packed chains.

The segment density distribution suggests that each terminally adsorbed molecule sweeps out a volume which can be represented by a prolate ellipsoid, as seen in Figure 5.9(d). Such an ellipsoid, retaining the same volume as the r.m.s. volume of the free molecule, will have a larger effective height h'. Figure 5.10 shows the variation of h' with the molecular weight of the PDMS, calculated as before assuming a volume equal to the r.m.s. volume of the free molecule. The minor axis of the ellipsoid was taken as the mean chain spacing (d) at the particle surface, and a planar surface was assumed.

The effective thickness of the FDMS layer as calculated from surface coverage information, will be compared with estimates of the layer thickness from rheology in Section 5.4.1.

5.3.3 Dispersion stability and stabilizer anchoring mechanism

PS dispersions

PS dispersions remained stable for long periods of time under ambient conditions. Particles which had sedimented under gravity were easily redispersed upon shaking, particularly when the particle size distribution was narrow. This would suggest that there was no significant desorption of stabilizer with time. The stability was to be expected, since the PS anchor block of the stabilizer would become incorporated within the matrix of the PS particle core, thus anchoring the PDMS block firmly to the particle.

Dispersions were, on occasion, subject to ultrasonic vibration. It was noted that D100, containing stabilizer with a low molecular weight PS block, eventually became unstable and gross flocculation occurred. This was probably due to the short PS anchor block being, as it were, "shaken out" of the core by the ultrasonic vibration. Any swelling of the core, either by the dispersion medium or unconverted monomer would have aided this process,as would any swelling of the anchor block itself. Dispersion D107, incorporating stabilizer of a high molecular weight anchor block, was quite stable to ultrasonic vibration.

The dimensions of the PS anchor block within the particle core would be expected to be the same as for a bulk polymer molecule. Flory [32] predicted that these would be unperturbed random coil dimensions,and this has recent ly been confirmed by neutron scattering studies [140-143]. The probable anchoring mechanism is illustrated in figure 5.11[a].

FIGURE   5.11

STABILIZER   ANCHORING   MECHANISMS

[a]
PS
particle

[b]
PMMA
particle
- model I

[c]
PMMA
particle
- model II

cyclohexane
333 K

"bald
spot"
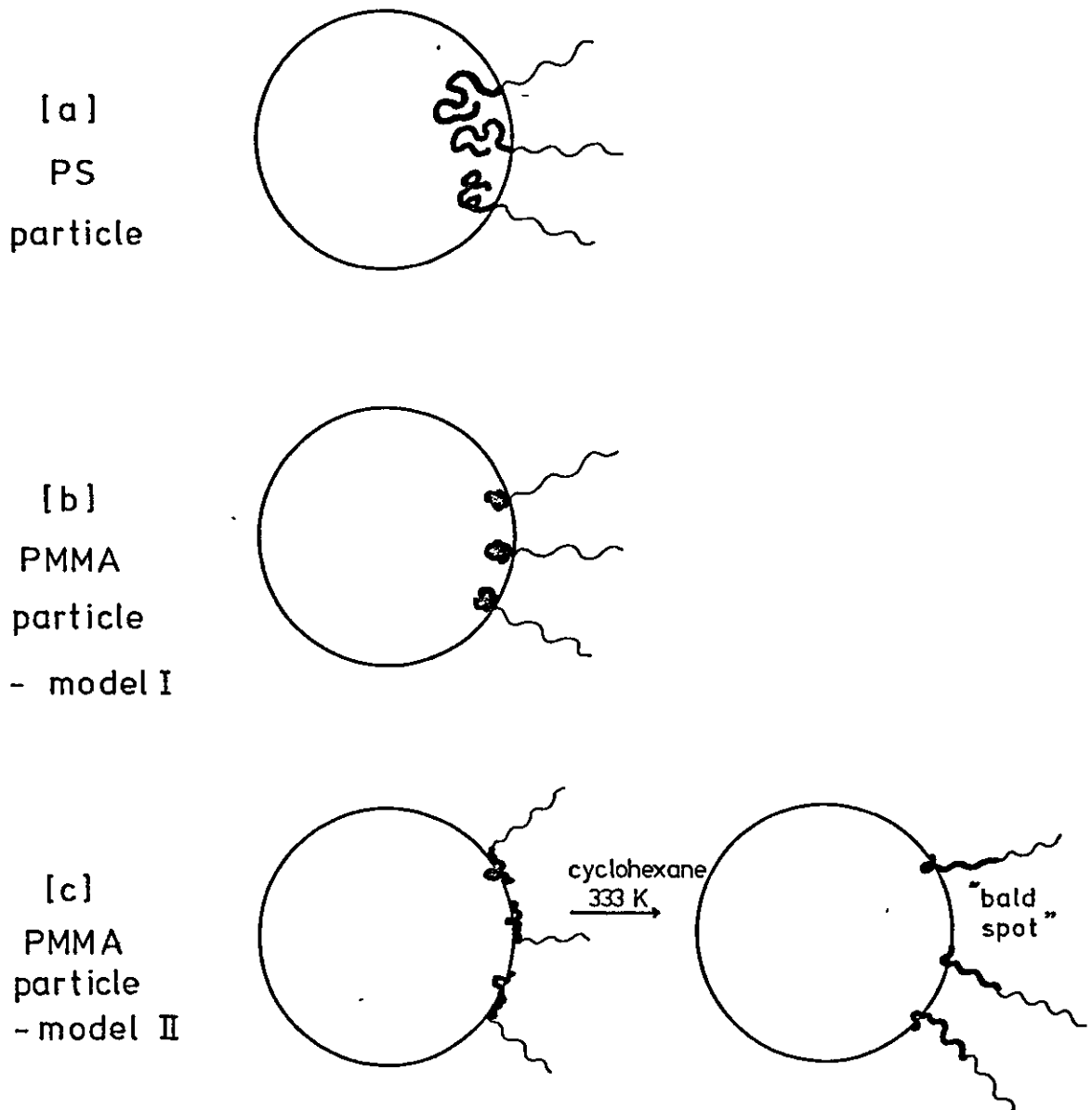
PMMA dispersions

The incompatibility of the bulk polymers PS and PMMA is well known [114]. It might,therefore,seem surprising that a PS-PDMS stabilizer could anchor to a PMMA particle. The present work has shown that such stabilizers were,in fact, suitable for stabilizing PMMA particles. Within the molecular weight range of the PS anchor blocks studied (8 800 - 44 000) no variation in anchoring efficiency was apparent. As with PS dispersions, long term stability suggested no desorption of the stabilizer, and stability under ultrasonic vibration showed that the anchoring mechanism was not weak.

In the dispersion polymerization of MMA, slightly higher concentrations of stabilizer in solution were required than commonly present in styrene polymerizations. PMMA dispersions could not be grown from a micellar dispersion seed (e.g. D78). This was to be expected since growing PMMA radicals would not readily diffuse into the incompatible PS core of the micelles. During a MMA dispersion polymerization,the incipient nuclei formed adsorbed stabilizer from the dispersion medium. The "driving-force" of this adsorption was the insolubility of the PS block of the stabilizer in the dispersion medium.

Analysis of a sample of the stabilizer isolated from a low molecular weight PMMA dispersion (Section 4.3.3) showed that the stabilizer chains had not been grafted onto the particle surface by a chain transfer mechanism. This was not surprising as the chain transfer constants for MMA onto both PS and PDMS are very small [29 $\times$ 10^{-5} [17] and 0.3 $\times$ 10^{-5} [145] respectively].

The PS anchor block is postulated to be in a collapsed state, in order to minimise polymer/polymer contact between

incompatible polymers. Two models for the anchoring mechanism
are proposed. One model involves the collapsed PS anchor
becoming trapped within the matrix of the PMMA particle as it
grows (figure 5.11(b)). In an alternative model, the anchor
block is adsorbed onto the particle surface in trains, with
an occasional loop being trapped within the surface of the
particle (figure 5.11(c)).

The efficiency of the anchoring mechanism was demonstrated
in studies of the particles of D44 and D55 redispersed in
cyclohexane. Such dispersions,when held at 333 K for 60 h ,
showed only slight flocculation, implied from a slightly
increased rate of sedimentation. Cyclohexane at 307 K is a
well-known θ-solvent for PS [17]. If the stabilizer were
not firmly anchored to the particles, heating such a disper-
sion to 333 K would lead to gross flocculation, owing to
desorption and dissolution of the PS anchor block. The slight
flocculation actually observed suggests a limited desorption
of stabilizer, which was reversible upon cooling the disper-
sion to 298 K.

The above study suggests the anchoring mechanism in
figure 5.10(c) might predominate. When the dispersion was
heated, the PS chains lying on the particle surface in chains
became swollen, and then extended into solution. This might
create "bald spots" on the particle surface which would
encourage either mild flocculation, or an increase in the
secondary-minimum effect discussed earlier. Upon cooling,
the PS anchor blocks are once again adsorbed onto the particle
surface, and deflocculation occurs.

An alternative explanation of the above behaviour is
based upon a model which is predominantly as in figure 5.11(b),

with a small proportion of stabilizer molecules anchored as in figure 5.11(c). Upon heating, the more weakly anchored molecules of model II are totally desorbed. This would lead to the limited flocculation observed, which would again be reversible on cooling.

5.4 PROPERTIES OF NON-AQUEOUS DISPERSIONS

5.4.1 Rheology

The rheology of systems of dispersed particles surrounded by a soluble polymer layer has been reported in the literature [6,124,147]. These studies were based on polymer particles surrounded by a layer of low molecular weight [1 600], soluble polymer, and irregular titanium dioxide particles with a surface layer of low molecular weight [< 9 000] polymer. Measurement of the apparent hydrodynamic volume of the dispersed phase was combined with a knowledge of the particle core dimensions to estimate the thickness of the adsorbed layer. Such an estimation was complicated by the ill-defined nature of the soluble polymer, which was the polydisperse product of a condensation polymerization. Also the thickness of the layer was small compared to the particle diameters, since the molecular weight was low.

The polymer dispersions prepared in the present work have made possible a more comprehensive study of the adsorbed layer. The PDMS layer was well-defined [of narrow molecular weight distribution] and monodisperse particles have been prepared with surface layers of PDMS of a range of molecular weights [3 200 - 48 000]. The rheology of both PS and PMMA dispersions was studied, with an emphasis on PMMA dispersions as a model system. The adsorbed layer thickness [δ] was measured for a

series of dispersions of varying particle size for both PS and PMMA systems. The effect of varying both the PS anchor block and PDMS soluble block molecular weight was studied for PMMA dispersions. The results of rheological studies are given in Section 4.4.1.

The effect of varying the particle size in a series of PMMA dispersions containing the same stabilizer, on δ, was investigated. Figure 4.44 shows that the plot of $[\alpha_o f]^{1/3}$ vs. D^{-1} was linear over the particle size range considered $(0.096 - 0.48 \mu m)$. This implies that δ was constant over this range of particle sizes. From the intercept of this curve, the effective Einstein coefficient $[\alpha_o f]$ was found to be 2.49 ± 0.08. As D^{-1} tends to zero, the surface layer thickness becomes negligible relative to the core diameter, and the effective Einstein coefficient approaches the true Einstein coefficient of 2.50. The good agreement of coefficients suggests that the particles were spherical and free from aggregation. The sphericity of the particles was confirmed by electron microscopy. Both light scattering and SAXS studies have suggested the possiblility of a limited flocculation of PMMA dispersions. This was not reflected in rheology studies, which suggests that any flocculation was in fact weak and was easily destroyed under shear.

The ratio of the slope to the intercept of figure 4.14 gave a value of 8.9 nm for the adsorbed layer thickness. Since δ was constant over the range of particle sizes considered, subsequent estimations of δ could be obtained directly from equation 2.44 for particles of known diameter. The absence of particle asymmetry and aggregation under shear was also confirmed for PS particles. Although the choice of

dispersions was more limited, figure 4.16 shows a plot of $[\alpha_0 f]^{1/3}$ vs. D^{-1} to be linear, with an intercept giving an Einstein coefficient of 2.54 $\pm$ 0.09.

The variation of δ with the molecular weight of the PDMS layer is shown in figure 4.20 for PMMA particles, and figure 4.21 for PS particles. The rather high value of δ for a PDMS chain of $\bar{M}_n$ 48 000 corresponded to a closer packing of the PDMS chains as seen in figure 5.7. Figure 4.20 shows that the molecular weight of the PS anchor block, at least in the range 10 - 40 000, does not affect the value of δ. This confirms that the anchor block does not extend significantly into solution, and the PDMS chains may be thought of as being terminally adsorbed at the particle surface.

The variation of δ with the molecular weight of the PDMS chains is shown along with estimates of layer thickness from surface coverage studies in figure 5.12. This figure shows that δ is in reasonable agreement with the thickness h' calculated from surface coverage studies based on the prolate ellipsoid model of a molecule. The parameter δ was basically derived from Einstein's equation (equation 2.35), and, therefore, represents a hydrodynamic dimension rather than a molecular dimension. Figure 4.20 showed that the r.m.s. volume of a free PDMS chain was slightly greater than its equivalent sphere hydrodynamic volume. It is suggested from both experimental [148] and theoretical observations [149] that the r.m.s. volume of a molecule when represented by a prolate ellipsoid in good solvent media is greater than its hydrodynamic volume. It is ,therefore,reasonable that values of δ are consistently slightly less than h' values. The values calculated for h' will also be slightly overestimated,

FIGURE 5.12

A COMPARISON OF δ, h and h' AS A
FUNCTION OF PDMS MOLECULAR WEIGHT
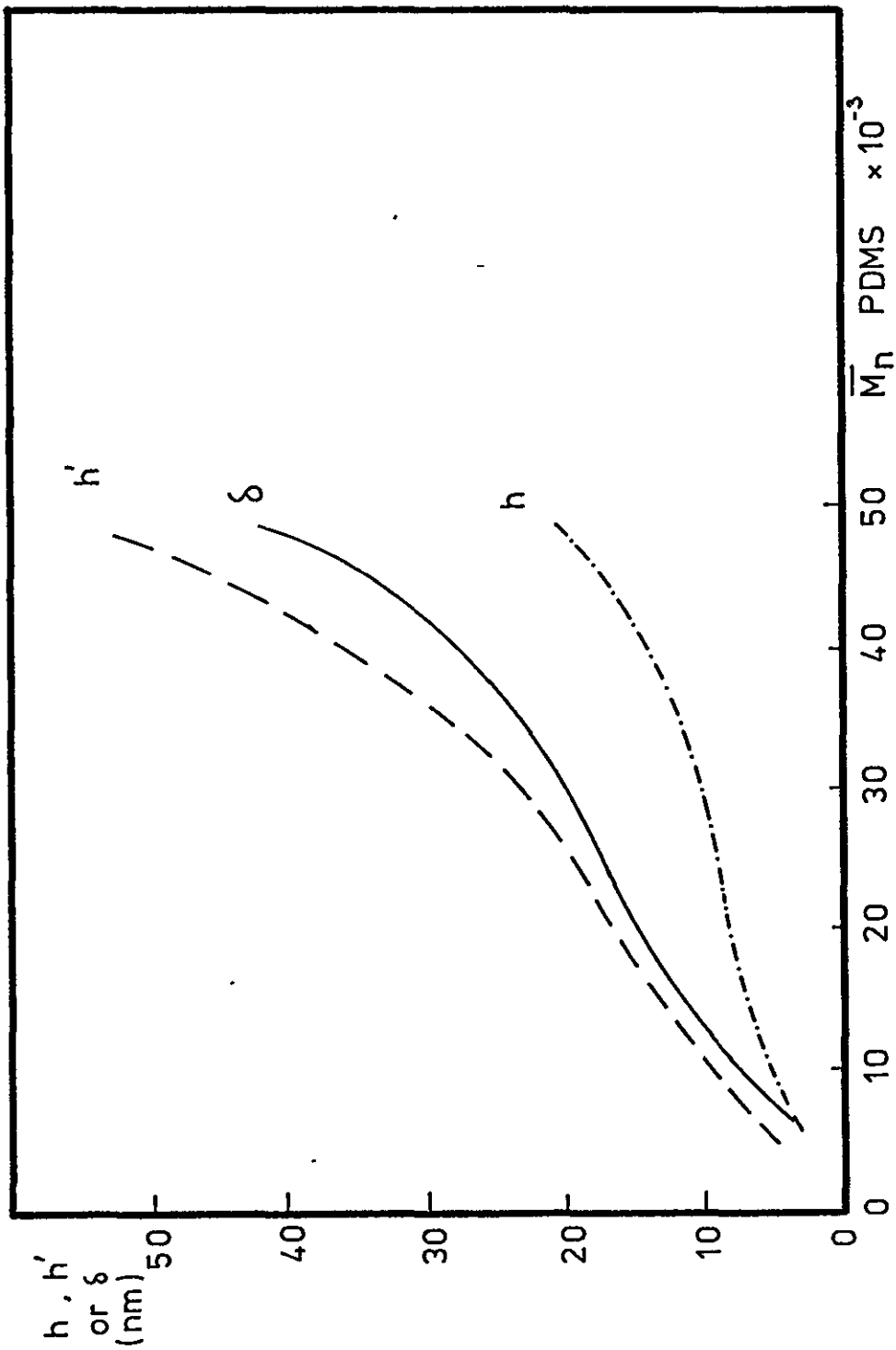
since on the convex surface of a particle, the prolate ellipsoid would become an ovoid, thus reducing the overall layer thickness. The suggestion that the PDMS chains could overlap was discussed in Section 5.3.2 and would also lead to a reduction in h'.

General conclusions can now be made about the configuration of the PDMS chains. Rheological studies have suggested that the PDMS molecules are extended over the random coil end-to-end distance of the free molecule in solution. The extension was seen to be less than for a fully extended chain (figure 4.20). An estimate of the layer thickness from surface coverage, based on a prolate ellipsoid model of a molecule, was in good agreement with the layer thickness derived from rheological studies.

The extension of the PDMS molecules might be expected, since it represents a balance between excluded volume effects extending the molecule to increase polymer-solvent contacts, and the loss of entropy associated with extending the molecule tending to oppose the extension. Whilst such extension occurs in solution, the elongation is even greater for a terminally adsorbed molecule, owing to the anisotropic situation. The molecule cannot penetrate the particle surface, and is severely restricted in penetration of neighbouring volumes. The molecule is, however, free to extend in a perpendicular plane to the surface, and, therefore, adopts an extended configuration.

Barsted et al. [124] have studied the rheology of polymer particles stabilized with a surface layer of poly(12-hydroxy stearic acid) of number average molecular weight 1 600. These workers found no variation of δ with particle size in the

range 0.04 to 2.0 μm, although Goodwin [86] has reworked these results to suggest that δ decreases at the smallest particle size. Barsted et al. reported a value for δ of 6.2 nm, which, according to their calculations, represents a layer thickness close to the hydrodynamic height of the molecule, and much less than the r.m.s. height. It is believed that these workers have calculated the r.m.s. dimensions incorrectly. From the intrinsic viscosity quoted for free poly[12-hydroxy stearic acid], a r.m.s. height of 4.9 nm was calculated, which is much less than Barsted's value calculated as 15.6 nm. Thus, their work is in agreement with the present findings for particles incorporating surface layers of PDMS. A relatively larger value of δ might be expected for short chain poly[12-hydroxy stearic acid] molecules, since such molecules are relatively inflexible, and approximate more closely to a non-overlapping, worm-like chain model.

5.4.2 Flocculation studies under θ-conditions

The behaviour of sterically stabilized dispersions in a medium which is a θ-solvent for the stabilizing chains was discussed in Section 2.1.3. Consideration of the "mixing term" gave equation 2.8, from which it was predicted that under θ-conditions [i.e. $\chi = 0.5$], ΔG_m becomes zero. In the absence of a repulsive force, the particles would flocculate. If an additional "volume restriction" term is considered, such systems would still experience a repulsive force under θ-conditions. Napper has studied the stability of sterically stabilized particles at θ-conditions. He reports results for an aqueous system [150,151] in which the molecular

weight of the stabilizing chains (polyethylene oxide) was varied from 10^3-10^6, although the molecular weight distribution of these soluble chains was rather broad. Napper has also studied non-aqueous sterically stabilized dispersions [14] ' under θ-conditions. Studies of PMMA particles in alkanes [14] were limited to low molecular weight stabilizing chains ($\bar{M}_n < 5\,000$) again of a polydisperse nature. For both aqueous and non-aqueous systems, Napper reported a loss of stability at θ-conditions or even at slightly better than θ-conditions.

The well-defined non-aqueous dispersions prepared in the present work were studied as a function of the solvency of the dispersion medium. Adding a non-solvent for PDMS (e.g. ethanol) to a dispersion eventually produced flocculation. This flocculation has been followed with larger particles ($> 1\ \mu$m) under the optical microscope. The minimum volume fraction of non-solvent added to produce visible flocculation was recorded as the critical flocculation volume (c.f.v.). The solvency of the dispersion medium was also reduced by lowering the temperature to give the critical flocculation temperature (c.f.t.). Flocculation could not be induced by cooling an aliphatic hydrocarbon-based dispersion, so the dispersion medium was changed to a heptane/ethanol mixture. All these studies were based upon stirred samples of dispersions. Thus, any inherent weak flocculation (Section 5.3.1) was removed under shear, as was shown by rheological studies (Section 5.4.1).

θ-conditions for PDMS homopolymer were determined by a cloud-point method as described in Section 4.8. The method used [42] was the same as that used by Napper [14], but since

the solubility parameters of PDMS and n-heptane are very close (both ≃ 7.4 [17]), the modification of Suh and Clarke [125] was adopted. The determined θ-temperature was checked by following the phase separation of PDMS at different molecular weights and applying the method of Talamini and Vidotto [126]. The good agreement of the determined θ-temperatures (Section 4.5.2) confirmed the applicability of the Suh and Clarke modification.

Table 4.15 shows that for particles stabilized by the same stabilizer, both the c.f.v. and the c.f.t. were insensitive to the particle diameter over the range studied. This is in agreement with Napper's work with aqueous systems [150] and confirms Fischer's prediction [11] that the interaction volume at constant surface separation is almost directly proportional to the particle core radius. For non-aqueous systems, Napper found a decrease in c.f.v. with increasing particle size, but this may be a result of incomplete surface coverage of the larger particles.

Table 4.16 shows the insensitivity of both c.f.v. and c.f.t. to the molecular weight of the PDMS chains. The errors involved in the determination of the c.f.v. were rather large owing to the experimental difficulty associated with mixing the non-solvent into the dispersion medium. The closer agreement of c.f.t. values reflects the more easily controlled experimental technique.

The θ-composition and θ-temperature for PDMS in equivalent solvents were found to be 38.7% (volume fraction of added ethanol) and 339.0 ± 1 K respectively. Hence, within experimental error, the c.f.t. values correspond closely to the determined θ-temperature for PDMS. The c.f.v. values all

occur at slightly worse than θ-conditions, but this could well be a result of the experimental difficulties mentioned above.

The accuracy of this particular experimental procedure must be considered. Flocculation was recorded as the point of a visible change in the turbidity of the stirred dispersion. The use of instrumentation capable of measuring the optical density of the dispersion would,perhaps,have been more sensitive, and it is possible that the critical flocculation points recorded do not in fact represent incipient flocculation. The reproducibility of both c.f.v. and c.f.t. determinations was, however, good. The concept of θ-conditions for a terminally adsorbed polymer molecule should be treated with caution, since these are not necessarily the same as the θ-conditions for a free molecule in dilute solution. With the above limitations in mind, however, these studies of flocculation do suggest some significant features.

It is evident that the dispersions chosen were in fact sterically stabilized, and that flocculation was induced by changing the solvency conditions for the PDMS layer. Flocculation occurred when the dispersion medium was of much better solvency than that required for phase separation of the particular stabilizing PDMS chain in solution. The critical flocculation point was insensitive to the molecular weight of the PDMS. These two observations suggest that the flocculation of a dispersion is not a result of a dimensional collapse of the PDMS chains. The dispersions reported in table 4.16 contained PS anchor block of molecular weights 8 800 - 44 000. The insensitivity of c.f.v. and c.f.t. to the anchor block length, again confirms that the anchor block

was not extended into the dispersion medium.

The overall conclusion of these studies is that these sterically stabilized dispersions lose stability and flocculate close to the point when the dispersion medium becomes a θ-solvent for the soluble stabilizing chains. Whilst the experimental techniques are open to improvement, there remains still the problem of defining θ-conditions for a relatively concentrated layer of terminally adsorbed polymer molecules. This problem must be resolved before more significant conclusions can be drawn.

CHAPTER 6

CONCLUSIONS

Well-defined systems of sterically stabilized polymer particles have been prepared. The particles were either PS or PMMA and the stabilizing mechanism was provided by a surface layer of PDMS. The stabilizing layer was anchored to the particle by incorporating the PDMS into an AB block copolymer of PS-PDMS.

High vacuum purification and polymerization techniques produced better-defined PS-PDMS stabilizers than inert gas blanket techniques. Anionic polymerization gave stabilizers of narrow molecular weight distribution $[\bar{M}_w/\bar{M}_n < 1.2]$ which produced well-defined layers of PDMS at the particle surface.

Three types of dispersion polymerization were compared:

[i] the radical dispersion polymerization of styrene

[ii] the anionic dispersion polymerization of styrene

[iii] the radical dispersion polymerization of methyl
    methacrylate

A comparison of the rates of polymerization yielded the following order for the above systems:

$$[ii] > [iii] \gg [i]$$

Phase separation studies have led to an estimate of the threshold molecular weight for precipitation of PS in the dispersion medium. It was shown that most of the polymerization in [i] actually occurs in solution. A reaction between polystyryl anions and the PDMS stabilizing chains in [ii] was

identified, and methods of minimising this adverse effect were developed.

The particle size and distribution of sizes was influenced by the composition and concentration of stabilizer present in the dispersion medium, and by the solvency of the medium. Smaller particles resulted from either an increase in the concentration of the stabilizer, an increase in the PDMS block molecular weight or a decrease in the solvency of the dispersion medium. The particle sizes were estimated by transmission electron microscopy and verified by SAXS.

The presence of the surface layer of PDMS was detected by both light scattering and SAXS studies, although it is doubtful if these techniques detected the full extent of the surface layer. Scattering studies also suggested that in at least two of the PMMA dispersions, there was limited particle flocculation. The rheology of these dispersions has shown any flocculation to be weak, and this type of behaviour was accounted for in terms of a secondary-minimum type of effect.

The surface coverage of the particles by PDMS chains was shown to be a function of the molecular weight of the PDMS, and was complete for all the particle sizes considered. Models were suggested for the packing of PDMS chains at the particle surface. Rheological studies have suggested that a good approximation might be a model in which each PDMS chain occupies an ovoid volume. Estimates of the PDMS layer thickness from surface coverage data, and of the hydrodynamic layer thickness from rheology both suggested that the PDMS chains are in an extended configuration. This configuration lies between random coil and a fully extended chain, and is a result of interactions between neighbouring chains.

The mechanism of anchoring of the PDMS chains to the surfaces of PS and PMMA particles is believed to be different. The PS block of a stabilizer molecule is thought to be incorporated within the matrix of a PS particle, and would,therefore, exhibit a configuration as in a bulk polymer. Owing to the incompatibility of PS and PMMA, a collapsed state was suggested for the PS anchor block on a PMMA particle. The anchoring efficiency in both systems was shown to be good. Surface coverage information, rheology and flocculation studies have all confirmed that the PS anchor block was not significantly extended into the dispersion medium.

Non-aqueous dispersions lost stability when the dispersion medium was changed to a θ-solvent for the stabilizing PDMS chains. Thus,the mechanism of stabilization was confirmed to be steric stabilization.

CHAPTER 7

RECOMMENDATIONS FOR FUTURE WORK

The present work has provided a method for preparing model sterically stabilized polymer dispersions. The stabilizing polymer layers were well-defined and of sufficiently high molecular weight for conventional polymer solution theories to be applicable. These dispersions would, therefore, provide an ideal model for experimental justification of the theories of steric stabilization. The large surface area of such a particulate system also offers a good basis for studies of adsorbed polymer molecules.

Compression studies could be used to obtain information about the extent and magnitude of the steric forces. Compression of a monolayer of a dispersion along the lines of work by Doroszowski and Lambourne [15 . 39], or perhaps even better, three-dimensional compression studies as performed by Ottewill et al. [152] and Homola and Robertson [153], would provide useful information.

The hydrodynamic volume of the particles, measured in the present study by rheology, could also be estimated by centrifugal methods [154], or even the newly emerging technique of hydrodynamic chromatography.[155].

Small-angle X-ray studies have been used to obtain information about the dimensions of block copolymer micelles [134]. The preliminary SAXS studies reported in the present work could be extended along the same lines to cover the range of dispersions prepared. Likewise, the preliminary light scattering studies could be extended to include the

different types of particles prepared. Light scattering from
a stirred sample of a dispersion might be used to identify
the extent of the limited flocculation suggested.

The configuration of both the anchor block and the
stabilizing block of the adsorbed stabilizer is of interest.
Work is currently in progress involving neutron scattering
studies from the dispersions [156]. Such a technique could
be used to measure the radius of gyration of each block, and
hence the configuration could be predicted.

REFERENCES

1. D.C. Blackley, "Emulsion Polymerization : Theory and Practice", Applied Sci. Publishers (1975).

2. British Patent 385 970 to British Thomson-Houston (1930).

3. British Patent 893 429 to Imperial Chemical Industries (1957).

4. British Patent 934 038 to Rohm and Haas (1958).

5. British Patent 941 305 to Imperial Chemical Industries (1958).

6. D.J. Walbridge and J.A. Waters, Discuss. Farad. Soc., $\underline{42}$, 294 (1966).

7. K.E.J. Barrett and H.R. Thomas, J. Polym. Sci. A-1, $\underline{7}$, 2621 (1969).

8. British Patent 1007 476 to Firestone Tire and Rubber Co. (1965).

9. G.B. Stampa, J. Appl. Polym. Sci., $\underline{14}$, 1227 (1970).

10. K.E.J. Barrett (Ed.), "Dispersion Polymerization in Organic Media", Wiley, London (1975).

11. E.W. Fischer, Kolloid-Z. Z. Polymere, $\underline{227}$, 108 (1958).

12. D.J. Meier, J. Phys. Chem., $\underline{71}$, 1861 (1967).

13. B. Vincent, Advances in Coll. and Interface Sci., $\underline{4}$, 193 (1974).

14. D.H. Napper, Trans. Farad. Soc., $\underline{64}$, 1701 (1968).

15. A. Doroszkowski and R. Lambourne, J. Polym. Sc. C, $\underline{34}$, 253 (1971).

16. G. Allen (Chairman), Science Research Council Report on Colloid Science (1972).

17. J. Brandrup and E.H. Immergut, "Polymer Handbook", Wiley, New York (1966).

18. German Patent 2 142 598 to Dow Corning (1972).

19. J.C. Saam and C.H. Tsai, J. Appl. Polym. Sci., 18, 2279 (1974).

20. F. London, Z. Physik., 63, 245 (1930).

21. H.C. Hamaker, Rec. Trav. Chim., 55, 1015 (1936)
                                       56, 3727 (1937).

22. J.Th.G. Overbeek and E.J.W. Verwey, "Theory of the Stability of Lyophobic Colloids", Elsevier, Amsterdam, (1948).

23. D.W.J. Osmond, B. Vincent and F.A. Waite, J. Coll. Interface Sci., 42, 262 (1973).

24. E.M. Lifshitz, J. Exper. Theor. Phys. of U.S.S.R., 29, 94 (1955).

25. B. Derjaguin and L. Landau, Acta Phys. Chem., 14, 633 (1941).

26. P.J. Flory and W.R. Krigbaum, J. Chem. Phys., 18, 1086 (1950).

27. R.H. Ottewill and T. Walker, Kolloid-Z. Z. Polymere., 227, 108 (1968).

28. D.H. Napper, J. Coll. Interface Sci., 29, 168 (1969).

29. F.Th. Hesselink, J. Phys. Chem., 73, 3488 (1969).

30. E.L. Mackor, J. Coll. Sci., 5, 490 (1951).

31. A.K. Dolan and S.F. Edwards, Proc. R. Soc. Lond. A., 337, 509 (1974).

32. P.J. Flory, "Principles of Polymer Chemistry", Cornell Univ. Press, New York (1953).

33. F.Th. Hesselink, A. Vrij and J.Th.G. Overbeek, J. Phys. Chem., 75, 2094 (1971).

34. D.W.J. Osmond, B. Vincent and F.A. Waite, Colloid and Polym. Sci., 253, 673 (1975).

35. E.J. Clayfield and E.C. Lumb, J. Colloid Interface Sci., 22, 269 (1966).

36. E.J. Clayfield and E.C. Lumb, J. Colloid Interface Sci., 22, 285 (1966).

37. R. Evans and D.H. Napper, Kolloid-Z. Z. Polymere, 251, 329 (1973).

38. J.B. Smitham, R. Evans and D.H. Napper, J. Chem. Soc. Faraday Trans. I, 71, 285 (1975).

39. A. Doroszkowski and R. Lambourne, J. Coll. Interface Sci., 43, 97 (1973).   .

40. D.M. Andrews, E.D. Manev and D.A. Haydon, Spec. Disc. Farad. Soc., 1, 46 (1970).

41. H.G. Elias, Makromol. Chem., 50, 1 (1961).

42. C.F. Cornet and H. van Ballegooijen, Polymer, 7, 293 (1966).

43. A.R. Shultz and P.J. Flory, J. Am. Chem. Soc., 74, 4760 (1952).

44. G.D. Parfitt (Ed.), "Dispersions of Powders in Liquids with Special Reference to Pigments," 2nd Edn., Applied Sci. Publishers, London (1973).

45. C. Sadron, Pure Appl. Chem., 4, 347 (1962).

46. H.G. Elias, J. Macromol. Sci.-Chem., A7, 601 (1973).

47. C.J. Stacey and G. Kraus, Polym. Prepr., 18, 323 (1977).

48. Z. Tuzar and P. Kratochvíl, Adv. in Coll. and Interface Sci., 6, 201 (1976).

49. C. Sadron, Angew. Chem. Internat. Edn., 2, 248 (1963).

50. T. Inoue, T. Soen, T. Hashimoto and H. Kawai, J. Polym. Sci.-A2, 7, 1283 (1969).

51. M.E.L. McBain and E. Hutchinson, "Solubilization and Related Phenomena", Academic Press, New York (1955).

52. G. Reiss, J. Kohler, C. Tournut and A. Banderat, Makromol. Chem., 101, 581 (1967).

53. T. Inoue, T. Soen, T. Hashimoto and H. Kawai, Macromol., 3, 87 (1970).

54. D.J. Meier, Polym. Prepr., 18, 340 (1977).

55. M. Szwarc, M. Levy and R. Milkovitch, J. Am. Chem. Soc., 78, 2656 (1956).

56. P.J. Flory, J. Am. Chem. Soc., 62, 1561 (1940).

57. D. McIntyre, L.J. Fetters and E. Slagowski, Science, 176, 1041 (1972).

58. L.J. Fetters, J. Polym. Sci. Part C, 26, 1 (1969).

59. M. Morton and L.J. Fetters, Rubber Chem. and Tech., 48, 359 (1975).

60. L.J. Fetters, J. of Research of N.B.S.-A Phys. and Chem.- 70A, 421 (1966).

61. J.C. Saam, D.J. Gordon and S. Lindsey, Macromol., 3, 1 (1970).

62. W.G. Davies and D.F. Jones, I. & E. Chem. Prod. Dev., 10, 168 (1971).

63. J.C. Saam and F.W.G. Fearon, I. & E. Chem. Prod. Dev., 10, 10 (1971).

64. J.G. Zilliox, J.E.L. Roovers and S. Bywater, Macromol., 8, 573 (1975).

65. A. Marsiat and Y. Gallot, Makromol. Chem., 176, 1641 (1975).

66. M. Morton, L.J. Fetters, R.A. Pett and J.F. Meier, Macromol., 3, 327 (1970).

67. D. Margerison and J.P. Newport, Trans. Farad. Soc., 59, 2062 (1963).

68. D.J. Worsfold and S. Bywater, Can. J. Chem., 38, 1891 (1960) 42, 2884 (1964)

69. O.J. Worsfold and S. Bywater, J. Organometallic Chem. <u>10</u>, 1 (1967).

70. T.L. Brown, J. Organometallic Chem., <u>5</u>, 191 (1966).

71. V.A. Bessnov, P.F. Alikhanov, E.N. Gur'yanova, A.F. Simonov, I.O. Shapero, E.A. Yakovleva and A.I. Shatenshtein, J. Gen. Chem. U.S.S.R. (Eng. Transl.), <u>37</u>, 96 (1965).

72. C.L. Lee, C.L. Frye and O.K. Johansson, Polym. Prepr., <u>10</u>, 1361 (1969).

73. Y. Minoura, M. Mitoh, A. Tabuse and Y. Yamada, J. Polym. Sci. A1, <u>7</u>, 2753 (1969).

74. C.H. Bamford, W.G. Barb, A.D. Jenkins and P.F. Onyon, "The Kinetics of Vinyl Polymerization", Butterworths Scientific Publications, London (1958).

75. R.G.W. Norrish and R.R. Smith, Nature (London), <u>150</u>, 336 (1942).

76. B. Vincent in Colloid Science, Vol. 1, Specialist Periodical Report, The Chemical Society, London (1973).

77. E. Trommsdorff, E. Köhle and F. Langally, Makromol. Chem., <u>1</u>, 169 (1948).

78. R.M. Fitch and C.H. Tsai, in "Polymer Colloids" (Ed. R.M. Fitch), Plenum Press, New York (1971).

79. M. Volmer, "Kinetic der Phasenhildung", T. Steinkopff, Dresden and Leipzig (1939); reprinted Edward Bros., Ann Arbor, Mich. (1945).

80. W.D. Harkins, J. Am. Chem. Soc., <u>69</u>, 1428 (1947).

81. G.V. Schulz and G. Harborth, Makromol. Chem., <u>1</u>, 106 (1947).

82. G.V. Schulz, Z. Phys. Chem., <u>8</u>, 290 (1956).

83. A. Einstein, Ann. Physik, <u>17</u>, 459 (1905)   (cont.)

83. A. Einstein, Ann. Physik, 19, 289 (1906)

34, 591 (1911).

84. R. Rutgers, Rheol. Acta, 4, 305 (1962).

85. H.L. Frisch and R. Simha, in "Rheology, Theory and Applications", Vol. 1, (Ed. F. Eirich), Academic Press, New York (1956).

86. J.W. Goodwin in Colloid Science, Vol. 2 (Ed. D.H. Everett), Chem. Soc. Specialist Period. Report, London (1975).

87. R.St.J. Manley and S.G. Mason, J. Coll. Sci., 17, 354 (1962).

88. D.G. Thomas, J. Coll. Sci., 20, 267 (1965).

89. M. Mooney, J. Coll. Sci., 6, 162 (1951).

90. F.L. Saunders, J. Coll. Sci., 16, 13 (1961).

91. C. Parkinson, S. Matsumoto and P. Sherman, J. Coll. Interface Sci., 33, 150 (1970).

92. H.C. van de Hulst, "Light Scattering by Small Particles", Wiley, New York (1957).

93. Lord Rayleigh, Proc. Roy. Soc. (London), A90, 219 (1914).

94. G. Mie, Ann. Physik, 25, 377 (1908).

95. S.H. Maron, P.E. Pierce and I.N. Ulevitch, J. Coll. Sci., 18, 470 (1963).

96. S.H. Maron, P.E. Pierce and M.E. Elder, J. Coll. Sci., 18, 391 (1963).

97. P.E. Pierce and S.H. Maron, J. Coll. Sci., 19, 658 (1964).

98. S.H. Maron, M.E. Elder and P.E. Pierce, J. Coll. Sci., 18, 733 (1963).

99. S.H. Maron, P.E. Pierce and M.E. Elder, J. Coll. Sci., 19, 591 (1964).

100. G. Dezelić and J.P. Kratohvil, J. Coll. Sci., 16, 561 (1961).

101. J.F. Kratohvil and C. Smart, J. Coll. Sci., 20, 875 (1965).

102. G.M. Burnett, R.S. Lehrle, D.J. Ovenall and F.W. Feaker, J. Polym. Sci., 29, 417 (1958).

103. J.W. Vanderhoff in "Kinetics and Mechanisms of Polymerization Series, Vol. 1, Vinyl Polymerization, Pt. II", [Ed. G.E. Ham], Dekker, New York (1969).

104. J.P. Kratohvil, Ann. Chem., 36, 5, 458R (1964).

105. M. Kerker, "The Scattering of Light and Other Electro-magnetic Radiation", Academic Press, New York (1969).

106. P. Debye, J. Phys. Chem., 51, 18 (1947).

107. T. Alfrey, Jnr., E.B. Bradford, J.W. Vanderhoff and G. Oster, J. Opt. Soc. Am., 44, 603 (1954).

108. D.P. Riley and G. Oster, Disc. Farad. Soc., 11, 107 (1951).

109. G. Porod, Kolloid Z., 124, 83 (1951).

110. G. Porod, Kolloid Z., 125, 51 (1952).

111. L. Kahovec, G. Porod and H. Ruck, Kolloid Z., 133, 16 (1953).

112. P. Debye, H.R. Anderson and H. Brumberger, J. Appl. Phys., 28, 679 (1957).

113. A. Guinier and G. Fournet, "Small-Angle Scattering of X-rays", Wiley (1955).

114. D.P. Jones, Dow Corning Ltd., Barry, Glamorgan, U.K.

115. H. Gilman and A.H. Haubein, J. Am. Chem. Soc., 66, 1515 (1944).

116. M. Morton and R. Milkovich, J. Polym. Sci.-A1, 443 (1963).

117. J. Young & Co., Acton, U.K.

118. ALC/GPC 501 Instruction Manual, Waters Ass., Framingham, Massachusetts (1970).

119. Pressure Chemical Co., Pittsberg, U.S.A.

120. Mechrolab Model 502 Instruction Manual, Mechrolab. Inc., Mountain View, California.

121. Parr Instrument Co. Ltd., Moline, Illinois, U.S.A.

122. Technicon Instruments Co. Ltd., Basingstoke, U.K.

123. V. Vand, J. Phys. Chem., 52, 277 (1948).

124. S.J. Barsted, L.J. Nowakowska, I. Wagstaff and D.J. Walbridge, Trans. Farad. Soc., 67, 3598 (1971).

125. K.W. Suh and D.H. Clarke, J. Appl. Polym. Sci., 12, 1775 (1968).

126. G. Talamini and G. Vidotto, Makromol. Chem., 110, 111 (1967).

127. N.N. Slavnitskaya, Yu.D. Semchikov, A.V. Rayabov, D.N. Bort, Vysokomol. Soed.-A12, 1756 (1970) (transl. in Polym. Sci. U.S.S.R. 12, 1993 (1970)).

128. H.E. Fickett, M.J.R. Cantow, J.F. Johnson, J. Appl. Polym. Sci., 10, 917 (1966).

129. T.G. Croucher, Ph.D. Thesis, Loughborough University (1976).

130. J.V. Dawkins, Br. Polym. J., 4, 87 (1972).

131. G.V. Schulz and E. Husemann, Z. Physik. Chem., B39, 246 (1938).

132. A. Dijkstra, G. Kortleve and G. Vonk, Kolloid-Z. Z. Polymere, 210, 121 (1966).

133. R.C. Weast (Ed.), "Handbook of Chemistry and Physics", 53rd Edn., C.R.C. Press (1972).

134. J. Plěstil and J. Baldrian, Makromol. Chem., 176, 1009 (1975).

135. J. Brandrup and E.H. Immergut, "Polymer Handbook", 2nd Edn., Wiley, New York (1975).

136. M. Szwarc, "Carbanions, Living Polymers and Electron Transfer Processes", Wiley Intersci. (1968).

137.   E. Papier and V.T. Nguyen, Polymer Letters, 10, 167
        (1972).

138.   D.H. Napper and R.H. Ottewill, J. Coll. Sci., 19, 72
        (1964).

139.   T. Tanaka, Macromol. 10, 51 (1977).

140.   H. Benoit, D. Decker, J.S. Higgins, C. Picot, J.P. Cotton,
        B. Farnoux, J. Jannink and R. Ober, Nature - Phys. Sci.,
        245, 13 (1973).

141.   J.P. Cotton, D. Decker, H. Benoit, B. Farnoux, J.S.
        Higgins, J. Jannink, R. Ober, C. Picot and J. des
        Cloizeaux, Macromol., 7, 863 (1974).

142.   R.G. Kirste, W.A. Kruse and J. Shelten,   Makromol.
        Chem., 162, 299 (1972).

143.   D.G.H. Ballard, J. Shelten and C.D. Wignall, Eur. Polym.
        J., 9, 965 (1973).

144.   M. Baer, J. Polym. Sci.-A2, 2, 417 (1964).

145.   J.C. Saam and D.J. Gordon, J. Polym. Sci.-A1, 8, 2509
        (1970).

146.   W.H. Tuminello, Ph.D. Thesis, Loughborough University
        (1973).

147.   A. Doroszkowski and R. Lambourne, J. Coll. Interface
        Sci., 26, 214 (1968).

148.   W.R. Krigbaum and D.K. Carpenter, J. Phys. Chem., 59,
        1166 (1955).

149.   W. Kurata and H. Yamakawa, J. Chem. Phys., 29, 311 (1958).

150.   D.H. Napper, J. Coll. Interface Sci., 32, 106 (1970).

151.   D.H. Napper and H. Netschey, J. Coll. Interface Sci.,
        37, 528 (1971).

152.   C. Barclay, A. Harrington and R.H. Ottewill, Kolloid-Z.
        Z. Polymere, 250, 655 (1972).

153.   A. Homola and A.A. Robertson, J. Coll. Interface Sci.,
        $\underline{54}$, 286 (1976).

154.   T. Allen, "Particle Size Measurement", Ch. 12, Chapman
        and Hall, London (1975).

155.   H: Small, J. Coll. Interface Sci., $\underline{48}$, 147 (1974).

156.   G. Allen, J.S. Higgins, A. Maconnachie, J.V. Dawkins and
        G. Taylor, work in progress.

157.   M. Hemming, Ph.D. Thesis, Lancaster University (1973).

158.   P.J. Flory, "Statistical Mechanics of Chain Molecules",
        Wiley, New York (1969).

159.   S.H. Maron, B.P. Madow and I.M. Krieger, J. Coll. Sci.,
        $\underline{6}$, 584 (1957).

CALCULATION OF MOLECULAR DIMENSIONS OF PDMS

(a) Root mean square (r.m.s.) end-to-end distance

The r.m.s. end-to-end distance was calculated from the intrinsic viscosity $[\eta]$. The Mark-Houwink equation relates $[\eta]$ to the molecular weight M of a polymer according to

$$[\eta] = K M^{a} \qquad .$$

where K abd a are constants for a given polymer/solvent system at a temperature T.

For PDMS in cyclohexane, at 308 K, the following relationship has been shown to hold

$$[\eta] = 6.3 \times 10^{-5} M^{0.76} \qquad [157]$$

The intrinsic viscosity of a molecule is proportional to the effective hydrodynamic volume of the molecule in solution divided by its molecular weight [32]. The effective volume is proportional to the cube of a linear dimension of the randomly coiling chain. Hence, if $\langle r^{2} \rangle^{1/2}$ is the dimension chosen,

$$\left[\eta\right] = \phi \frac{\langle r^{2} \rangle^{\frac{3}{2}}}{M}$$

where ϕ is a universal viscosity constant, which will be taken as 2.1×10^{23} cc g^{-1}. Thus the r.m.s. end-to-end length of PDMS at various molecular weights was calculated.

These r.m.s. dimensions were calculated at 303 K. The change in dimensions of a molecule with temperature can be calculated [158]. This was found to be very small for a PDMS

molecule over a 10° range.

(b) Radius of gyration

The radius of gyration of a molecule $\langle s^2 \rangle^{1/2}$ is defined as the r.m.s. distance of the elements of the chain from its centre of gravity. For linear polymer molecules, the mean square end-to-end distance and the square of the radius of gyration are simply related:

$$\langle r^2 \rangle = 6 \langle s^2 \rangle$$

(c) Extended chain dimensions

An extended PDMS chain on a crystal lattice adopts the conformation of lowest energy. This has been shown to be helical, with six repeat units per revolution [158]. Crystallographic measurements yielded a value of 0.138 nm for the linear repeat unit length [17]. Hence, the fully extended chain length was calculated for PDMS of various molecular weights.

(d) Hydrodynamic volume

The hydrodynamic volume of a chain can be derived from Einstein's equation, by assuming the molecule and associated solvent can be represented by a non-draining equivalent sphere. The hydrodynamic volume (V_h) can thus be obtained from the intrinsic viscosity,

$$[\eta] = 2.5 \; No \; V_h \; [M]^{-1}$$

where No is Avagadro's Number.

The hydrodynamic radius or diameter can then be obtained from V_h.

(e) Root mean square volume

The r.m.s. volume was calculated from the radius of gyration:

$$r.m.s.\ volume\ =\ \frac{4}{3}\pi \langle s^2 \rangle^{\frac{3}{2}}$$